APPENDICES A1-A3

APPENDIX A1 - Seismic Interpretation Maps

The seismic interpretation of the main three horizons (base of Sequence 2, base of Sequence 3 and top of Sequence 3) are shown. A few block names are shown for reference.

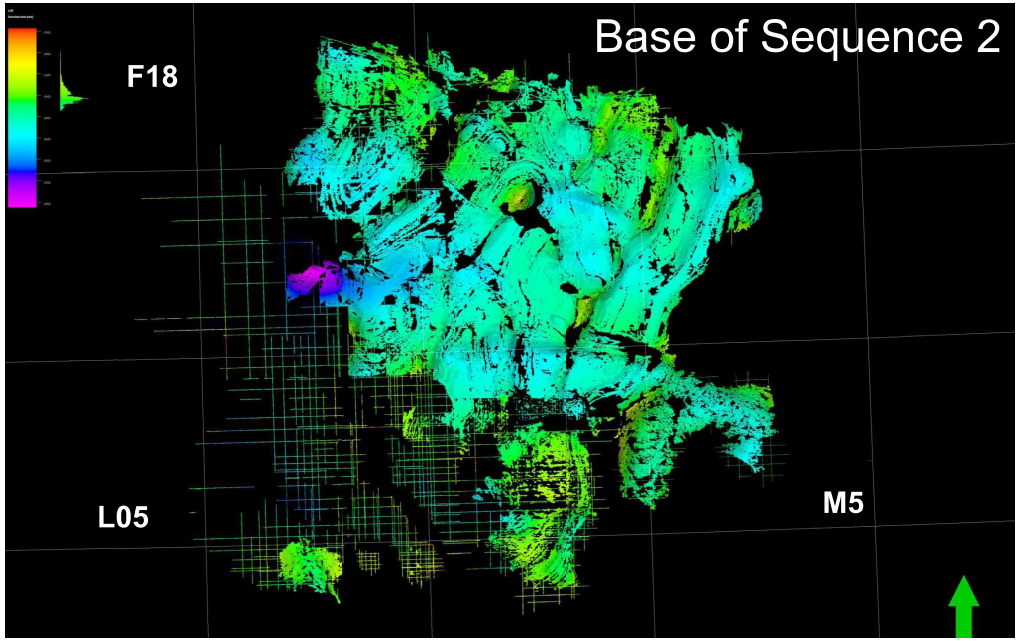

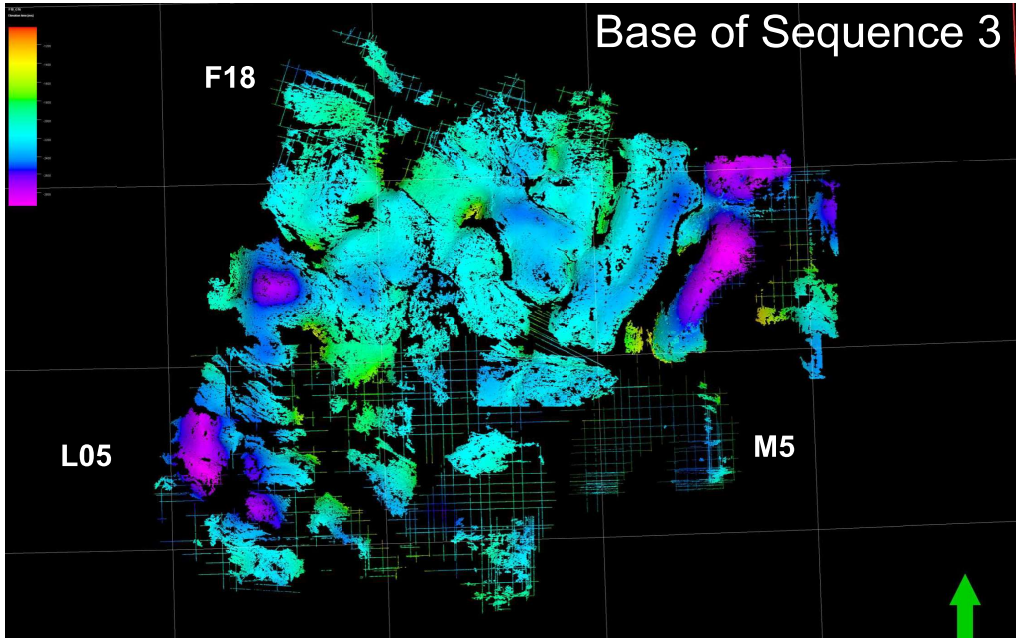

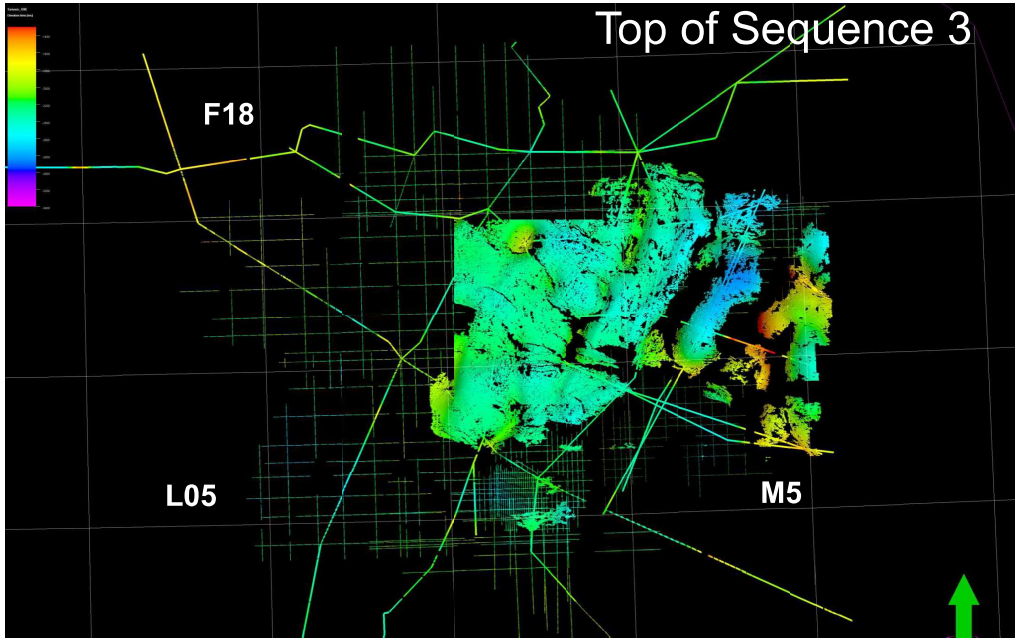

APPENDIX A2 - Panel H

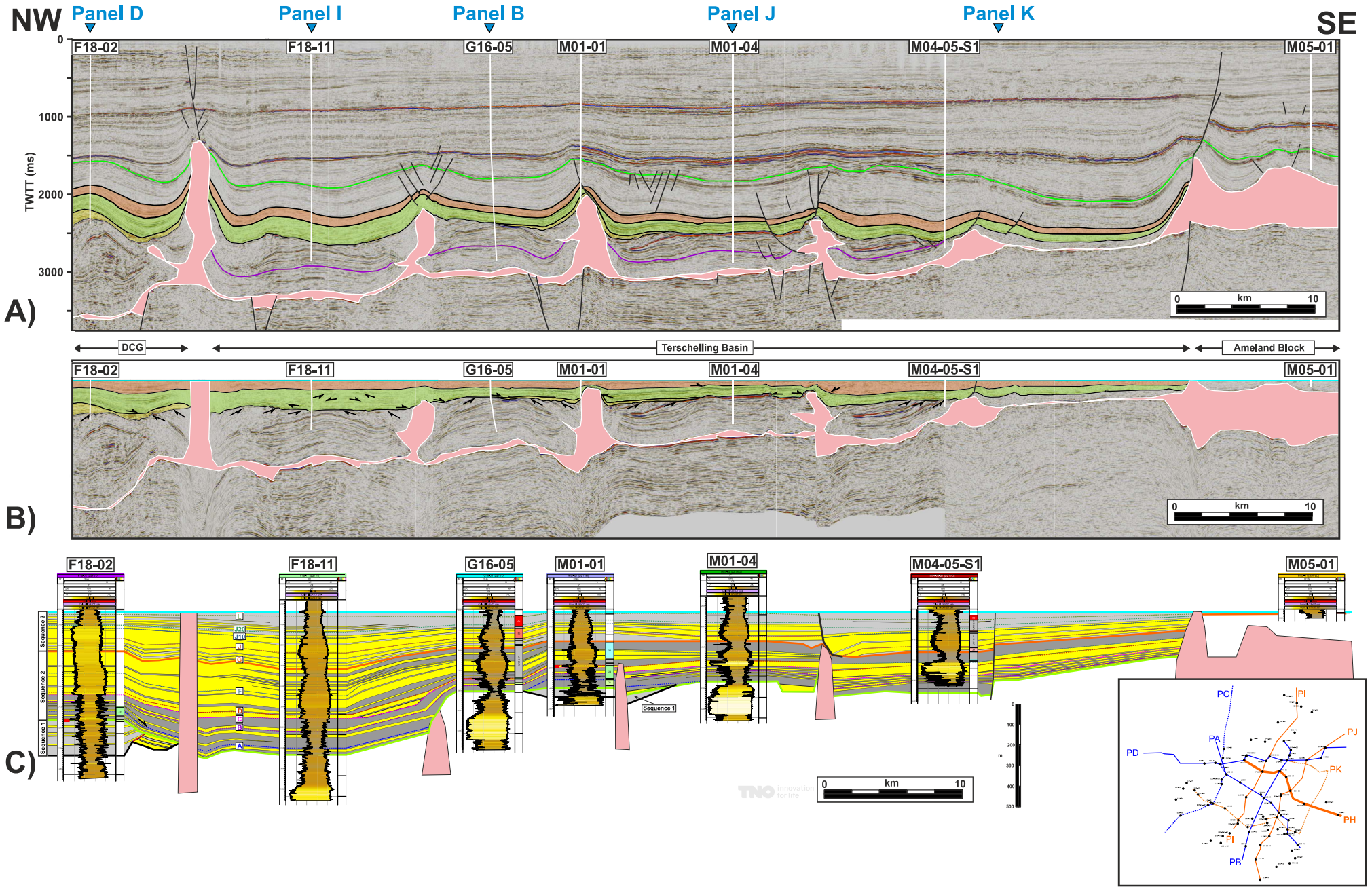

APPENDIX A2 - Panel I

TNO innovation for life

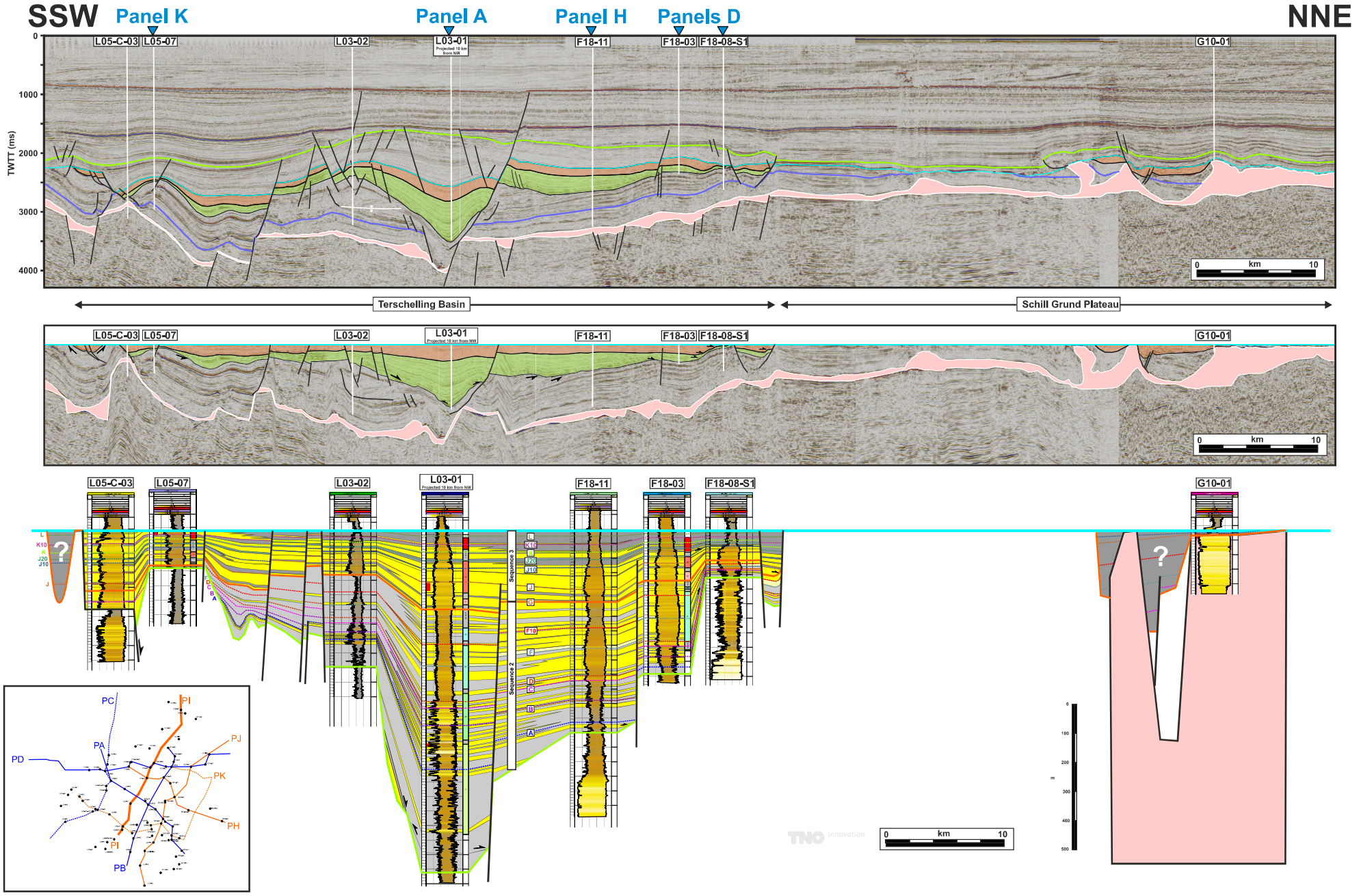

APPENDIX A2 - Panel J

TNO innovation for life

A)

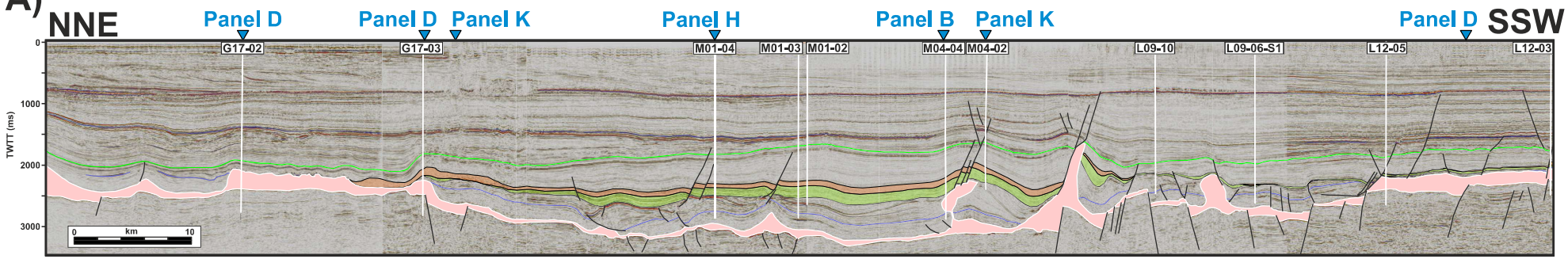

B)

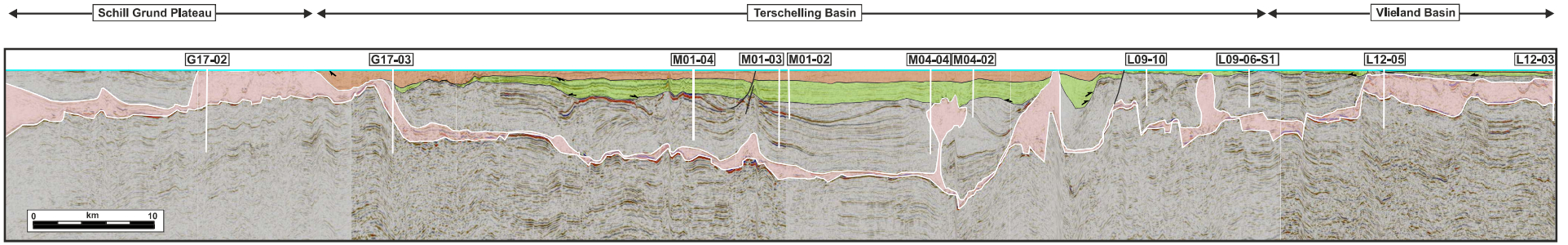

C)

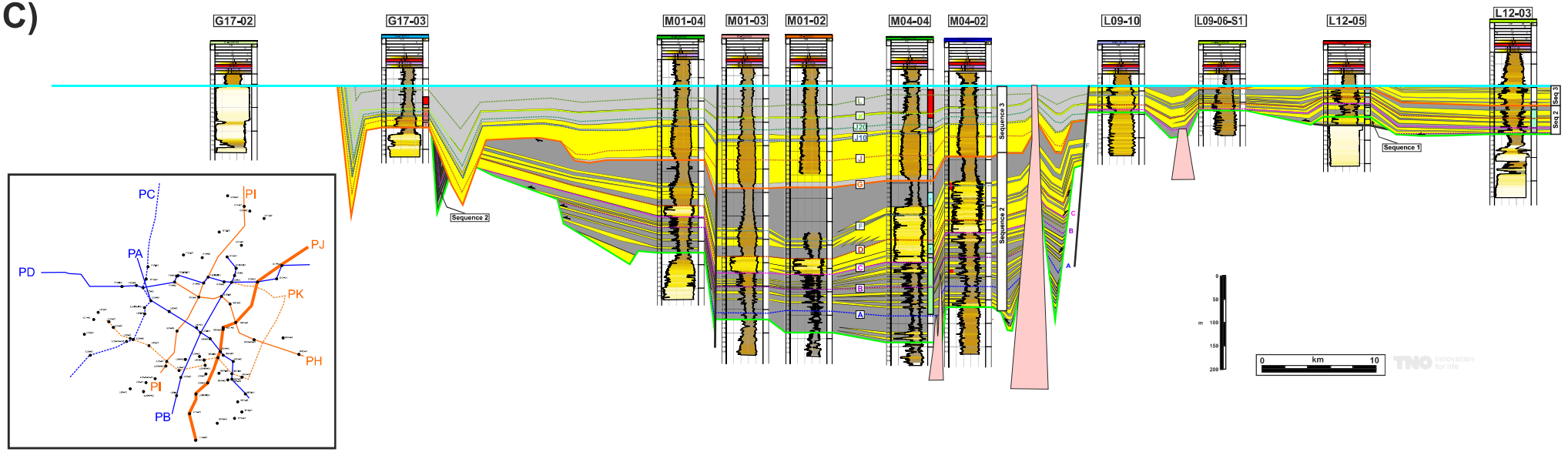

APPENDIX - Panel K

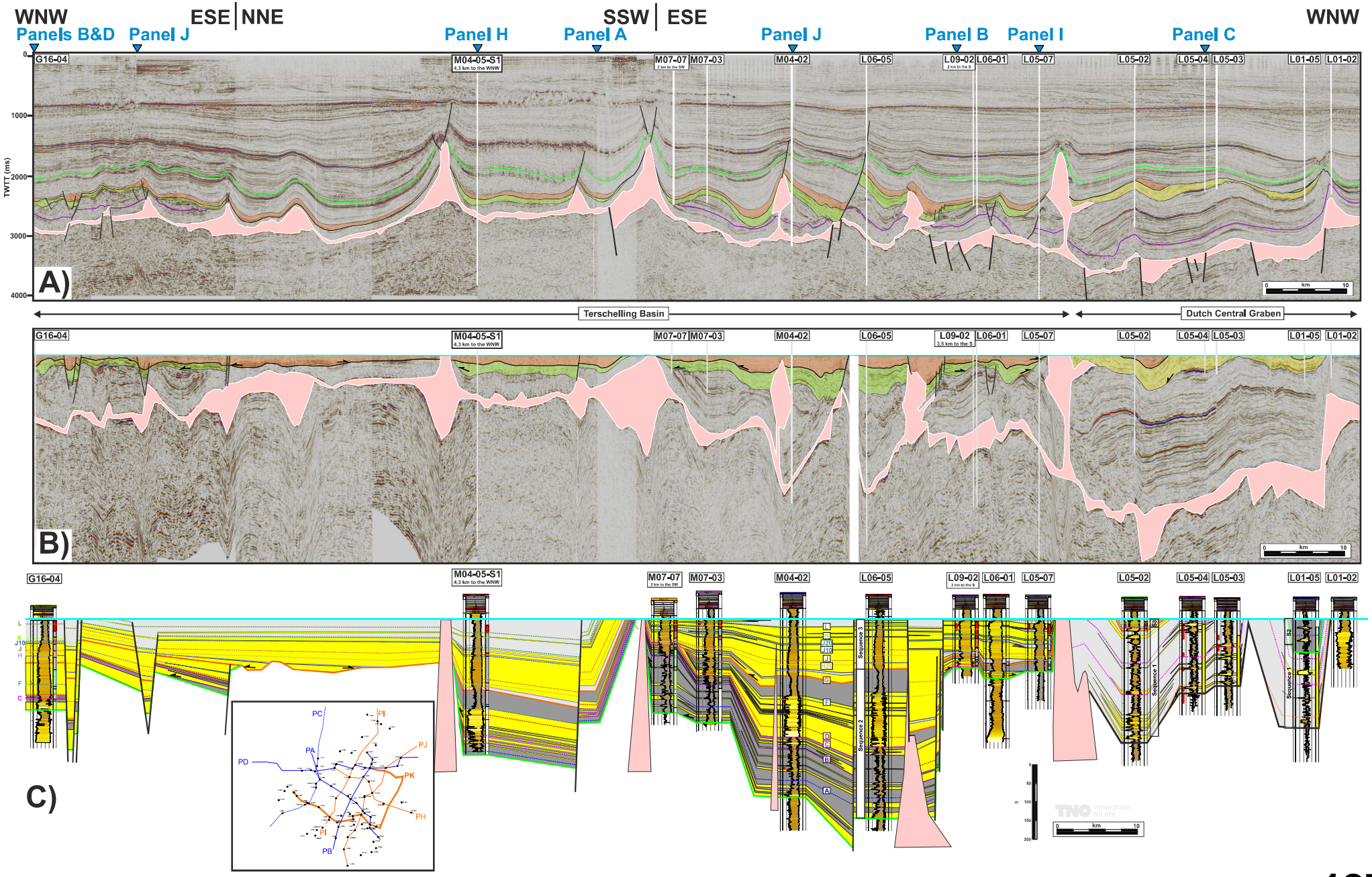

Appendix A3 - Regional Panels from Focus Project

Seven regional panels that include interpreted seismic sections, flatten seismic section and corresponding stratigraphic correlation have been constructed for the Focus Project. Each seismic section and its corresponding well correlation panels where analyzed at the same time, by the same interpreter (Fig. A4.1). This allowed for a integrated interpretations of seismic and well data. In the present report, three panels from the Focus Projects are used (A, B and D) since they cover part or all of the Terschelling basin. They are display in the following pages.

Note that Panel A has two versions (A1 and A2) with the southeastern part of the seismic panels following a different trend: 1) Panel A1, from M04-01 to the southeast toward M08-02; Panel A2 (dashed in Fig. A4.1) from M04-01 to the south toward M07-03, M07-07, M07-08 and M07-01. The location maps (Figure A4.1) shows the location of each of the regional panels presented.

Below is the list of wells that are included for each panel:

Panel A1
F17-06, F17-05, L02-05, L03-01, L03-03, L03-04, L06-02, M04-04, M04-03, M04-01,(M08-02), M07-03, M07-07 and M07-01.

Panel A2
F17-06, F17-05, L02-05, L03-01, L03-03, L03-04, L06-02, M04-04, M04-03, M04-01, M07-03, M07-07, M07-08, M07-01

Panel B
G13-02, G16-03, G16-04, G16-05, L03-04, L06-03, L09-02, L09-01

Panel C
B18-03, F03-08, F03-05-S1, F03-06, F03-03, F06-01, F08-01, F08-02, F11-01, F14-05, F14-06, F17-01, F17-06, F17-09, L02-05, L02-03, L02-FA-101, L02-06-S1, L05-04, L05-05, L04-05, L04-01

Panel D
E18-01, E18-07, F16-A-05, F16-04, F16-02, F17-04, F17-09, F17-05, F18-02, F18-01, F18-09-S1, F18-03, F18-08, G16-02, G16-04, G17-03, G17-01, G17-02

Panel E
F07-02, F11-03, F11-02, F11-01- F12-03, G10-03

Panel F
A08-01, A12-02, B13-02, B14-02, B14-01, B14-03, B18-02, B18-03, F03-07

Panel G
A12-01, A18-02-S1, F01-01, F04-02-A, F09-01

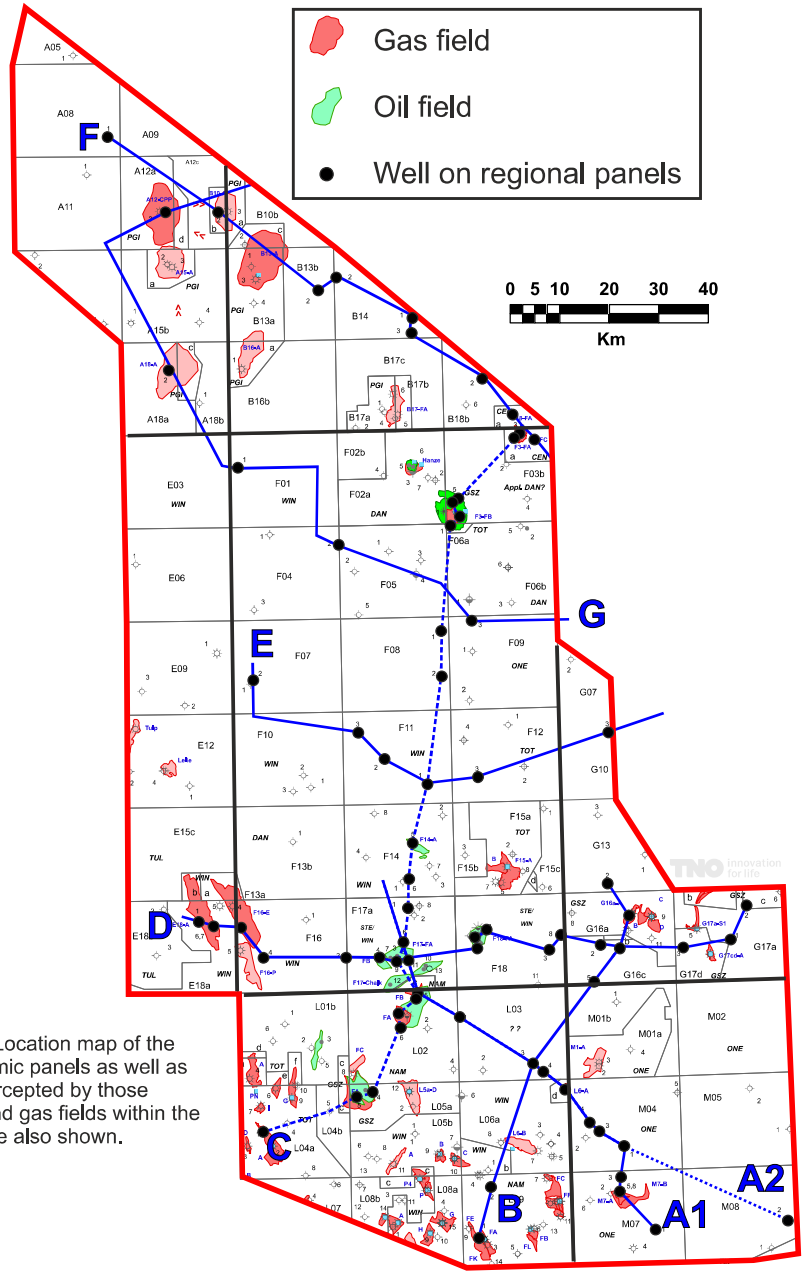

Figure A4.1: Location map of the regional seismic panels as well as the wells intercepted by those panels. Oil and gas fields within the study area are also shown.

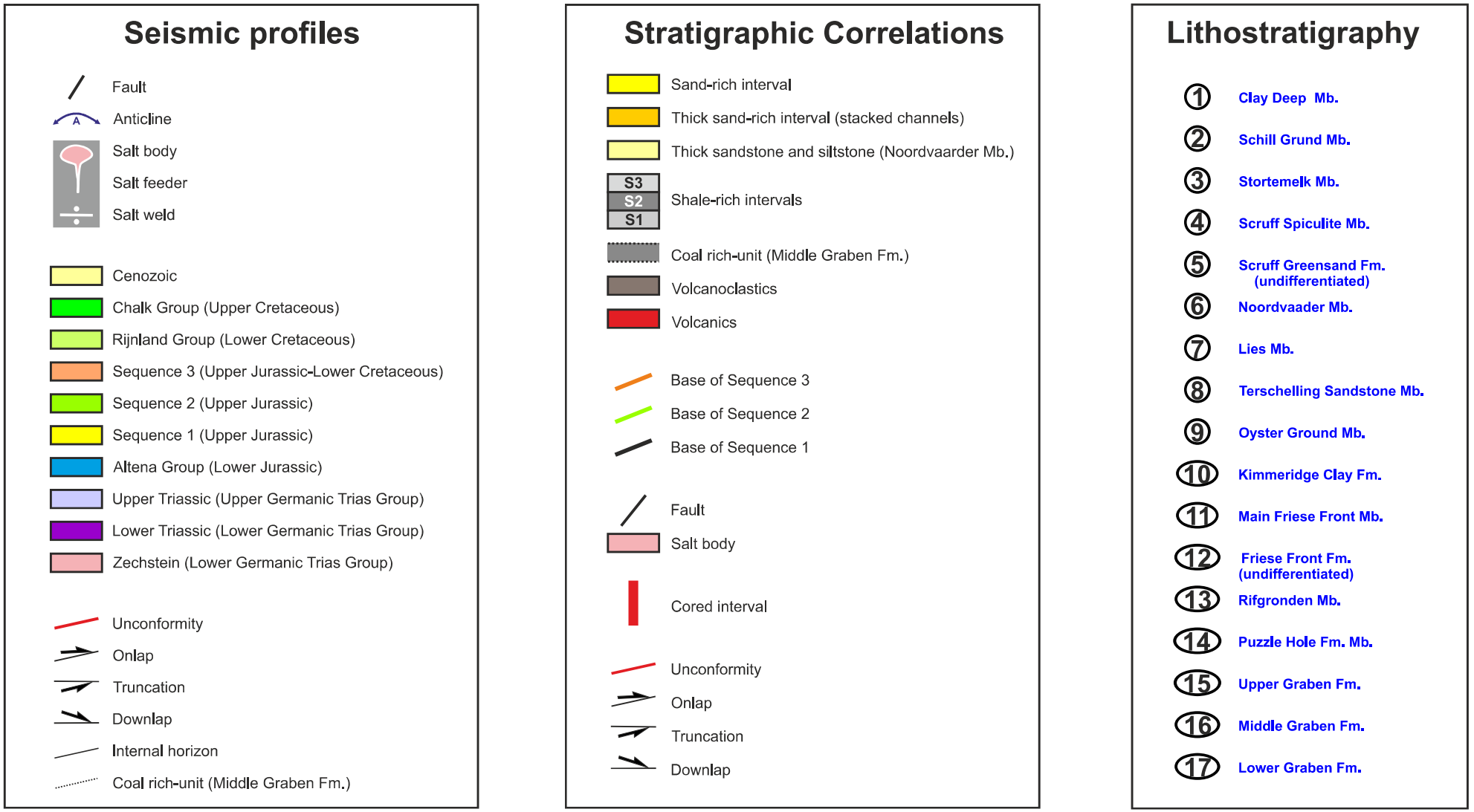

Figure A4.2: Legend for seismic and correlation panels

Appendix A3 - Regional Panels from Focus Project - Panel A1

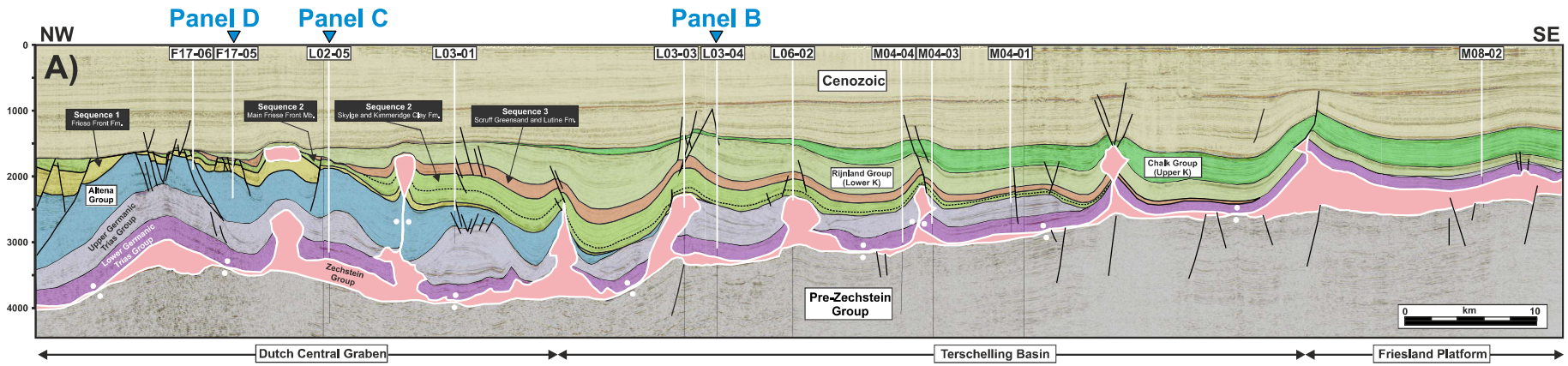

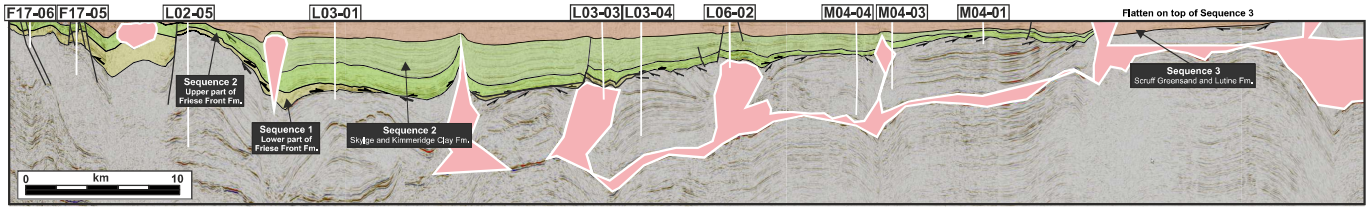

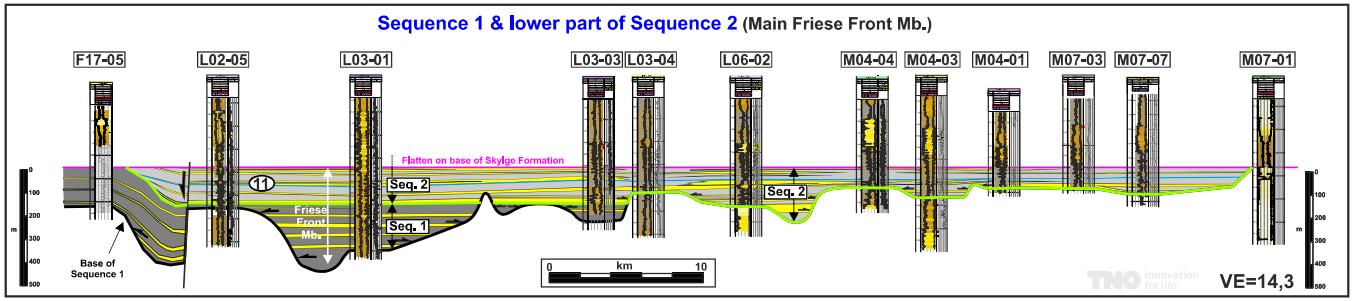

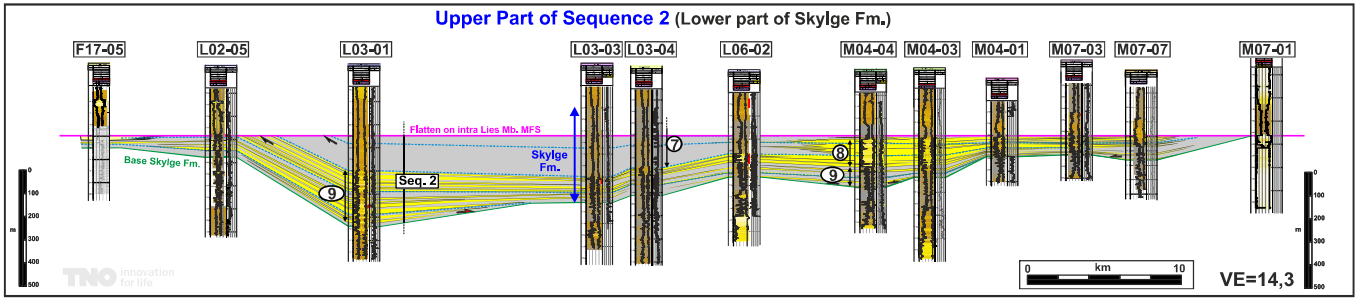

Panel A1 is located across three structural provinces, namely from SE to NW, the Friesland Platform, the Terschelling Basin and the southern part of the DCG, and is trending SE-NW. **A)** 111,5 km long interpreted seismic section that intercepts 11 wells. **B)** 87,5 km long, flattened and interpreted seismic section. The section is flattened on the Top of Sequence 3 (top of the Skylge Formation) and intercepts 10 wells. This seismic profile is the same as the one shown above but slightly shorten to the NW and SE. **C)** Well correlation section for Sequence 1 and the lower part of Sequence 2. This section is flattened on the base of Sequence 3 (Skylge Formation). This section intercepts 12 wells in total and is slightly different from the seismic section A and B in the SE part (from well M04-01) where a SSE trend is used to add wells M07-03, M07-07 and M07-01 to the section. The vertical exaggeration is 14.3. **D)** Well correlation section for the upper part of Sequence 2. This section is flattened on a well recognizable on GR and Sonic logs maximum flooding surface of the Lies Member. The vertical exaggeration is 14.3. See Fig. A4.1 for location map and Fig. A4.2 for legend.

⑦ Lies Mb.

⑧ Terschelling Sandstone Mb.

⑨ Oyster Ground Mb.

⑪ Main Friese Front Mb.

Appendix A3 - Regional Panels from Focus Project - Panel A2

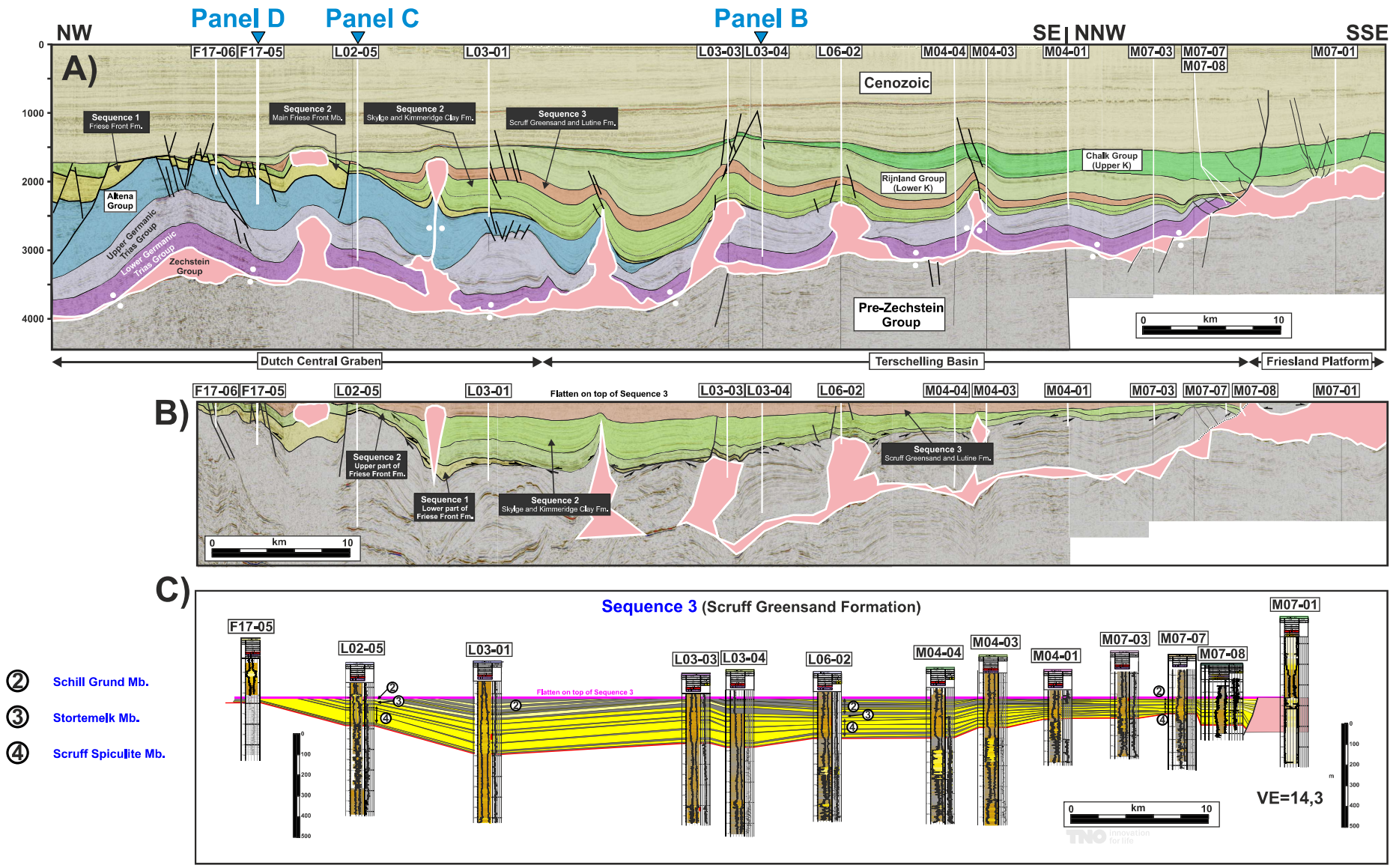

Panel A2 is trending SE-NW and is located across three structural province, namely from SE to NW, the Friesland Platform, the Terschelling Basin and the southern part of the Dutch Central Graben. It is composed of three figures. **A)** 98,4 km long interpreted seismic section that intercept 14 wells. **B)** 86,4 km long, flattened and interpreted seismic section. The section is flattened on the top of Sequence 3 (top of the Skylge Formation) and intercepts 14 wells. This seismic profile is the same as the one shown above (A) but slightly shorten to the NW. **C)** Well correlation section for Sequence 3. This section intercepts 13 wells and is flattened on the top of Sequence 3 (Skylge Formation). The vertical exaggeration is 14.3. See Fig. A4.1 for location map and Fig. A4.2 for legend.

Appendix A3 - Regional Panels from Focus Project - Panel B

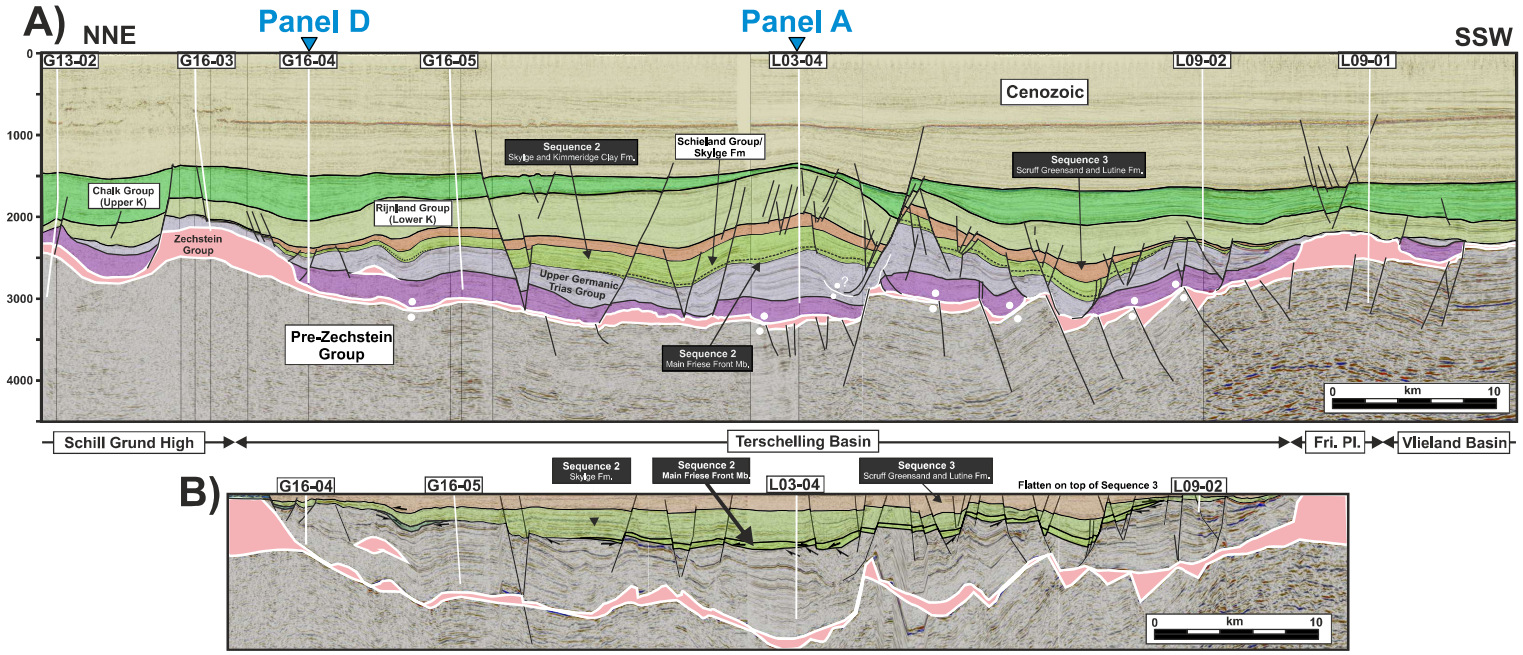

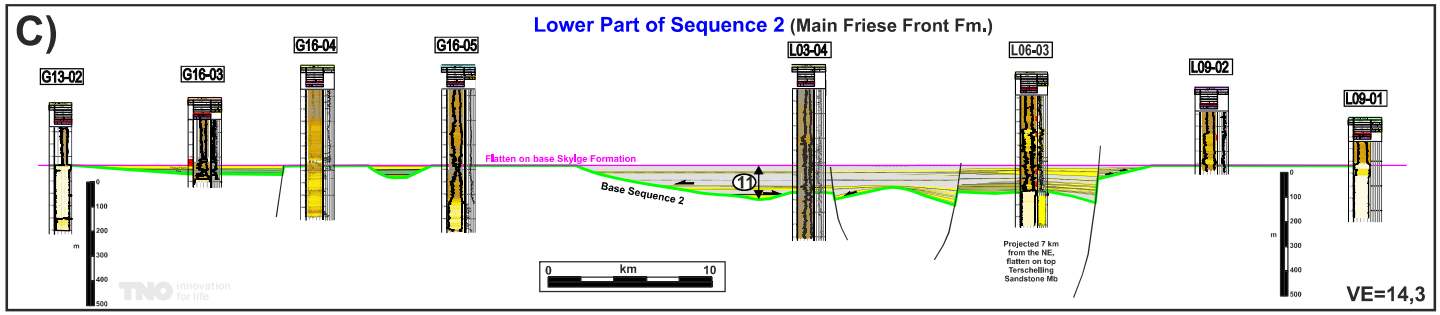

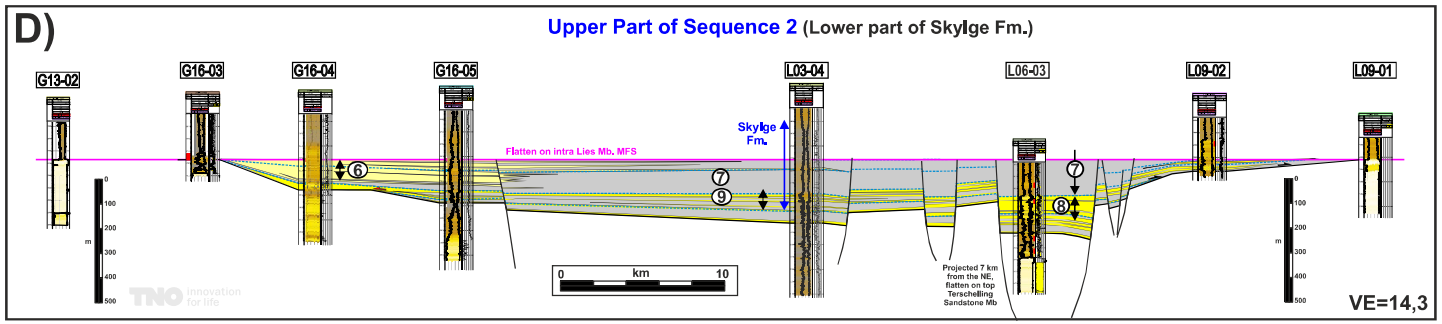

Panel B1 is located across four structural provinces, namely from north to south, the Schill Grund High, the Terschelling Basin, the Friesland Platform and the Vlieland Basin. This panel trends NNE-SSW and is composed of four figures. See Fig. A4.1 for location map and Fig. A4.2 for legend.

A) 91,5 km long interpreted seismic section that intercept 7 wells.

B) 69,5 km long, flattened and interpreted seismic section. The section is flattened on the top of Sequence 3 (top of the Skylge Formation) and intercept 4 wells. This seismic profile is the same as the one shown above (A) but slightly shorten to the NNE and SSW.

C) Well correlation section for the lower part of Sequence 2. This section is flattened on the base of Sequence 3 (base of Skyge Formation). Note that Sequence 1 is not observed in this part of the basin. This section intercepts 7 wells, with the addition of well L06-03 that is projected 7 km from the NW. The vertical exaggeration is 14.3.

D) Well correlation section for the upper part of Sequence 2. This section is flattened on a recognizable maximum flooding surface in the lower part of the Lies Member. This section intercepts the same wells as in (C). The vertical exaggeration is 14.3.

⑥ Noordvaader Mb.

⑦ Lies Mb.

⑧ Terschelling Sandstone Mb.

⑨ Oyster Ground Mb.

Appendix A3 - Regional Panels from Focus Project - Panel B

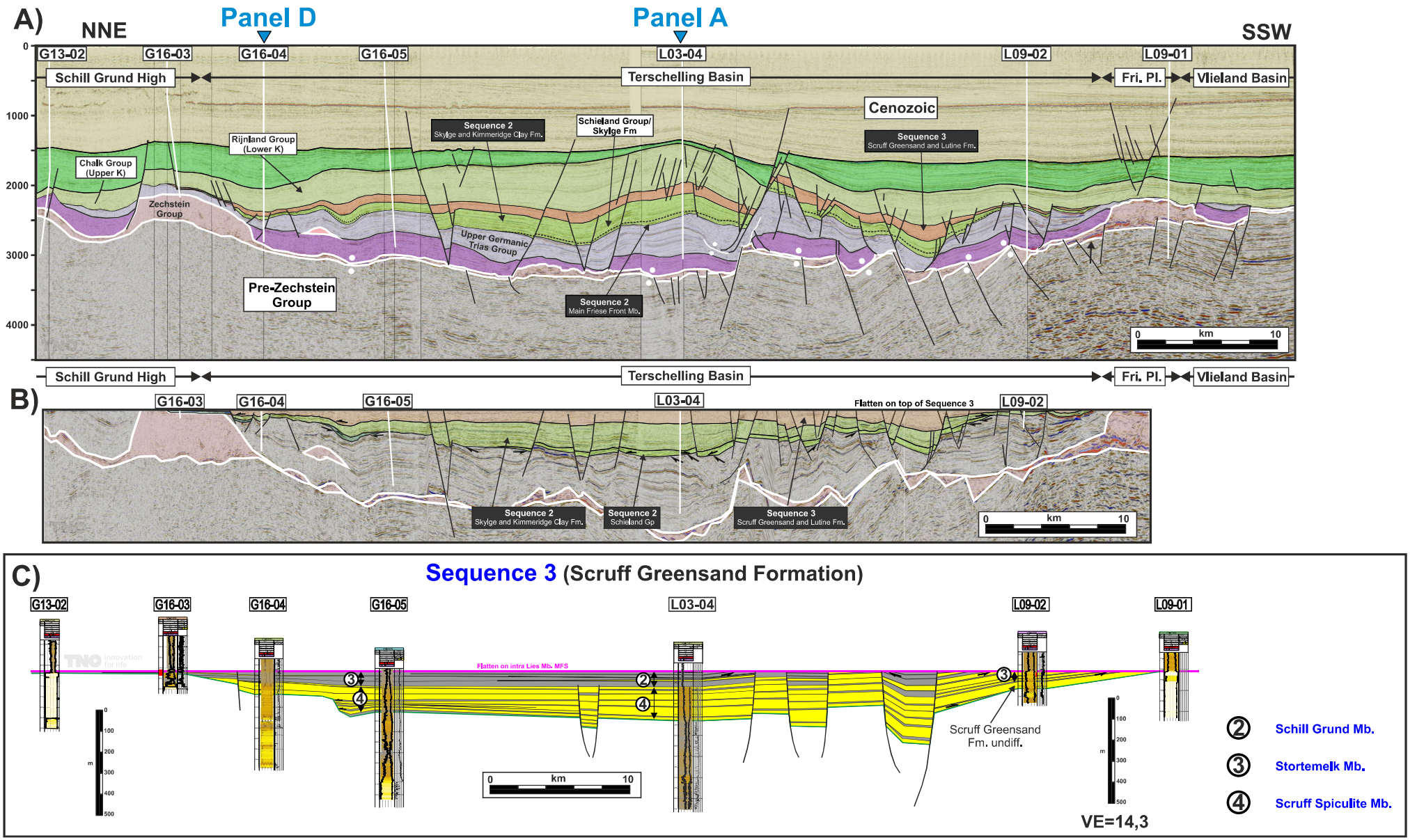

Panel B2 is located across four structural provinces, namely from north to south, the Schill Grund High, the Terschelling Basin, the Friesland Platform and the Vlieland Basin. This panel trends NNE-SSW and is composed of three figures. **A)** 91,5 km long interpreted seismic section that intercept 7 wells. **B)** 69,5 km long, flattened and interpreted seismic section. The section is flattened on the top of Sequence 3 (top of the Skylge Formation) and intercept 4 wells. This seismic profile is the same as the one shown above (A) but slightly shorten to the NNE and SSW. **C)** Well correlation section for Sequence 3. This section is flattened on the top of Sequence 3 (top of Skylge Formation). This section intercepts 7 wells. The vertical exaggeration is 14.3. See Fig. A4.1 for location map and Fig. A4.2 for legend.

Appendix A3 - Regional Panels from Focus Project - Panel D

TNO innovation for life

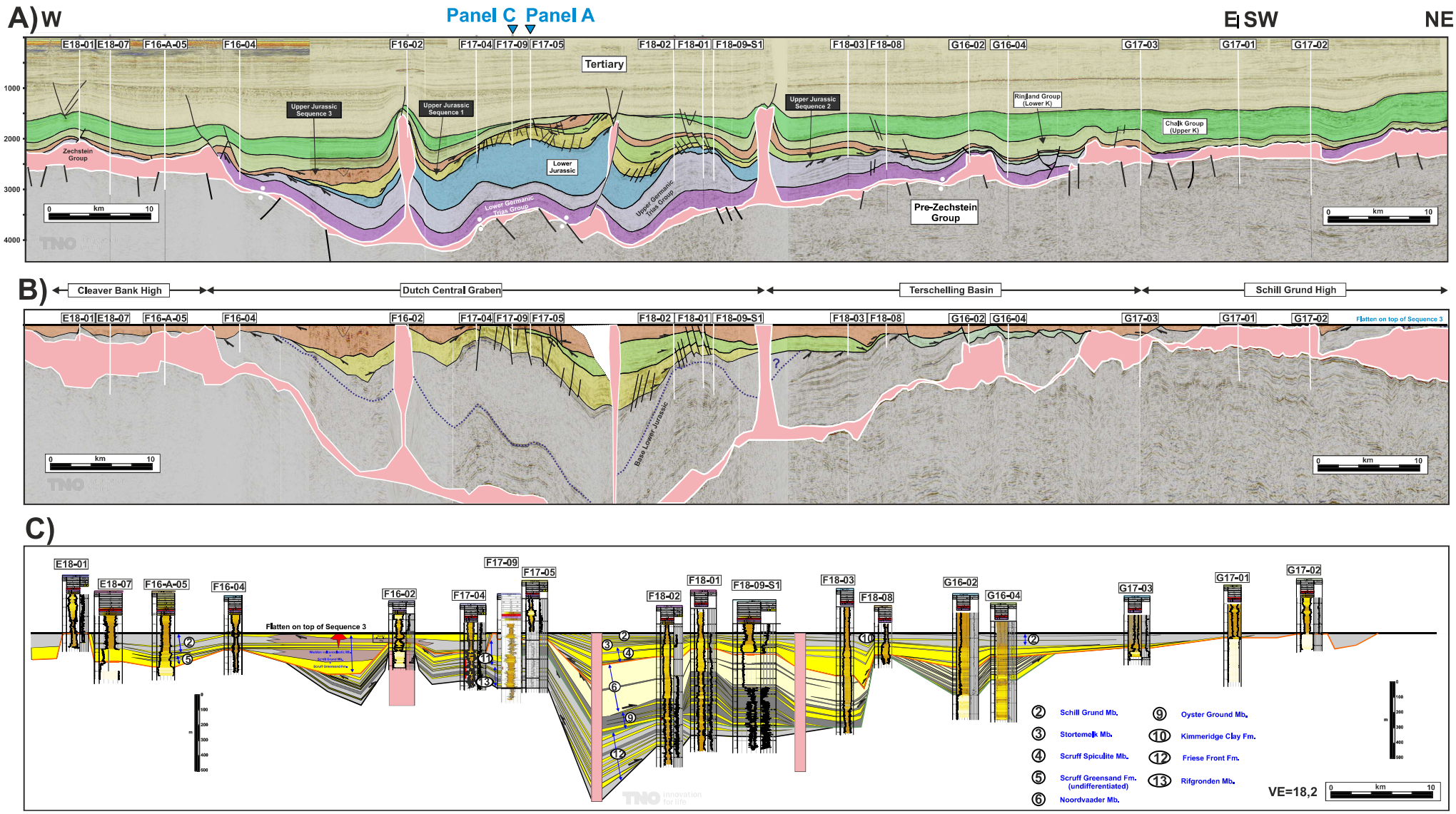

Panel D is located across four structural provinces, namely from east to west, the Cleaver Bank High, the Dutch Central Graben, the Terschelling Basin and the Schill Grund High.. This panel is trending NW-SE. This panel is composed of three figures: **A)** 144,2 km long interpreted seismic section that intercept 9 wells. **B)** 144,2 km long, flattened and interpreted seismic section. The section is flattened on the top of Sequence 3 and intercept 9 wells. This seismic profile is the same as the one shown above (A). **C)** Well correlation section for Sequences 1, 2 and 3. This section is flattened on the top of Sequence 3, intercepts 9 wells and has a vertical exaggeration of 17,7. See Fig. A4.1 for location map and Fig. A4.2 for legend.

APPENDIX A4

MSc. Report: Daniel Korosi

Tectono-stratigraphy of the northeastern margin of the Dutch Central Graben during the Late Jurassic:

Effects of paleo-topography on continental and shallow water depositional systems

Dániel Korösi
Utrecht University
TNO

MSc thesis - May 2016

Supervisors:
Dr. Renaud Bouroullec, TNO
Prof. Dimitrios Sokoutis, UU
Dr. Jeroen Smit, UU

Utrecht University

TNO innovation for life

Table of contents

Abstract

Detailed 3-D seismic analysis of the F6 block was carried out to evaluate the tectono-stratigraphic history of the margin of the Dutch Central Graben during the Late Jurassic. Isopach and attribute mapping suggests that the basin physiography, sediment accumulation and sediment transport directions were significantly controlled by active tectonics in the NE part of the Dutch Central Graben.

Ten seismic stratigraphic units are defined and enabled to study thickness distributions of intra-Upper Jurassic intervals in 3-D, which provide insights into the paleo-topographic effects on sedimentation, as well as the evolution of differential subsidence in space and time. Seismic attribute analysis was carried out and revealed several tectonically influenced geobodies that provide information about varying sediment transport directions and rate of structural control. With the aid of palynological data, sedimentation rates were estimated for each defined unit in order to constrain the overall subsidence evolution during the deposition of the Upper Jurassic growth units.

Stratigraphic thickness distributions show high variability of differential subsidence during the deposition of the Lower-, Middle-, and Upper Graben Formations. In contrast, the subsidence is occurring at a broader scale during the deposition of the Kimmeridge Clay Formation.

For the first time, several fluvial channels and small deltas have been clearly imaged using attribute mapping in the Lower Graben Formation and at the base of Middle Graben Formation. These features show east to west, transverse sediment transport direction from the basin margin to the basin axis. An extensive channel-delta system in the Upper Graben Formation suggests SE to NW sediment transport direction and fluvio-deltaic sedimentary development. A submarine channel was detected in the lower part of Kimmeridge Clay Formation, while slumps and a potential deepwater slope fans are interpreted in the upper part of the Kimmeridge Clay Formation.

Estimated sedimentation rates of the purely seismically defined intra-Upper Jurassic stratigraphic units suggest four phases of subsidence during the deposition of the Upper Jurassic units. High values during the deposition of the Lower Graben Formation and the middle Kimmeridge Clay Formation are in contrast with low values for the Middle- and Upper Graben Formations, earliest and latest Kimmeridge Clay Formation and the Scruff Greensand Formation.

Integration of seismic horizon, isopach and attribute mapping combined with sedimentation rate quantification allowed to further constrain the relation between paleo-topographic features, controlled by active structures, and depositional systems in the Dutch Central Graben and highlight the potential for detailed stratigraphic/structural analysis.

1. Introduction

Stratigraphic development of extensional rift basins has been widely studied in the past decades. Sedimentary architecture proved to serve as a good indicator of the activity of active structural elements, such as faulting, folding, salt diapirism and the coeval combination of those (Gawthorpe & Leeder, 2000, Dawers & Underhill, 2000).

Models have been developed for the evolution and deformation of syn-tectonic growth strata architecture related to salt diapirism, based on field studies (Rowan & Weimer 1998, Giles & Lawton 2002), subsurface data (Hearon *et al.* 2014), analogue (Vendeville & Jackson 1992) or numerical modeling (Poliakov *et al*. 1993). Previous work suggests that salt diapirism exerts a major control on the evolving growth strata. In terms of the external shape of growth sequences, the main relationship appears to be between the rate of salt rise and the rate of sedimentation (Hearon *et al.* 2014). Models suggest that sedimentation influences salt diapirism as well, moreover, differential loading exerts the major control on salt diapirism (Poliakov *et al.* 1993, Hudec & Jackson, 2007, Rowan et al. 2012)). However, others suggest that the main initiating and controlling mechanism of salt diapirism is active tectonics, (e.g. Brun & Fort, 2011). Fault patterns can define the preferential location of salt diapirism, which can be organized as elongated salt walls following prominent fault trends, as it can be observed in the Central Graben in the North Sea (van Wijhe 1986).

Deep-water depositional environments in salt-controlled basins have been studied in detail (Posamentier, 2003; Kolla 2007). These publications describe tectonically controlled or influenced submarine channels, turbidite development and mass flow deposits in deepwater settings. However, studies focusing on shallow water settings are scarce (Aschoff & Giles, 2005, Mannie *et al.* 2014). Fluvial sedimentary environments adjacent to and influenced by salt diapirism were studied in detail by few authors e.g. Banham and Mountney (2003), Andrie *et al.* (2012) based on outcrop work and provide models for fluvial channel development in periods of differing accommodation/sedimentation ratios.

In the present study, the evolution of the basin margin and the paleo-topography are attempted to reconstruct in the northern part of the Dutch Central Graben which was an active salt-controlled rift basin during the Late-Jurassic (De Jager 2007). This is done by putting constraints on the rate of subsidence, differential subsidence and sedimentary development and the relation of these with active extension and salt diapirism. Seismic stratigraphic division of the Upper Jurassic is carried out to reveal stratigraphic external forms i.e. thickness variations of intra-Upper Jurassic units. Three-dimensional interpretation of several tectono-stratigraphic units and their thickness distributions allow to define paleolows and highs (corresponding to paleothicks) and spatial and temporal variations in sediment accumulation that are likely controlled by active tectonics in the extensional basin. Possible lateral lithological variations and the detection of distinct depositional features potentially controlled by active tectonics are interpreted with the help of attribute analysis of several selected horizons. The continental to shallow marine succession reveals distinct geobodies such as fluvial or submarine channels and mass transport deposits, which are influenced, triggered or diverted by active tectonics.

Sedimentation rates are estimated for each stratigraphic unit defined with the aid of absolute geologic ages from playnological data, and used to define relative changes in basin

subsidence between the different units, and so, to come up with an approximate qualitative subsidence rate evolution of the NE part of the Dutch Central Graben.

Integration of seismic, seismic attribute, well-log data together with sedimentation rates allowed to constrain the paleo-topographic evolution of the NE-basin margin area in the salt controlled Dutch Central Graben.

2. Geological setting

2. 1. Regional geological evolution

The evolution of the Dutch Central Graben, as part of the Southern North Sea Basin dates back to the period of the assembly of Pangea. In its final phase the Southern North Sea Basin is characterized by the Variscan orogenesis, which was completed in the Late Carboniferous-Early Permian. Post-orogenic magmatism induced thermal uplift of the region resulting in widespread exposure and erosion (De Jager, 2007).

In the **Permian**, the cease of the thermal uplift triggered subsidence in the so-called Southern-Permian Basin (SPB) and resulted in the deposition of the Rotliegend Group clastic sediments, which originate from the erosion of the Variscan Mountain Belts. The SPB was an east-west trending basin extending from today's North-West Europe to North-Poland. Continuing subsidence during the Permian created a widespread depression under arid conditions with no obvious connection to the sea, which triggered the deposition of evaporates of the Zechstein Group. In the following basin evolution stages, halokinesis of the Zechstein salt played a major role in the subsequent evolution of the basin.

The break-up of Pangea initiated in the **Early Triassic** by rifting between Greenland and Scandinavia and represented the northern part of the Proto-Atlantic Ocean. During the Triassic and Early Jurassic, thermal subsidence occurred. In the Early Triassic, the Buntsandstein Subgroup was deposited in saline, fluvial and eolian environments, represented by fine- to coarse-grained clastics. The **Middle Triassic** is characterized by marine and evaporitic conditions with the deposition of claystones, carbonates and evaporites (Röt and Muschelkalk Formations). Based on the recognition of thickness trends, an early phase of halokinesis occurred during the Early Triassic in the form of salt pillows and swells in the Southern North Sea. Piercement of salt first occurred during the Middle Triassic with salt diapirism developing preferentially along pre-Zechstein faults that were reactivated as normal faults during the Middle Triassic (Remmelts, 1996). The **Late Triassic** is characterized by little tectonic activity accompanied by regional, slow subsidence.

In the **Early Jurassic**, an eastern arm of the Atlantic rift began to intrude southeastwards, into the North Sea Basin. As a consequence, the SPB separated into several sub-basins (Munsterman *et al.* 2012). The continuous, slow subsidence during the Early Jurassic is characterized by the deposition of fine-gained clastics of the Altena Group that comprise the source rocks of the Posidonia Shale Formation.

During the **Middle Jurassic**, thermal doming of the Mid-North-Sea uplifted the North Sea Basin resulting in erosion and non-deposition of Middle and Early Jurassic sequences. Sediments deposited and preserved only in isolated depocenters such as the Central Graben.

In the **Late Jurassic**, a new phase of rifting commenced in the North Sea rift system, triggering accelerating subsidence and deposition of Upper Jurassic sediments. In the Dutch Central Graben, this period is recorded by the Schieland and Scruff Groups. East-west extension occurred during the deposition of the entire Schieland Group, which changed to northwest-southeast during the deposition of most of the Scruff Group.

In the **Early-Cretaceous**, the Jurassic sub-basins of the Southern North Sea filled up. Coeval with subsidence in these sub-basins, such as the Dutch Central Graben, neighbouring highs were uplifted and eroded during the Early Cretaceous. Subsequent regional sea-level fall

resulted in the exposure and erosion of the Upper Jurassic sequences that is marked by the widely recognizable Early-Cretaceous Unconformity. The regional extent of the Upper Jurassic and Earliest Cretaceous can be observed in Figure 3 and 4.

In the **Late-Cretaceous** extension focused in the northern Mid Atlantic that resulted in the cease of rifting in the North Sea. For this reason, the North Sea Rift is often referred to as failed rift system, since no oceanic crust developed. Subsidence continued due to thermal relaxation that, along with global sea level rise, triggered widespread flooding of the Southern North Sea and the deposition of shallow marine carbonates of the Chalk Group.

Late-Cretaceous initiation of the Alpine orogeny by the convergence of Africa-Arabia and Eurasia plates exerted compressional stresses in the North Sea area. Alpine orogeny triggered the inversion of the North Sea Basin, which occurred in four main phases in the Late Cretaceous, Paleocene, end of Miocene, and at the end of the Oligocene (De Jager 2007).
The **Late Neogene** clastic sedimentation filled the Southern North Sea basin by the dominantly westward progradation of fluvio-deltaic sequences.

2. 2. Upper Jurassic tectono-stratigraphy

In the Dutch subsurface, the Upper Jurassic has been subdivided into three main tectono-stratigraphic sequences (Abbink *et al.* 2006) (Figure 1). The following brief description of these sequences and associated formations are based on Munsterman *et al.* (2012).

Sequence 1 is characterized by east-west extension in the Callovian-Oxfordian and earliest Kimmeridgian, affecting mainly the DCG axial zone. Sequence 1 is recorded by the deposition of the Schieland Group which is represented by the Lower-, Middle- and Upper Graben Formations and the Lower Part of the Kimmeridge Clay Formation in the DCG (Figure 1).

Lower Graben Formation consists of very fine to fine grained, well sorted sandstones, which were deposited in fluvial and deltaic/coastal plain environment. An overall coarsening upward trend can be observed, especially in the upper part of the formation (Figure 2).

The major part of Middle Graben Formation is represented by carbonaceous claystones. The base of Middle Graben Formation is marked by three extensive coal beds (Figure 2). Munsterman *et al.* (2012) propose that these sediments are deposited in lacustrine to marginal marine shallow water depositional environments. In the northern corner of the DCG, two sandstone beds are locally present, forming the Middle Graben Sandstone Member. These beds are composed of fine to medium grained sandstones with coal intercalations and have been deposited in lacustrine and deltaic environments (Munsterman *et al.* 2012).

The Upper Graben Formation consists of fine-grained carbonaceous sandstones and silty claystones. A marine barrier-island system has been proposed as depositional environment with a north to south sediment transport direction.

Sequence 2 includes the rest of the Kimmeridge Clay Formation (Figure 1) and most of the Tithonian strata, when the direction of extension changed from E-W orientation, being dominant during the deposition of Sequence 1, to SW-NE. The Kimmeridge Clay Formation is composed of silty claystones with dolomite fragments (Figure 2) and its depositional environment of Kimmeridge Clay has been interpreted as outer shelf.

Sequence 3 is characterized by continuing subsidence and the flooding of the platforms neighbouring the DCG. In this period, the greyish-green fine-grained argillaceous and calcareous sandstones of the Scruff Greensand Formation were deposited, in shallow marine shoreface to offshore setting.

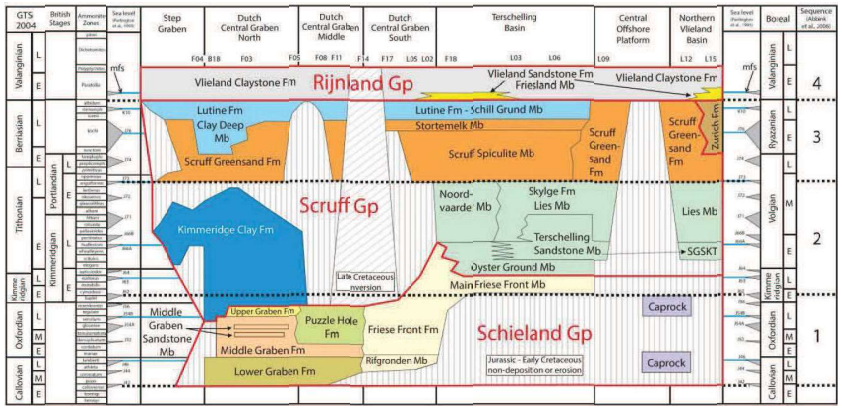

Figure 1. Lithostratigraphy of the Upper Jurassic and Lower Cretaceous in the Dutch Mesosoic basins. Note the formations present in the Northern Dutch Central Graben in the second column and the tectonic sequence boundaries in the right by Abbink *et al.* (2006). (Munsterman *et al.* 2012)

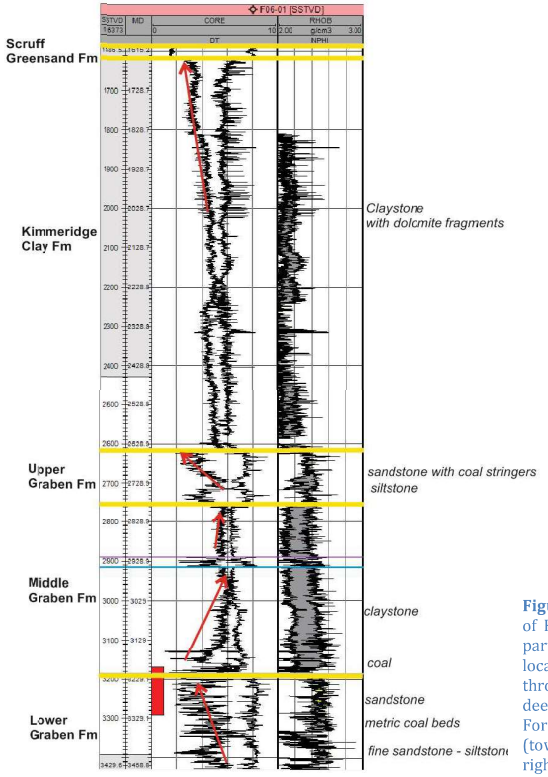

Figure 2. Gamma ray and sonic log response of F-06-1 well, located in the northwestern part of the study area, see Figures 6-7 for location. The well does not penetrate through the whole Upper Jurassic but its deepest reach lies within the Lower Graben Formation. Red arrows indicate coarsening (towards the left) and fining (towards the right) upwards grain size trends.

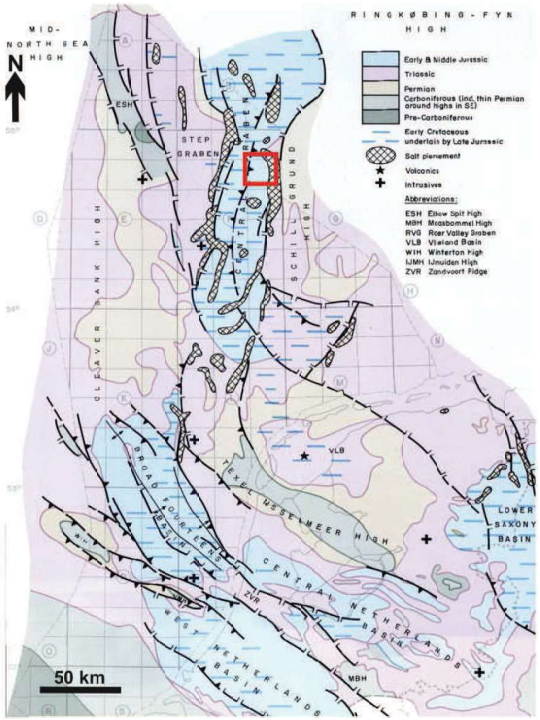

Figure 3. Basement fault trends, salt structures, and the distribution of Upper Jurassic sediments in the Dutch offshore. The salt wall, located in the east of the study area, follows the north-south trend of a major basement fault, bounding the Dutch Central Graben. The study area is marked by red. (from Van Wijhe, 1987)

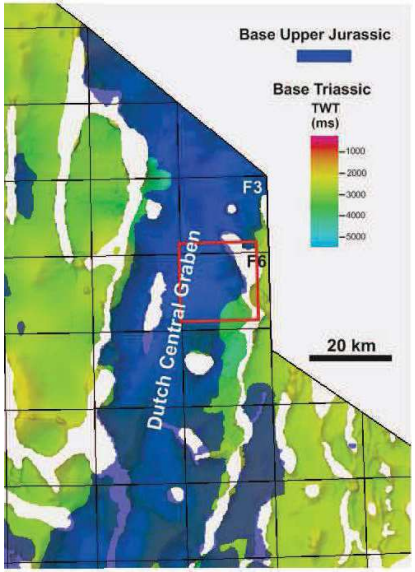

Figure 4. Regional base map displaying the Base Triassic (rainbow colours) and the distribution of Base Upper Jurassic (in blue) in the Northern Dutch Offshore. Elongated and circular white zones correspond with salt structures (see Figure 3 map). The Upper Jurassic is deposited and preserved only in extremely deeply subsided sub-basins, such as the Central Graben. The study area is marked by the red rectangle.

3. Data and methodology

3. 1. Seismic data

In this project, a three-dimensional seismic cube of pre- stack depth migrated data has been studied in detail by different seismic interpretation softwares and techniques. The seismic cube (F06_Z3PET1992F) is located at the northeastern margin of the Dutch Central Graben and covers large part of the F6 block minor part of F3 (Figure 4). It covers an area of 25 x 24 km, and 5000 milliseconds (in two-way travel time, TWT) in depth. However, quality of the data is insufficient below ~4600 milliseconds to perform detailed analysis. The survey was selected from the publicly available seismic surveys of the Dutch Offshore based on seismic quality, preservation of the Upper Jurassic and the fact that the seismic survey covers a well exposed basin margin area (northeastern margin of the DCG), including basin-bounding salt structures.

3. 2. Well Data

F06-01 is one of the few wells penetrating the Upper Jurassic succession within the study area and it is located in the northwestern part of the study area (Figure 2). The wireline log information of this well has been interpreted in terms of lithology and the depositional environments in the different tectonostratigraphic units have been established using previous work (Munsterman *et al.* 2012). Palynological data of F03-3 well were used to estimate ages for the defined unit boundaries. The ages along with thicknesses allowed to estimate sedimentation rates for each unit at the well and in different locations representing the basin axis and the basin margin.

3. 3. Seismic interpretation

Interpretation of seismic horizons was originally carried out in Petrel software (Schlumberger) using a north-south and east-west grid along selected reflectors, i.e. unit boundaries (Figure 5). Where reflector continuity allowed, autotracking method was preferred in order to capture irregularities and spatial amplitude changes of single reflectors, since they may reflect geological heterogeneities. Where reflectors ceased, or their continuity was not sufficient, manual interpretation was applied. Existing 2-D interpretation of tectonic sequence boundaries (1-2-3) crosscutting the study area were used as stratigraphic constraints.

The interpreted horizons were used to create thickness maps of the main tectono-stratigraphic units. Thickness maps were generated by 'true stratigraphic thickness' calculation for each unit. This approach measures the distance between two horizons along a line perpendicular to the upper horizon and results in isopach maps. It is in contrast with the 'true vertical thickness' calculation, where distance is measured vertically regardless of horizon dips, and resulting in isochore maps. Dipping reflectors are characteristic in the study area, so applying true stratigraphic thicknesses is essential in order to avoid the distortion of thickness trends.

It is important to note that thicknesses are measured only in time in the software, since no reasonable time-depth conversion model was available. It poses a limitation on the results, being seismic waves propagate through different lithologies with varying velocities, which may

result in distorted reflector patterns. Dipping reflectors complicate seismic wave reflection patterns and might also result in different reflector orientations.

3. 4. Stratal slicing and attribute mapping

Horizons were generated not only by the grid-interpretation but also by the so-called model-grid interpretation approach. The horizons interpreted in Petrel were used as constraints for horizon stack generation in another seismic interpretation software (PaleoScan by Eliis) through the selected seismic volume. This technique enabled extremely dense stratal slicing, even below the resolution of a single reflector. Different number of modelled horizons were tested depending on the size of the studied seismic sub-volume of interest, ranging from 80 to 250.

Since the number of horizons were not restricted to the grid interpretation, attribute mapping was carried out along numerous horizons, by applying a given attribute calculation to a whole horizon stack.

Several seismic attribute algorithms exist in different seismic interpretation softwares but all of them were designed to enhance and highlight the heterogeneities in seismic amplitude, frequency, continuity or other type of seismic signal, along given surfaces and/or vertical windows. Several attributes were tested in this study, among which Root Mean Squere (RMS), Sweetness and Frequency filtering proved to be the most useful for the aim of this research project.

The heterogeneities highlighted by attributes can be of different origin. It is the interpreter's task to differentiate potentially geology-related patterns from artifacts and noise (e. g. tuning), or seismic interpretation mis-picks. Therefore, when interpreting 3-D attribute maps, identified features were checked on 2-D cross sections as well to validate or discard the interpretation of geobodies. Although with limitations, amplitude changes can mimic lithological changes along a vertical column, as well as along reflectors and so were used to reconstruct sedimentary distribution patterns.

Frequency filtering was applied not only to check the spatial patterns of dominant frequencies along particular horizons but to create colour-blended spectral decomposition maps as well. During spectral decomposition, a horizon is filtered by three different frequency values. The proper frequencies can be selected from the frequency data curve of a horizon. The choice is not too challenging if the frequency distribution shows peak values. However, when the distribution is more gradual, a trial-and-error approach has to be also applied to find the right set of three frequencies. For each of these frequencies, the primary colours (red, green, blue) are adjusted. The integrated coloured image can thus well visualize the spatial distribution, overlap, or lack of the selected frequencies and potentially highlight features that are not detected for example on amplitude-based attribute maps. As other attributes, spectral decomposition was applied on whole horizon stacks. The dense stratal slicing also enabled to produce movies, which in one case helped to visualise display channel avulsion and lateral migration.

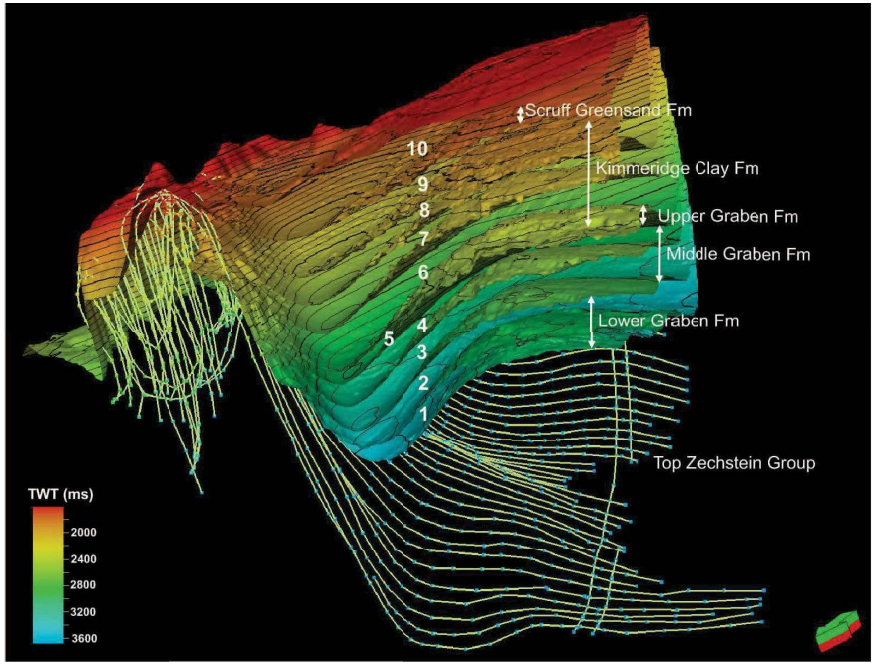

Figure 5. Three-dimensional display of the 11 interpreted horizons, which define the stratigraphic units (1-10) used in this study, along with the corresponding formations (arrows), and the Top Zechstein Group.

4. Results

With the aid of 3-D seismic data, several structural elements were identified in the study area. The basin bounding salt wall and additional salt structures were mapped. Clear fault trends were detected in the basin axis and at the basin margin as well. Horizon interpretations provided the boundaries of the newly defined tectono-stratigraphic units (Figure 5). Their external forms were studied with the help of isopach maps, while their internal characteristics were detected by tracking stratal terminations and attribute analysis. Amplitude- or frequency-related features of selected horizons are displayed in map view, which may provide additional information about lateral variations in lithology along certain stratigraphic levels.

4. 1. Structural setting and structural elements

In the following, the basic structural division of the study area i.e. basin margin and basin axis, as well as the major structural elements present in the study area are discussed. The structural elements include Zechstein salt structures, either autochthonous or allochthonous and faults located in the basin axis and the basin margin too.

4.1.1. Basin axis and basin margin

In the present project, two main zones in the study area are frequently referred within each unit, namely the basin axis and the basin margin. Zones where prominent thinning of a certain unit can be observed, is considered the basin margin. It is a zone for each unit with no exact boundary, in the rather proximity of the eastern salt wall. Basin axis is regarded as the zone where minor or no thickness change can be observed, and located west from the basin margin, further from the salt wall (Figures 11-17).

4. 1. 2. Zechstein salt and basement faults

The unique rheological characteristics of Zechstein salt, along with the load of overburden, triggered extensive salt diapirism in the Dutch Central Graben. The geometry of salt diapirs and salt walls mimic well the basement fault pattern (Figure 3). Normal faulting caused significant differences in sedimentation rate and accumulation on the two sides of the faults, being higher on the hanging wall and lower on the footwall side. Active normal faulting and extension along with the difference in sediment loading triggered the underlying Zechstein salt to move towards the thinner overburden, i.e. from the hanging wall towards to footwall. This way, the existing fault pattern facilitated the formation of continuous salt walls along basin bounding faults, preferentially along their footwall side (ten Veen *et al.* 2012; Vendeville & Jackson, 1992; Jackson & Vendeville, 1994). In the study area, the basin bounding salt wall is located in the east and oriented NNW-SSE in its present state (Figure 6).

Apart from the basin bounding salt wall, two allochthonous salt bodies (referred as S1 and S2 in the maps) with characteristic discontinuous seismic facies were detected on 3-D seismic data. They are located 2-3 km to the west of the salt wall (e.g. in Figure 6) and probably originated from the Zechstein salt. In their present state they are detached from the Zechstein feeder layer.

Basement faults were not observed in the study area, since the seismic survey does not penetrate deeper than Zechstein. Their orientation which correspond to the basin bounding salt wall, is known from earlier publications (Figure 3, Van Wijhe, 1987)

4. 1. 3. Basin axis faults

In the basin axis, different fault sets can be observed, with NNW-SSE and NNE-SSW trending faults being the most prominent (Figure 6, in red). These faults crosscut most of the Upper Jurassic (Figure 8 in red), with the exception of the Lower Graben Formation. The offset of the faults increases upwards (Figure 8 in red). These faults have a clear normal component but lateral offset of faults can also be detected. No wedge shaped stratal forms can be observed related to these faults within the Upper Jurassic, which suggests a post-depositional origin for these basin axis faults. Apart from the roughly north-south trends, a radial and concentric trend (Figure 6 in yellow and blue) can also be observed in the northwestern part of the study area. These faults are related to a turtleback structure, which plays an essential role in the structuration of the F03-FB gas field and reported in previous studies (Doornenbal & Stevenson, 2010).

4. 1. 4. Basin margin faults

Westward dipping N-S oriented faults can be followed close and roughly parallel to the basin margin in the middle part of the study area. The fault set is located between the two allochthonous salt bodies (Figure 7) and crosscuts nearly all of the stratigraphic units except Unit 10 (Figure 8 and see chapter 4.2 for unit division of this study). Although the same N-S fault trend affects most of the units, some faults themselves are not entirely continuous but show small-scale offsets vertically, i.e. are composed of small detachment faults (Figure 8). Moreover, the fault tips generally extend into younger strata towards the east. By comparing the two amplitude maps shown in Figure 6B in dotted and in Figure 7, less faults are present in the Kimmeridge Clay Formation (Figure 6A-B) than in the older Lower Graben Formation (Figure 7). Apart from the dominant N-S trend, amplitude maps locally reveal some faults running radially away from the salt bodies (Figure 6B, in orange at S1; and in Figure 7, at S2).

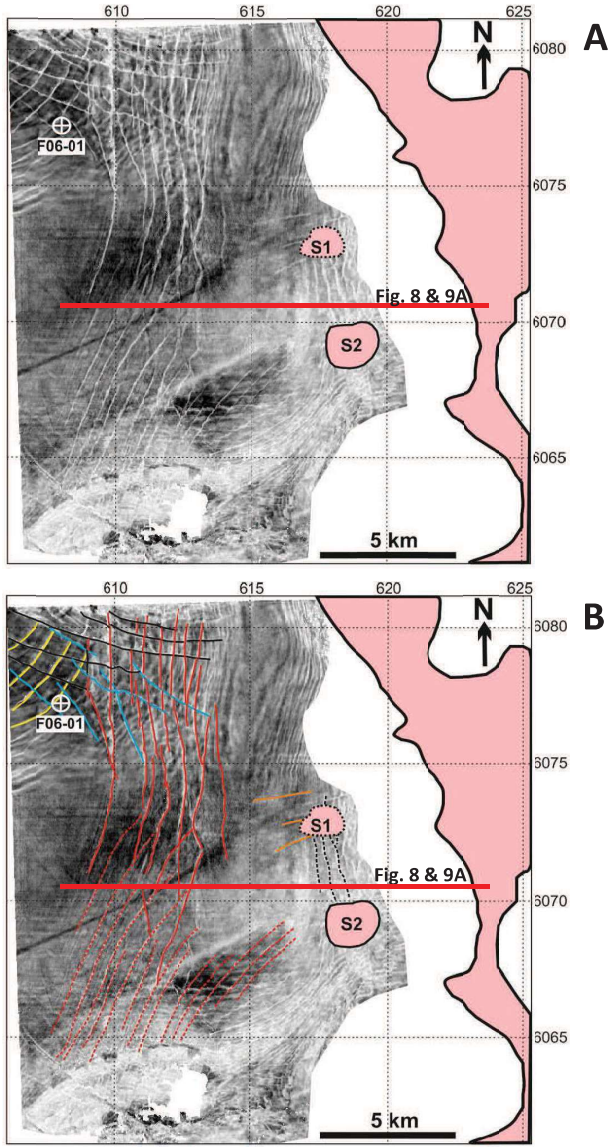

Figure 6. A, RMS amplitude map from the Kimmeridge Clay Formation (Base Unit 7) depicting fault pattern in the basin axis and at the margin between the two salt bodies. B, Interpreted fault sets marked by different colours. Note radial and concentric fault trends (blue and yellow) in the NW and roughly N-S trends in the basin axis (red).

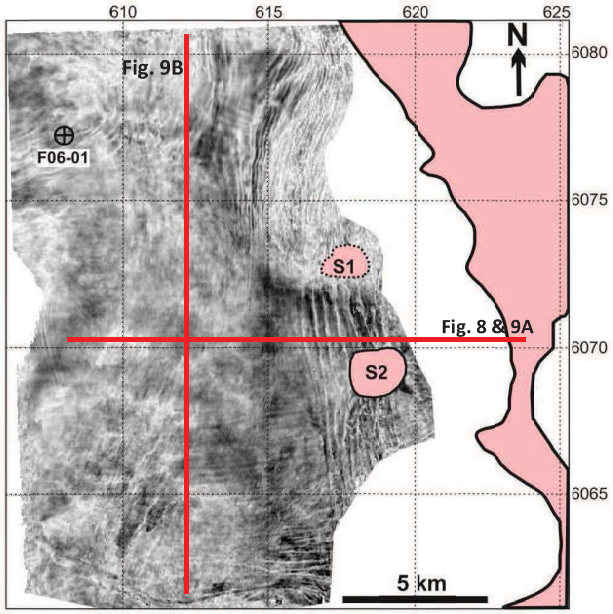

Figure 7. RMS amplitude map of intra Unit 1 horizon in the lower part of Lower Graben Formation depicting fault pattern at the basin margin in the proximity of the salt bodies. Faults are oriented N-S and radially from salt body 2. Note the higher number of faults in this map in the Lower Graben Formation and their minor occurrence in the younger Kimmeridge Clay Formation (Figure 6).

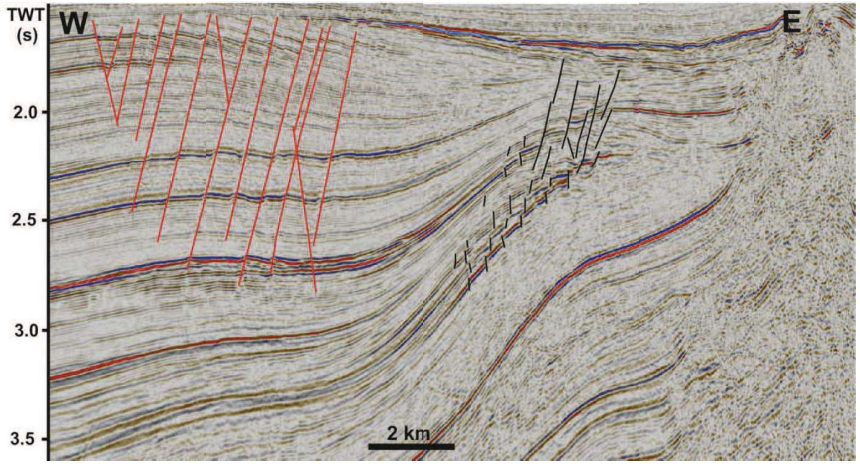

Figure 8. E-W seismic cross section with some interpreted basin axis (in red) and basin margin faults (in black) in 2-D cross section from the middle of the study area (see Figures 5-6 for location). (5x vertical exaggeration)

4. 2. Seismic stratigraphy

Three-dimensional seismic interpretation of eleven horizons in the Upper Jurassic allowed the creation of ten stratigraphic units within the Upper Jurassic. Isopach maps of these units reveal the thickness distributions of each unit. The thickness distributions define different stratigraphic external shapes, which are describe for each unit in chapter 4. 2. 2. along with prominent stratal seismic terminations observed and mapped. Isopach maps also allowed to quantify thinning that occurs characteristically towards the margin in case of most units, by calculating thinning rates for each unit in chapter 4. 2. 3.

4. 2. 1. Stratigraphic units

Ten stratigraphic units were defined based on seismic facies, stratigraphic external form, potential depositional features, and thickness distributions (Figure 9A-B). The unit boundaries take into account regional Upper Jurassic tectonic sequences 1, 2, 3 defined in earlier studies (Abbink et al. 2006, Munsterman et al. 2012) and formation boundaries. However, several intra-formational units were also identified and mapped, e.g. units 6 to 9 in the Kimmeridge Clay Fm.

The Lower Graben Formation, being the lowermost Upper Jurassic formation, is divided into Unit 1 and 2, the Middle Graben Formation is composed of Unit 3 and 4 and the Upper Graben Formation corresponds with Unit 5. The Kimmeridge Clay Formation is represented by Units 6-7-8-9. Unit 10 represents Scruff Greensand Formation, capped by the Cretaceous Unconformity (Figure 9A-B).

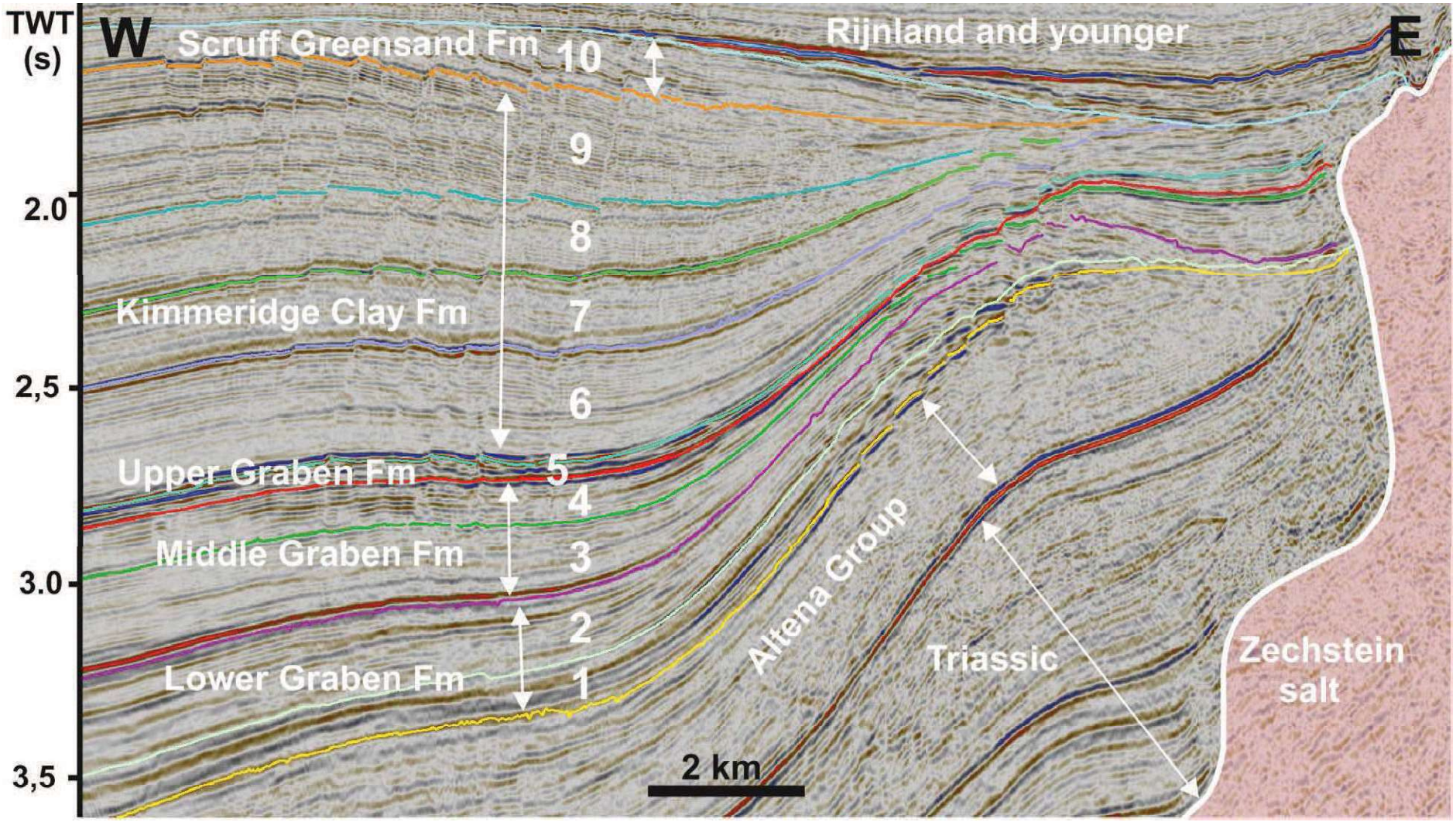

Figure 9 A. Characteristic W-E seismic cross section (5x vertical exaggeration) depicting the seismic signature of the Upper Jurassic in the Middle of the study area with stratigraphic subdivision in this study (1-10) and corresponding formations. See **Figures 6-7** for location.

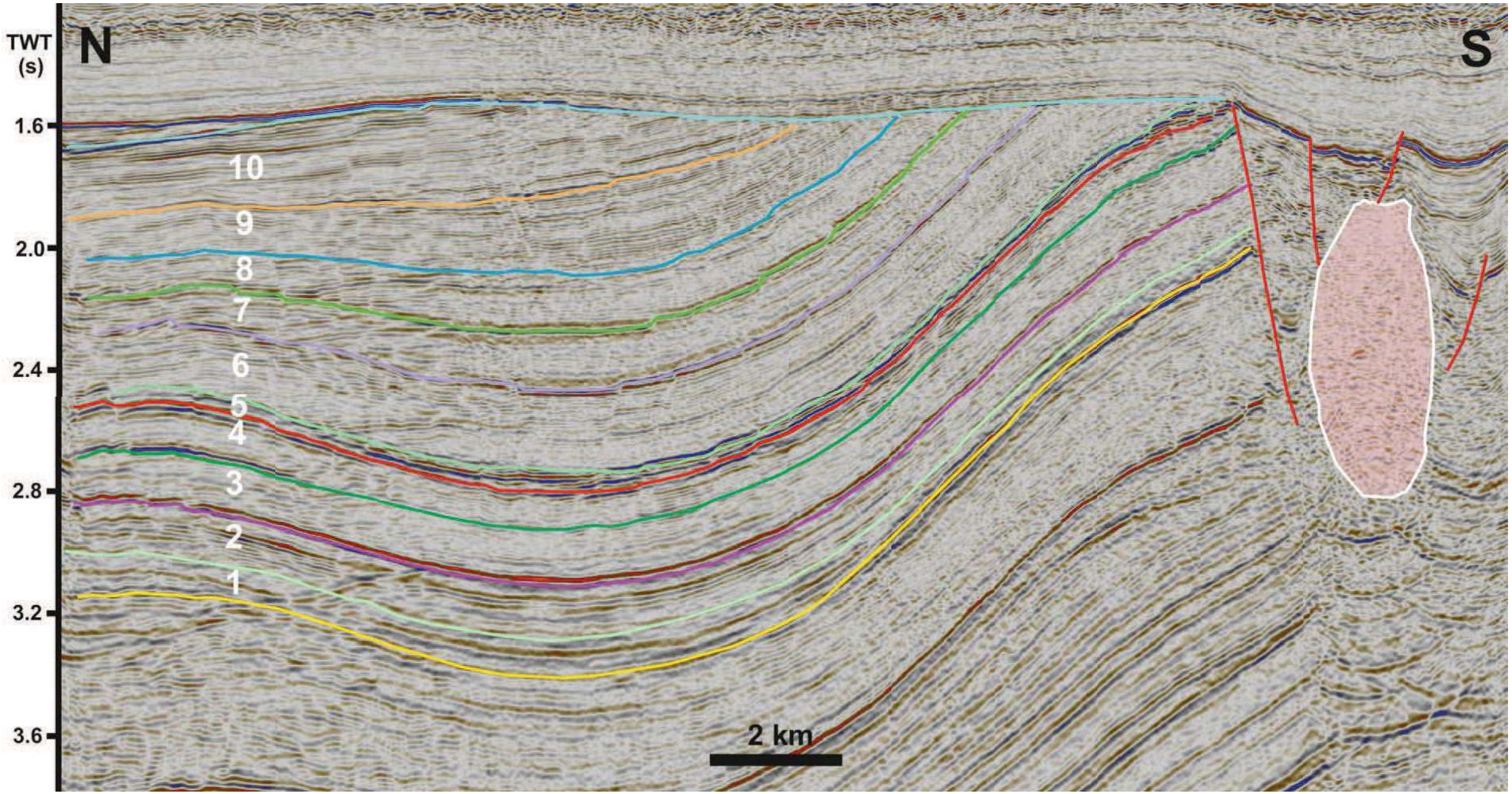

Figure 9 B. Characteristic W-E seismic cross section (5 times vertical exaggeration) depicting the seismic signature of the Upper Jurassic in the middle of the study area, with stratigraphic subdivision in this study (1-10) and corresponding formations. See **Figure 7** for location

4. 2. 2. Stratigraphic external forms and stratal seismic terminations

Thickness variations can define different stratigraphic external forms (Bouroullec et al. in press, Rowan & Weimer, 1998) with the end members of sheet, wedge, fault-related wedge, bowl and trough external forms (Figure 10). Isopach maps provide good insight into the external forms of the defined units (Figures 11-17). These external forms reveal the type of structural control that affects the stratigraphy, such as growth faults and salt withdrawal, and their characterization helps understanding the orientation and the rate of tectonic movement (e.g. faulting or three dimensional salt migration). Thickness changes can be described by introducing two terms, the thinning ratio and thinning rate. Thinning ratio represents the ratio between the maximum thickness of the unit measured in the basin axis and the minimum thickness measured at the basin margin, while thinning rate represents the ratio between the difference of the minimum and maximum thickness and the distance along which it is measured.

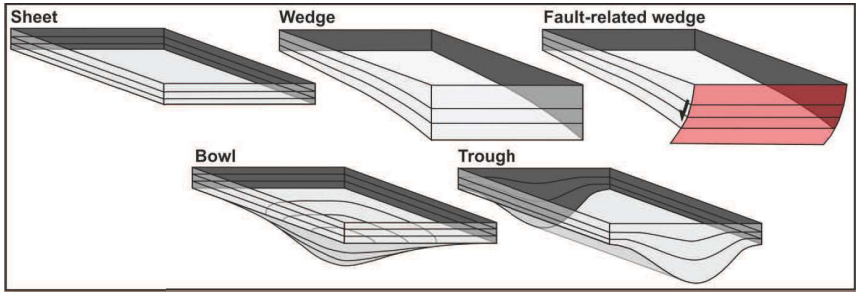

Figure 10. Stratigraphic external forms of growth packages. From Bouroullec *et al.* (in press)

In some cases seismic resolution may not enable to discriminate a single reflector thinning out from being truncated and the recognition of the exact termination points of a certain reflector can also be challenging. However, with seismic data of good quality, spatial trends of reflector terminations can be certainly extracted. Where stratal terminations correspond with high amplitude change, stratal slicing with attribute analysis also helped to reveal prominent stratal termination patterns. The edges of units are mostly characterized by stratal terminations. These were tracked in 3-D along the basin margin and plotted on corresponding isopach maps (Figures 11-17). Unit boundaries are marked by either terminations against the salt structures or terminations against younger units (lines dashed or in pink in Figures 11-17). It is important to delineate the basinward limit of boundary truncations because thicknesses beyond these limits may be affected by erosion, therefore do not represent true stratigraphic thicknesses.

Isopach maps of each unit reveal that thinning occurs multiple directions among which west to east can be considered the most dominant (Figure 10). Most units cannot be described by only one form, but different shapes can be observed within the same units. In the following, each defined unit is described in terms of stratigraphic external forms and prominent stratal terminations. The salt wall is delineated approximately at its shallowest representation with pink and pink unit boundaries refer to direct contact of the units with the salt wall. Since the salt wall is not vertical but has a rather irregular shape, its outline may vary at greater depths and so, salt wall boundary and unit boundaries marked by the contact with the salt may not correspond (see Figure 12 for example). It is important to note that the range of thickness scales vary between the units, since the defined units have highly variable thicknesses compared to each other.

Unit 1 – Lower Graben Formation (lowermost part)

Compared to the overlying units, the earliest interval of the Upper Jurassic and the Lower Graben Fm is characterized by unique thickness distributions. The most prominent thickness trend can be observed in the middle of the study area, where thickness increases radially towards salt body 2, which resulted in a bowl external form of approximately 2,5 km radius (Figure 11). To the north of the bowl, thickness decreases towards the margin to the east, although thinning occurs along a curved line which correspond to a major reflector termination. Apparent downlaps can be traced at the base of Unit 1, oriented NW-SE (Figure 18A). However, in a flattened section it can be clearly observed that these are rather onlaps, corresponding with the boundaries of the bowl shaped sub/zone of the lowermost interval of the Upper Jurassic (Figure 18B) The base reflector of the unit show abrupt termination in the north

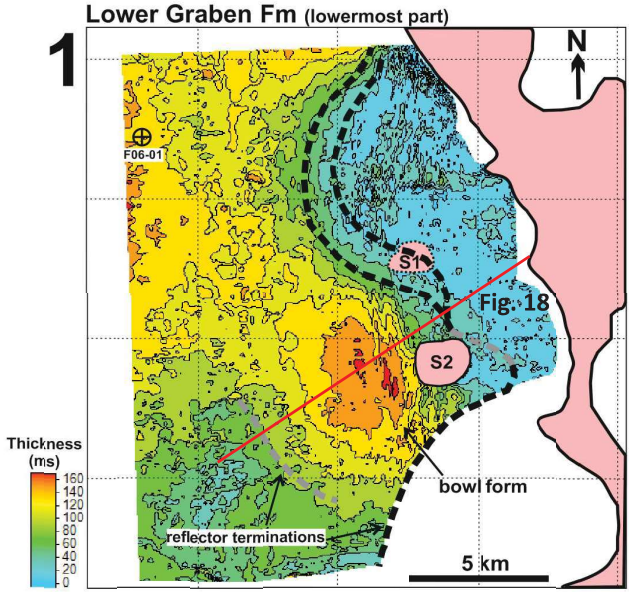

Figure 11. Isopach map of Unit 1, representing the lowest interval of the Lower graben Fm. Anomalously thick zone is described as a bowl external form west from salt body 2. Prominent reflector terminations mapped and marked by dashed lines. Pink depicts the basin bounding salt wall and allochthonous salt bodies S1 and S2. Coordinates are same as in Figure 6 and 7. See cross section (red line) in Figure 18.

Unit 2 – Lower Graben Formation (middle and upper part)

Unit 2 shows more homogenous thickness distribution along the margin than Unit 1 (Figure 12). The unit thins gradually from a maximum value of 250 in the basin axis towards the margin, curving isopach lines show differing directions of thinning. Therefore, the unit can be regarded as the eastern half of a north-south oriented trough on a large scale, or a wedge in the scale of this study. The basin axis depocenter is located in the middle of the study area (Figure 12). A remarkable sub-zone of Unit 2 can be observed between the two salt bodies, which is

thicker than the surrounding areas in the north, south and east. This zone represents close to constant thicknesses resulting in a sheet-like thickness distribution locally (Figure 12 & 19).

Its youngest interval shows laterally discontinuous terminations in the basin axis. In the north and south, the upper reflectors terminate against to overlying Unit 3 in the basin margin zone. These terminations correspond with areas of high rate of thinning in the north and south, in contrast with the sheet-like sub-zone in the middle.

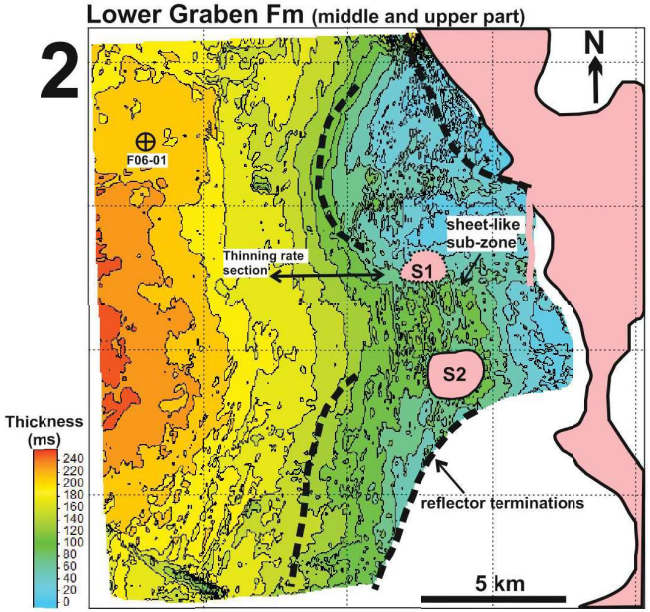

Figure 12. Isopach map of Unit 2 representing the Upper part of Lower Graben Fm. The main thickness trend is thinning towards the margin. Note very low rate of thinning between the two salt bodies that creates a sheet-like sub-zone. Prominent reflector terminations mapped and marked by dashed and dotted lines. Pink zones depict the basin bounding salt wall and allochthonous salt bodies S1 and S2, pink line refers to direct contact with salt wall.

Unit 3 – Middle Graben Formation (lower part)

Compared to Unit 2, thinning occurs more homogenously in Unit 3, trending roughly west to east across the whole study area (Figure 13). Apart from the dominant thinning trend, a thickening, wedge-shaped paleo-thick zone can also be observed within the unit, located between the basin bounding salt wall and the two salt bodies (Figure 13 and 20). This zone thickens radially from about 80 ms the northeast, reaching a maximum of 200 ms adjacent to the salt wall. Unlike in Unit 2, the basin axis depocenter is located in the SW of the study area.
The most extensive zone of stratal terminations within the entire studied stratigraphic interval can be observed along base Unit 3 The termination of reflectors moves towards the east with younging (Figure 13 and 19). The basinward extent of onlaps is marked by the termination of a high amplitude reflector at the base, which can be tracked the easiest on an RMS amplitude map as well (Figure 28).

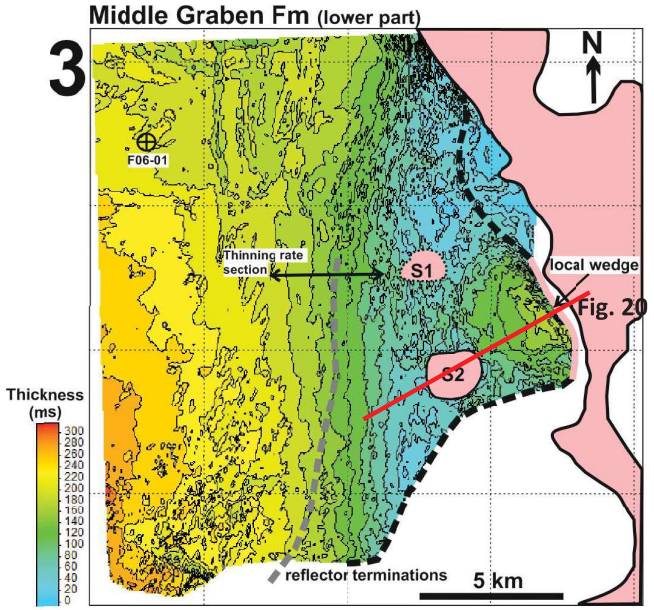

Figure 13. Isopach map of Unit 3, representing the lower part of the Middle Graben Fm. The unit thins generally from west to east. Locally thickening can be observed between the salt wall and the salt bodies creating a wedge external form. Prominent reflector terminations are marked by dashed lines.. Pink zones depict the basin bounding salt wall and allochthonous salt bodies S1 and S2, pink line refers to direct contact with salt wall. See cross section in **Figure 20.** Stratal termination marked my grey dashed line can be observed in **Figure 23** amplitude map, as well.

Unit 4 – Middle Graben Formation

Similar to Unit 3, Unit 4 is characterized by overall thinning towards the margin. However, thinning rate appears to be higher than that of Unit 3 (Table 1), and no local thickening can be observed between the salt wall and the two salt bodies. (Figure 14).

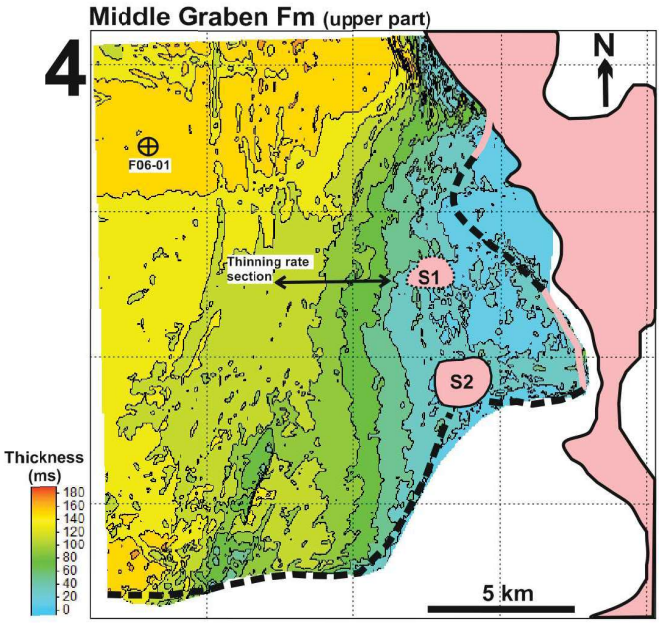

Figure 14. Isopach map of Unit 3 representing the lower part of the Middle Graben Fm. The unit thins generally from west to east. Prominent reflector terminations are marked by dashed and dotted lines. Pink zones depict the basin bounding salt wall and allochthonous salt bodies S1 and S2, pink line refers to direct contact with salt wall.

Unit 5 – Upper Graben Formation

Based on high amplitude, low frequency, discontinuous seismic facies, a thin, up to 60 ms thick interval was defined as Unit 5 in the Upper Graben Fm. The general thinning trend is characteristic in this unit too, but thickness distribution appears to be highly heterogeneous in this narrow interval (Figure 15). Thick zones tend to be organized into linear or circular shapes. The most prominent linear feature is oriented SE-NW. It terminates in a triangular shaped thicker zone in the basin axis. This linear feature has a sidetrack on its southwestern side which also terminates in a thicker area but in a rather circular shape.

Comparable to Unit 3, Unit 5 includes a local thickened zone adjacent to the salt wall , east of the salt bodies (Figure 15 and 20). The north-eastward direction of thickening creates a bowl form which differs from the north-eastward thickening wedge in Unit 3.

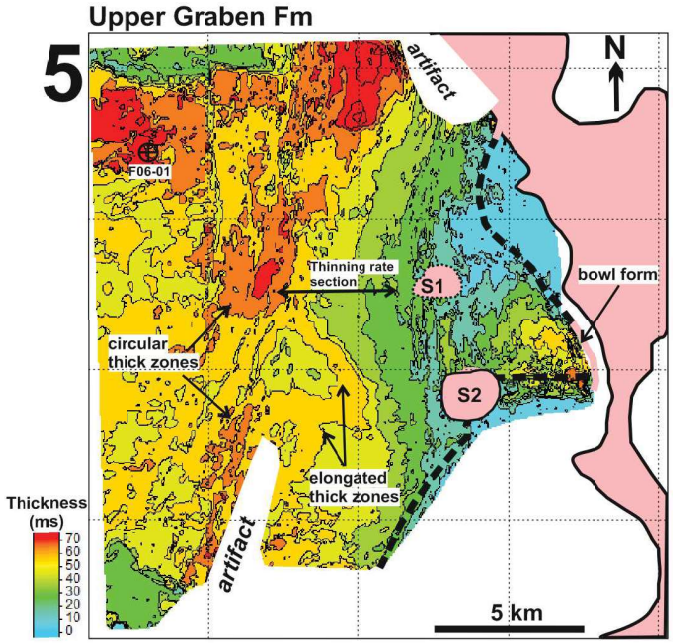

Figure 15. Isopach map of Unit 5, representing the Upper Graben Fm. Locally thickening can be observed between the salt wall and the salt bodies creating a bowl external form. Prominent reflector terminations are marked by dashed and dotted lines. Pink zones depict the basin bounding salt wall and allochthonous salt bodies S1 and S2, pink line refers to direct contact with salt wall.

Unit 6, 7, 8 and 9 – Kimmeridge Clay Formation

Units of the Kimmeridge Clay formation show similar thickness characteristics (Figure 16 A-D) therefore they are described in the same section .

Basin axis depocenters of all units defined by zones of maximum thicknesses are located in the southwestern part of the study area. In the north, thinning from the basin axis occurs to the east and west too, resulting in NE-SW oriented troughs (Figure 16 A-D). These troughs are bounded by the basin margin in the east and circular-shaped thinner areas in the west. Within the basin axis, thickness decreases towards the northeast. This decrease is more pronounced in Unit 9 than in Unit 6-7-8, which show similar SW-NE thinning trends in the basin axis.

Thinning rates along the margin show differences internally as well as between these units. In Unit 6, thinning rate is higher in the north than in the south, i.e. isopach lines are located closer to each other. (Figure 16A). In Unit 7, radial thickness decrease is more gradual in the middle than in the south and north (Figure 16B). Unit 8 shows roughly homogenous thinning rate towards the margin (Figure 16C), while Unit 9 thins more rapidly towards the south (Figure 16D), related to the southward thickening of the basin axis mentioned above.

One remarkable difference within the Kimmeridge Clay units is the presence of a local bowl adjacent to the salt wall in Unit 6 (Figure 16A and 20), which is not observed in the other units.

The defined intra-Kimmeridge units are getting less preserved and their southern boundaries move towards the north with younging (Figure 16A-D and Figure 9B).

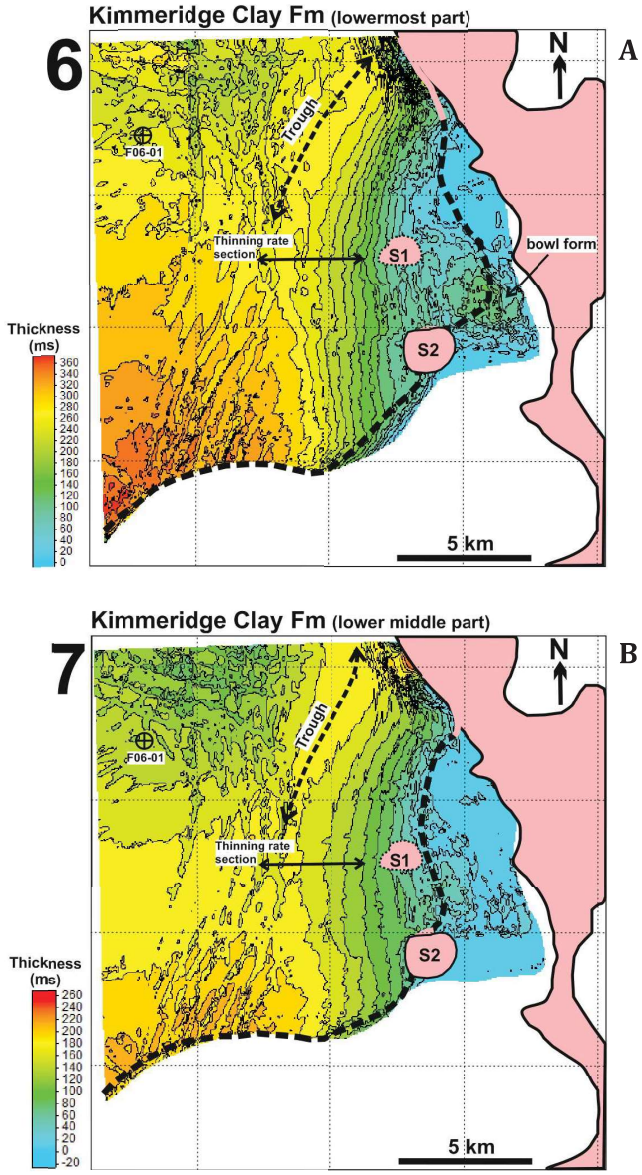

Figure 16 A-D. Isopach maps of Units 6-9, representing the Kimmeridge Clay Fm, and showing similar thickness distributions. Apart from the W-E thinning at the margin zone, radial thinning can be observed in the northwest that creates a NE-SW oriented trough in the north in case of each unit. In Unit 6, a local bowl form can be observed in the east adjacent to the salt wall, similar as of Unit 5.

Unit 10 – Scruff Greensand Formation

The Scruff Greensand Fm is highly affected by erosion (see cross sections Figure 9A-B) and restricted only in the northern half of the study area (Figure 17). Its depocenter is located in the middle in the north and creates an apparent bowl shape. The thickest zone is however bordered by prominent reflector terminations. Similar to the Kimmeridge Clay units, the northwestern zone is characterized by radial thinning.

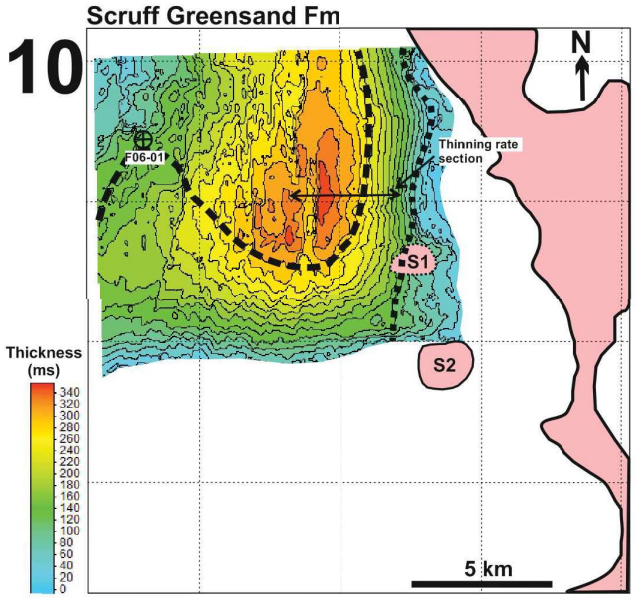

Figure 17. Isopach maps of Unit 10, representing the Scruff Greensand Fm. Prominent reflector terminations are marked by dashed and dotted lines. Pink zones depict the basin bounding salt wall and allochthonous salt bodies S1 and S2, pink line refers to direct contact with salt wall.

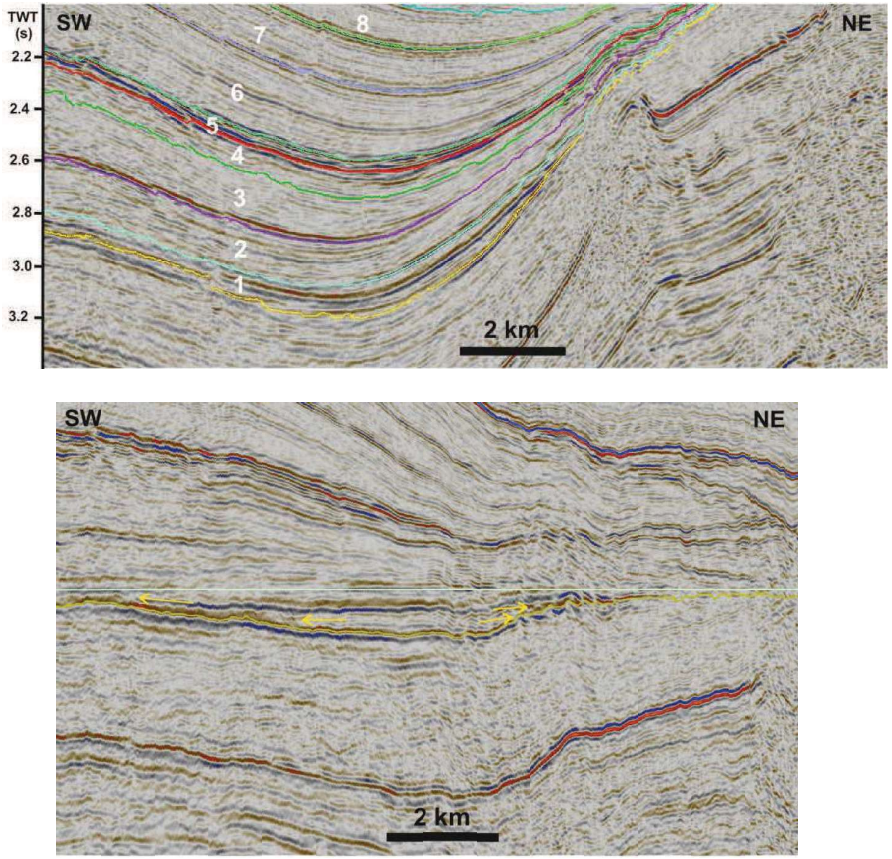

Figure 18 A, SW-NE section depicting the bowl shape of Unit 1**. B,** Flattened cross section on Base Unit 2, highlighting the bowl shape of Unit 1 and prominent reflector onlaps. For location see Figure 11.

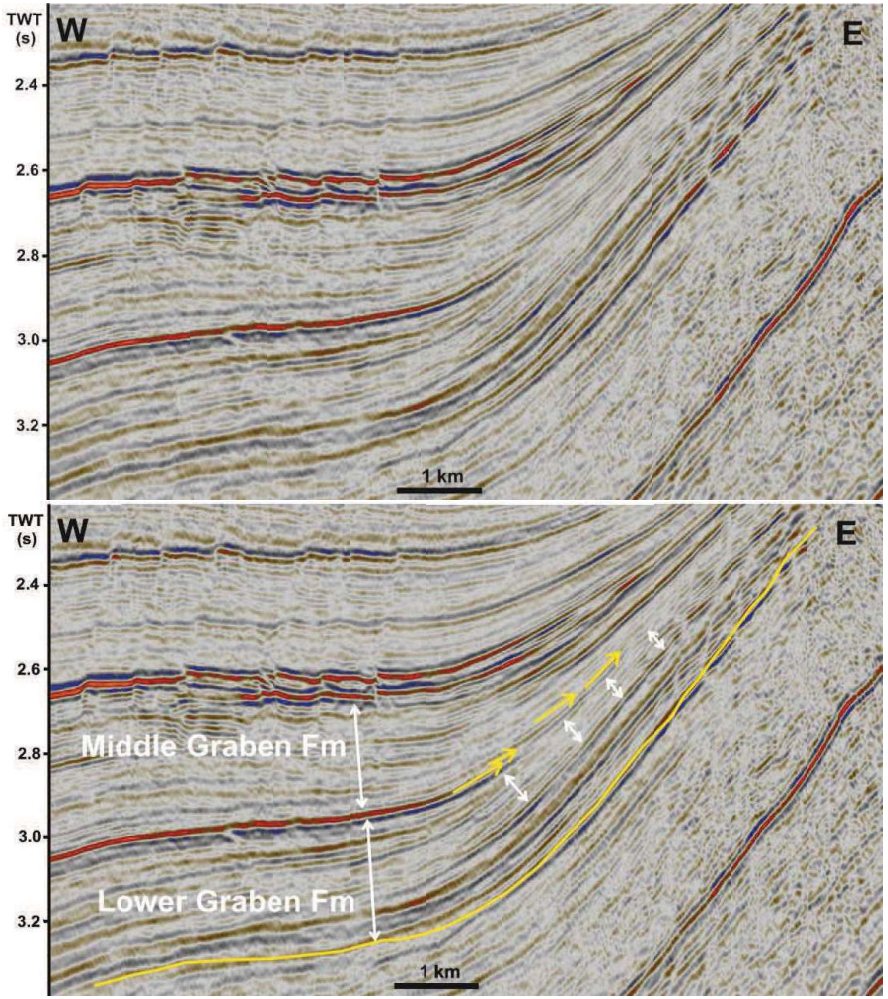

Figure 19. Terminating reflectors in Unit 2, 3 and 4, in the Middle Graben, and Lower Graben formations in the middle part of the study area. Note low rate of thinning in Unit 2, upper part of Lower Graben Formation. (white arrows)

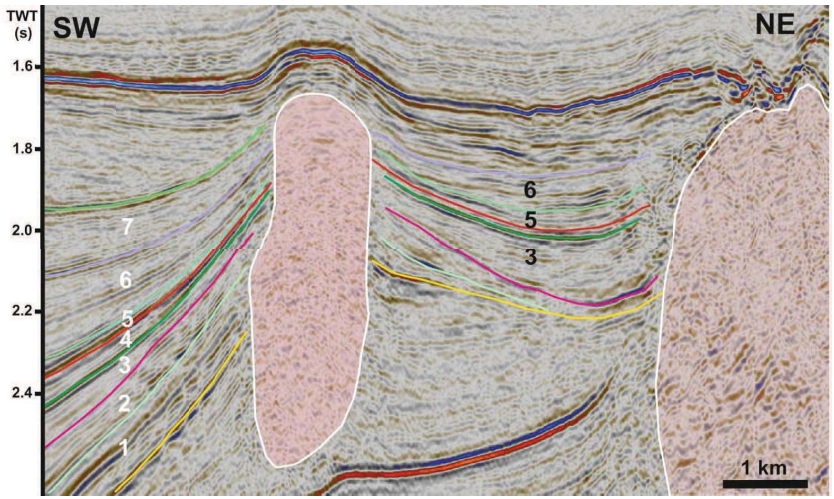

Figure 20. Cross section highlightingthe wedge exterenal form of Unit 3 and local thickening trends in units 5 and 6. See location in Figure 13.

4. 2. 3. Thinning rates between the basin margin and basin axis

With the aid of thickness maps, rates of thinning were estimated for each unit, which were measured along the same W-E line from the middle of the area (see Figures 11-17 for location), being characteristic for the units. The only exception is Unit 10 which is not well preserved in the middle, so its section of measurement was shifted to the northern part. Being the unique thickness distribution of Unit 1, Unit 2 and 1 has been merged in this estimation. Maximum thinning rates can be observed in case of Unit 1+2 (Lower Graben Formation) and Unit 10 (Scruff Greensand). In this simple calculation, thinning rate equals the thickness in the axis divided by the thickness at the margin, and it is therefore dimensionless. Thickness values (in milliseconds TWT) in the axis and at the margin and the calculated thinning rates can be observed in Table 1 per stratigraphic unit. Highest thinning rates can be observed in Unit 1-2 (Lower Graben Formation) Unit 5 (Upper Graben Formation, and Unit 10 (Scruff Greensand Fm), while Kimmeridge Clay units (Unit 6-9) show low thinning rate.

Unit #	Thickness axis (ms)	Thickness margin (ms)	Thinning rate
10	310	90	**3,44**
9	285	150	**1,90**
8	180	100	**1,80**
7	195	115	**1,70**
6	275	130	**2,12**
5	63	26	**2,42**
4	105	40	**2,63**
3	195	90	**2,17**
1 + 2	300	100	**3,00**

Table 1. Thickness values in the basin axis and at the basin margin with the calculated thinning rates per stratigraphic unit. See location used for the calculation in Figures 11-17.

4. 2. 4. Seismic attribute maps

Beyond highlighting stratal termination patterns along particular stratigraphic levels, attribute maps revealed several other amplitude and/or frequency related patterns that are potentially of geological origin. Well-defined linear, elongated, radial, or triangular features were detected along several horizons within the Upper Jurassic originating from seismic amplitude and/or frequency anomalies.

Linear patterns

The lowest stratigraphic level with linear amplitude patterns is located in the middle of Lower Graben Fm (Unit 2), in the northern part of the study area (Figure 21). The linear elements are represented by lower seismic amplitudes than their surroundings. At its southern termination, it seems to show multiple bends and from the east and west, additional linear elements are connected to the main feature (Figure 21). In cross section (Figure 22), it can be clearly observed that the anomalously low amplitude is caused by the disruption of a positive (red) reflector.

The second stratigraphic level with linear amplitude zones correspond to the base of the Middle Graben Formation, at the boundary of Units 2 and 3 (Figure 23). An approximately 600 m wide zone can be observed in the northern area. Starting from the east it can be traced going perpendicular to the margin, then suddenly turning to the north along the basin margin. In the basin it shows a large bend of 1 km radius, then terminates abruptly (Figure 23). At the margin, it can be traced just until the location of salt body 1. Cross-sections at different locations (Figure 24 & 25) show significantly different seismic character of the same element. IN a W-E cross section (Figure 24) it is represented by a depression of about 20 milliseconds in the east, while in the western side it is hardly or not even recognizable in 2-D. North-south cross section of the feature (Figure 25) at the margin shows again totally different seismic signature, being a flat high amplitude zone, with slightly elevated flanks on the sides.

The third main level of remarkable linear features is best highlighted by spectral decomposition from the Upper Graben Formation (Unit 5) (Figure 26-27). Generally SE-NW oriented linear features can be observed, which terminate in well-defined triangular or circular zones in the basin axis (Figure 27). When comparing the spectral decomposition map with the thickness map of 5, key features strikingly correspond. The linear elements, as well as the triangular and circular shapes can be observed in both maps at the same locations (Figure 27). Below this level but still within 5, other levels show linear elements in spectral decomposition maps. These have similar overall orientation, either SE-NW, or NE-SW, but are much narrower than the linear features of the upper level (Figure 26-27).

In the lower part of Kimmeridge Clay Formation (Unit 6), a prominent high amplitude zone is revealed on amplitude maps, oriented WSW-ENE in the southern section of the unit (Figure 28).

Other amplitude patterns

At the base of the Upper Jurassic two prominent high amplitude zones can be observed (Figure 29). A circular high amplitude area is located in the south and an elongated high amplitude zone in the east along the margin. The eastern end of the elongated zone is marked by the termination of the high amplitude reflector against younger units.

Only two reflectors above the base Lower Graben, at the boundary between Unit 1 and 2, a distinct zone of discontinuous seismic facies can be observed (Figure 30), and tracked in 3-D. It is located close to the margin and bounded by continuous, low frequency reflectors. The width of the zone increases towards the basin, reaching a maximum of 1km (Figure 30 and 41. 1).

At the base of Unit 2, within Lower Graben Formation, high amplitudes are organized into a prominent radial shaped zone in the middle of the study area (Figure 31). Similar patterns with smaller size were detected at the top (Figure 32) and the base (Figure 33) of Unit 4, Middle Graben Formation (Figure 17).

Seismic facies of Unit 8 and 9 in the Kimmeridge Clay is discontinuous in the vicinity of salt body 2. (see Figure 24.8 and 24.9 for map view) Enclosed in this zone, a high amplitude feature was detected in 2-D, which can be traced on RMS amplitude map as well (Figure 34).

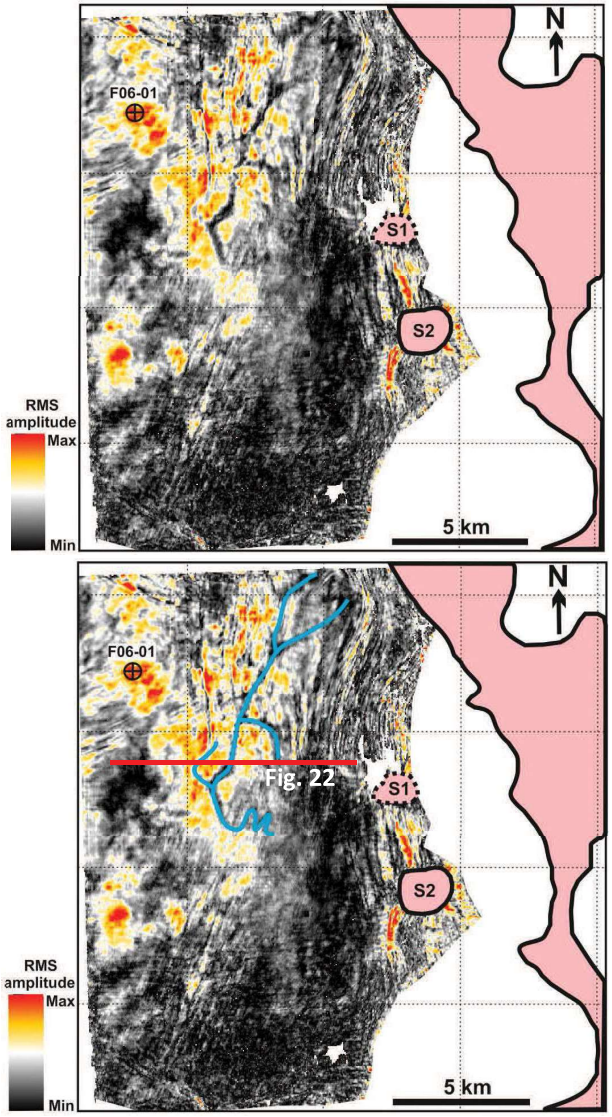

Figure 21. RMS amplitude map from the upper part of Lower Graben Fm in Unit 2. Low seismic amplitudes in the northern part of the study area organized into linear patterns, marked by blue lines.

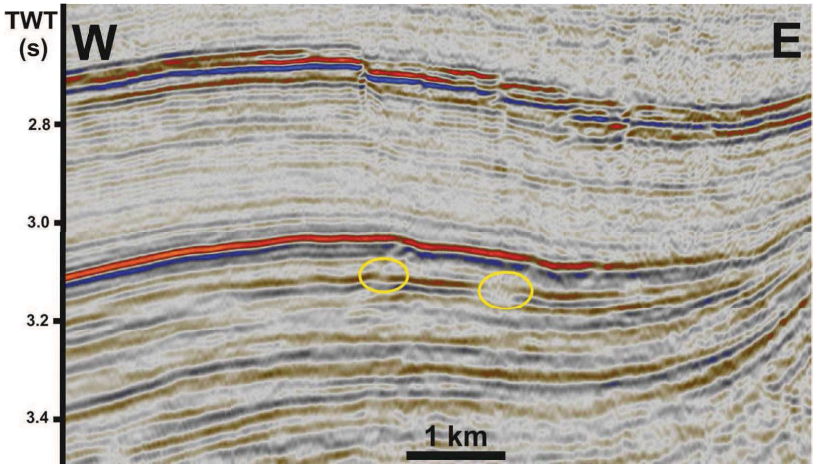

Figure 22. Cross-section highlighting the 2-D representation of the linear amplitude features (yellow circles) shown in Figure 21. Linear elements correspond to decreased amplitudes and disruption of the underlying reflector (see circle on the right)

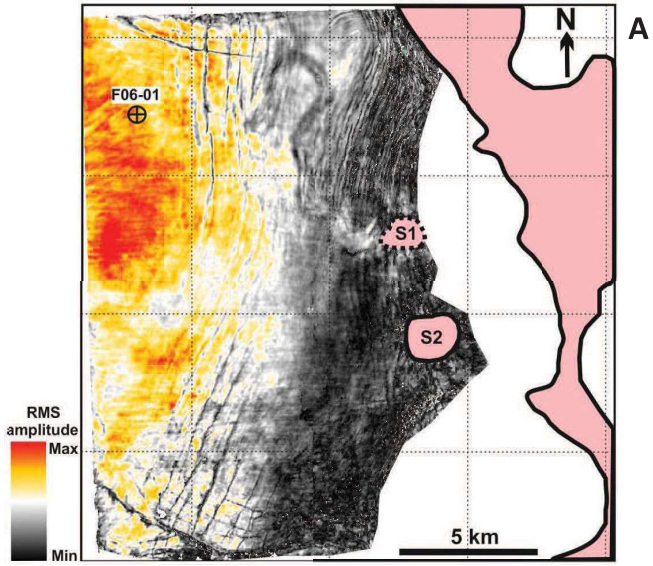

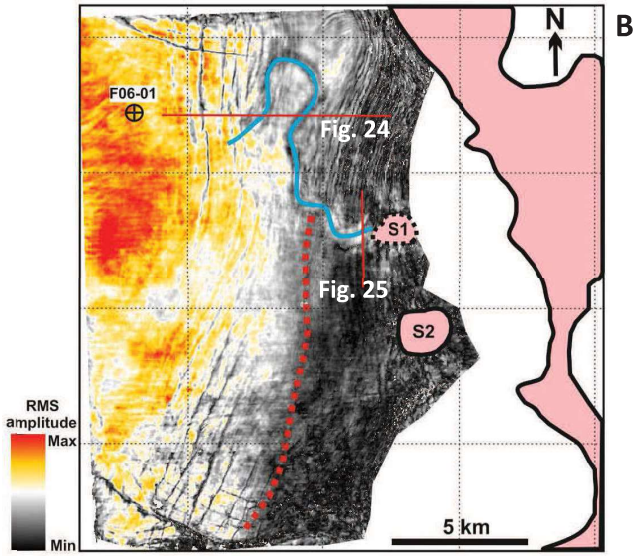

Figure 23. A-B. RMS amplitude map from base Middle Graben Fm in Unit 3 depicts linear amplitude pattern in the north of the study area. The feature shows rapid bends at the basin margin in contrast with the sinuous bend of 2 km radius in the basin axis. Red lines indicate cross sections of Figures 24 and 25. Dotted red line indicates N-S oriented boundary between high and low amplitudes, which correspond to prominent stratal termination at Base Middle Graben Fm (Unit 3) in Figure 19.

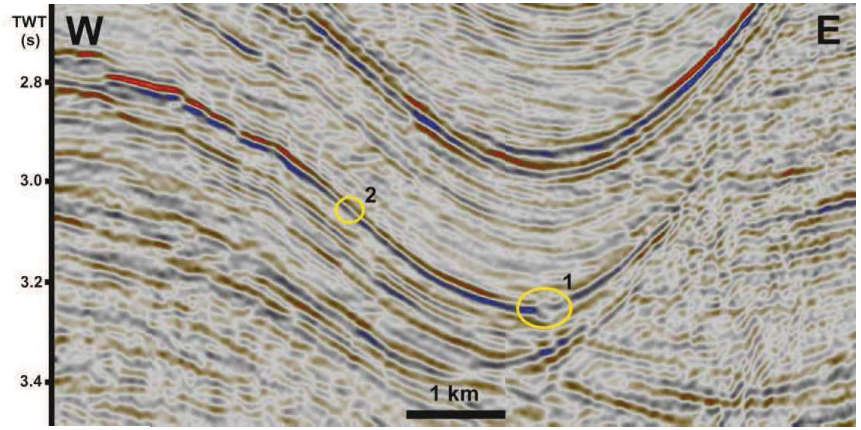

Figure 24. W-E cross sections showing 2-D seismic representation of linear amplitude feature of Figure 23, marked by yellow circles and rectangle. In the E-W section the feature shows prominent reflector heterogeneity in the east (circle 1) which is in contrast with the western side (circle 2), where amplitude variation is subtle.

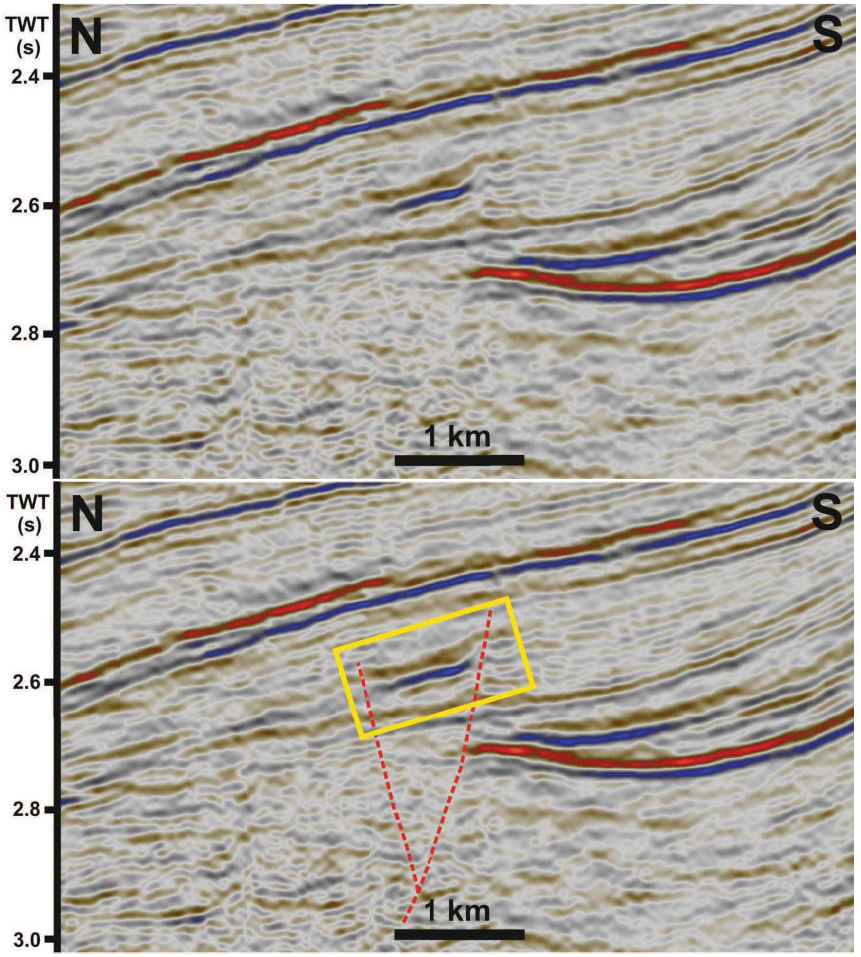

Figure 25. N-S cross sections showing 2-D seismic representation of linear amplitude feature (yellow rectangle) of Figure 23. The high amplitude zone is bounded by elevated flanks.

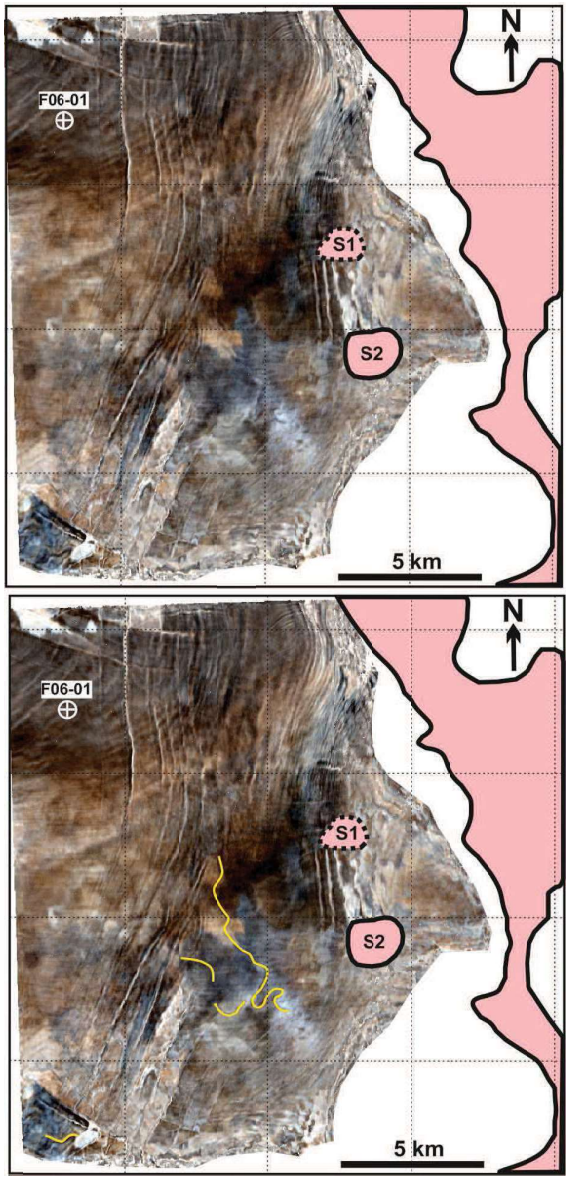

Figure 26. Color blended spectral decomposition map from the upper part of Upper Graben Formation in Unit 5, right below surface depicted in Figure 27. Linear elements show similar overall orientation (SE-NW), but are narrower.

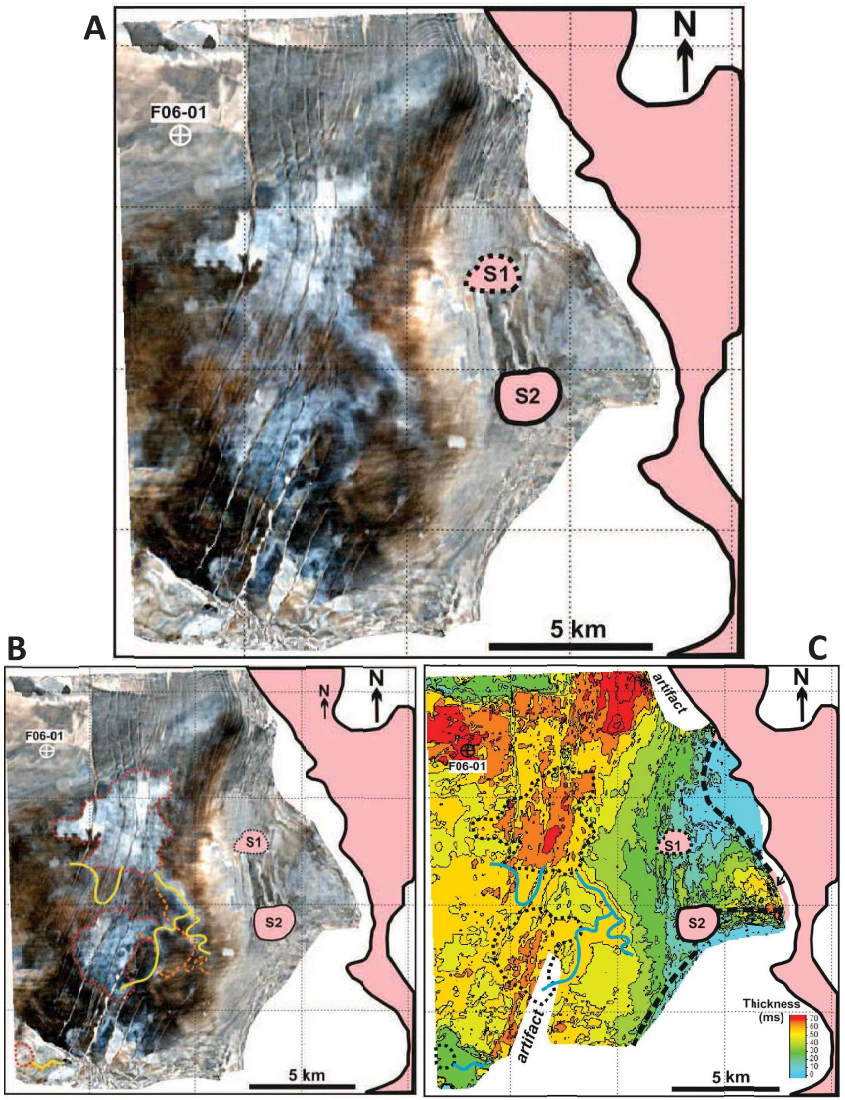

Figure 27. A, Color-blended spectral decomposition map from the upper part of Upper Graben Formation (Unit 5), highlighting linear elements terminating in well-defined triangular or circular zones. B, Red and yellow: outlines of identified features in Figure C, Isopach map of Unit 5 (Upper Graben Fm) showing correspondence of frequency features and zones of increased, orange: linear elements of Figure 31B. C: Isopach map of Unit 5, Upper Graben Formation.

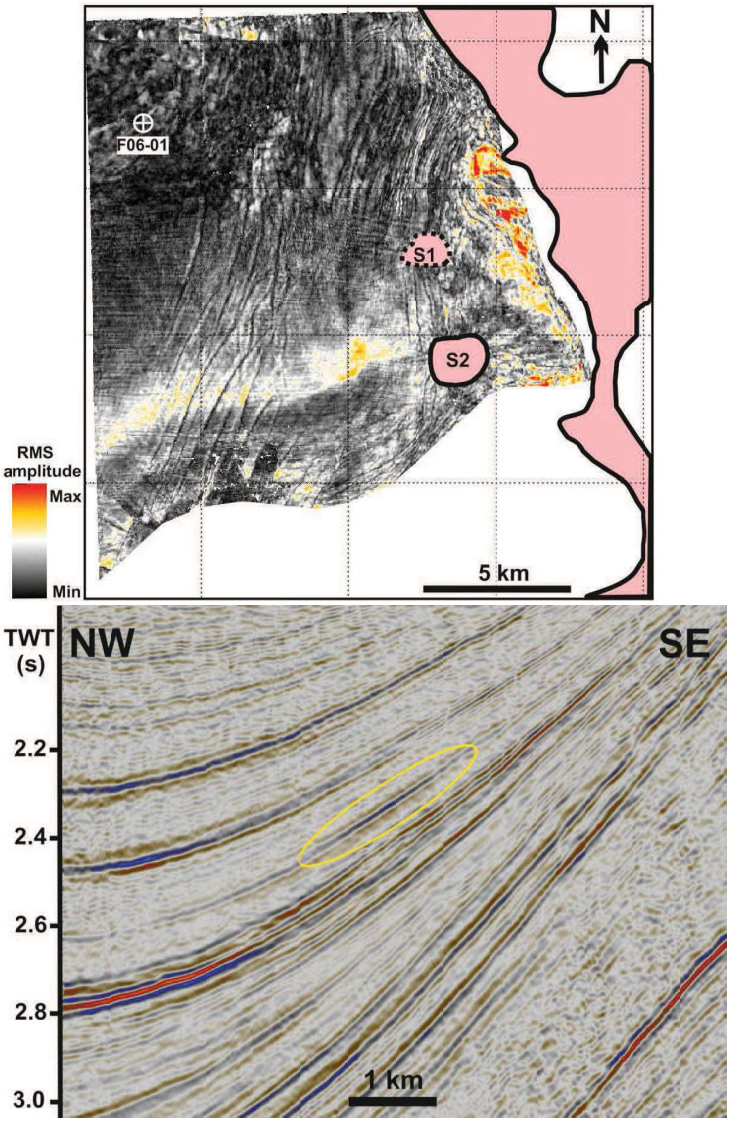

Figure 28. A, RMS amplitude map from middle Unit 6, the lowermost unit of Kimmeridge Clay Fm, depicting a WSW-ENE oriented elongated high amplitude zone B, 2-D signature of the zone can be detected along a NW-SE cross section, as well.

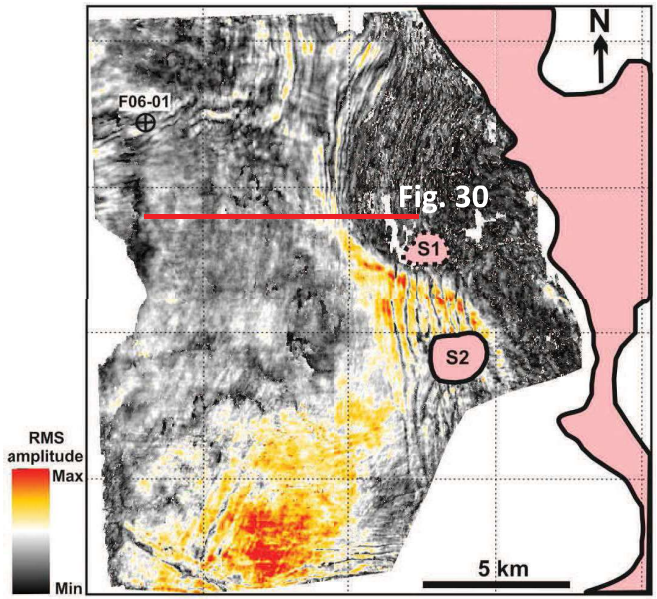

Figure 29. RMS amplitude map of base Lower Graben Fm depicting an elongated high amplitude zone at the marginal zone and rounded high amplitude zone in the south.

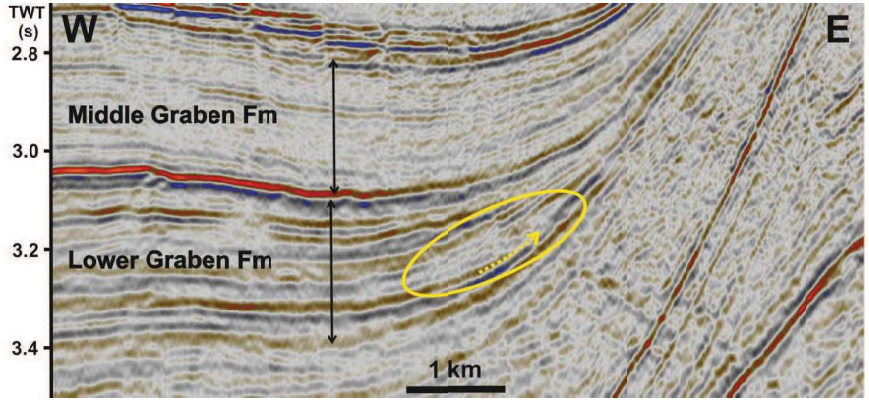

Figure 30. W-E cross section showing a distinct zone of discontinuous seismic facies in the Lower Graben Formation (yellow circle). The discontinuous zone is underlain by a clearly truncated reflector (yellow arrow).

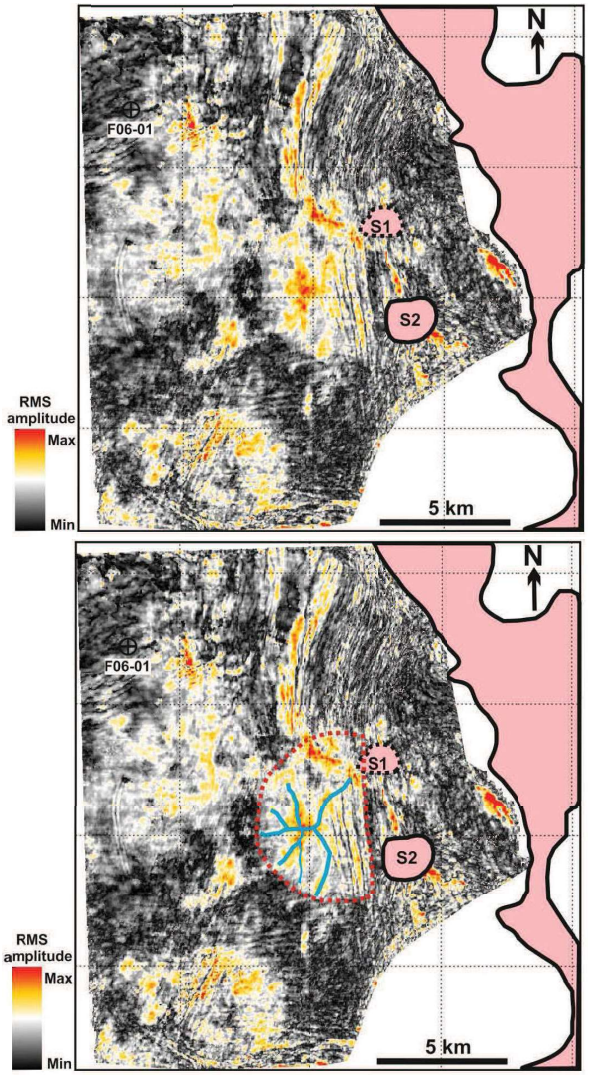

Figure 31. RMS amplitude map along Base Unit 2 in the Lower Graben Formation. Higher amplitudes are organized into a four-km wide circular zone west from the salt. See Figure 41. 2. for interpretation of the feature.

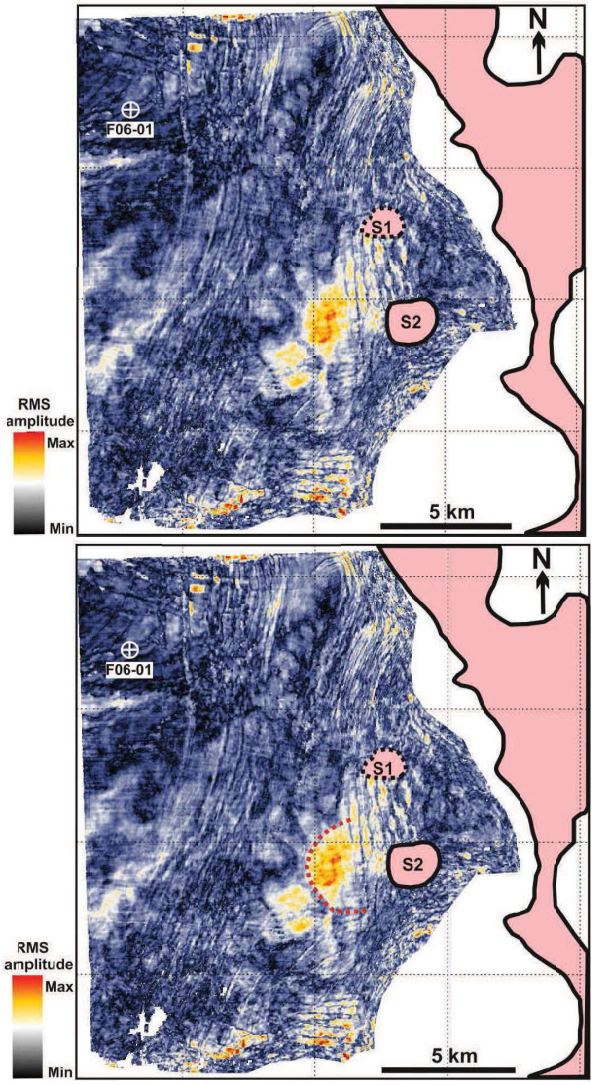

Figure 32. Sweetness attribute map from base Unit 4 in the Middle Graben Fm depicting high amplitude radial pattern at the margin-axis transition, west from salt body 1. Outline is plotted on Figure 41. 4 isopach map.

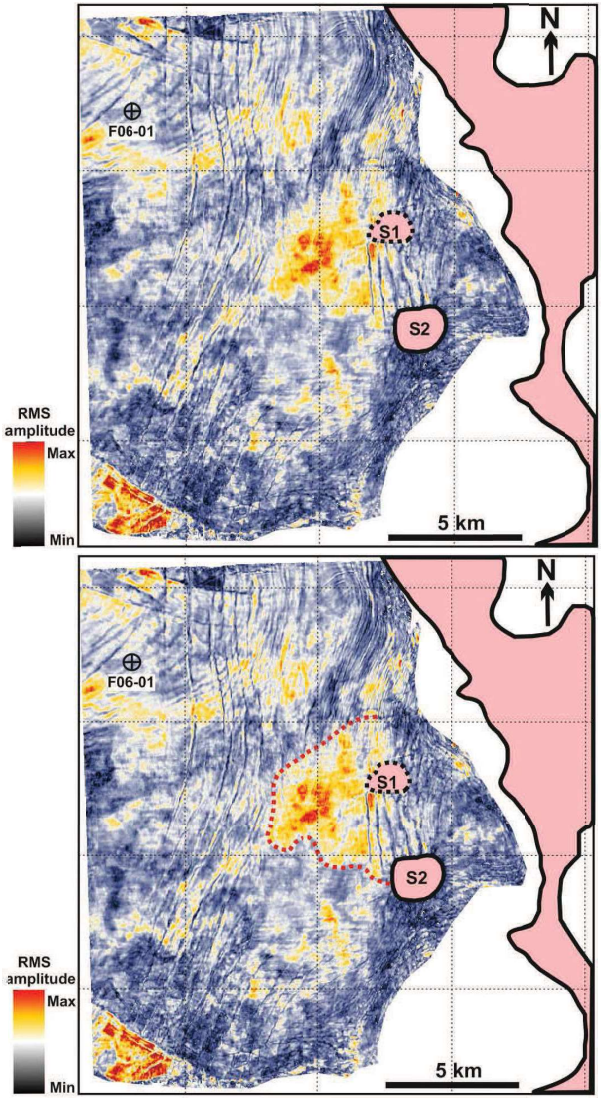

Figure 33. Sweetness attribute maps from Top Unit 4 in the Middle Graben Formation, depicting high amplitude radial pattern at the margin-axis transition, west from salt body 1. Outline is plotted on Figure 41. 4 isopach map.

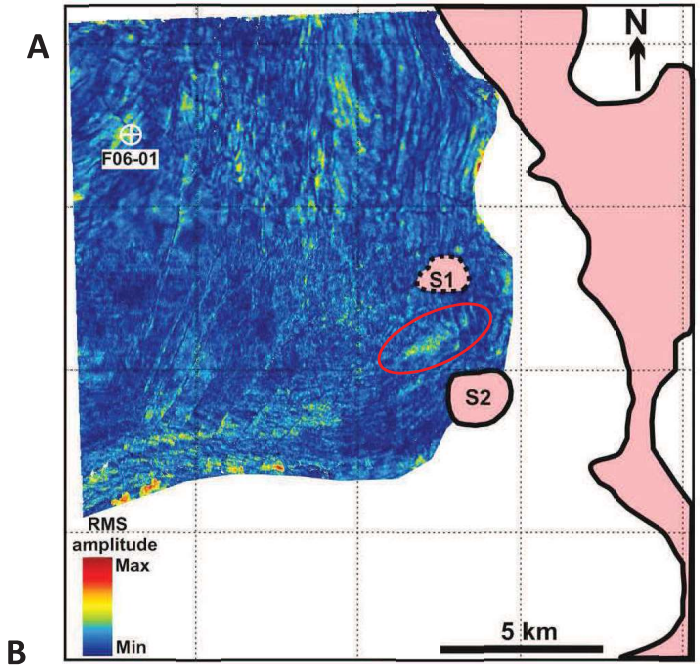

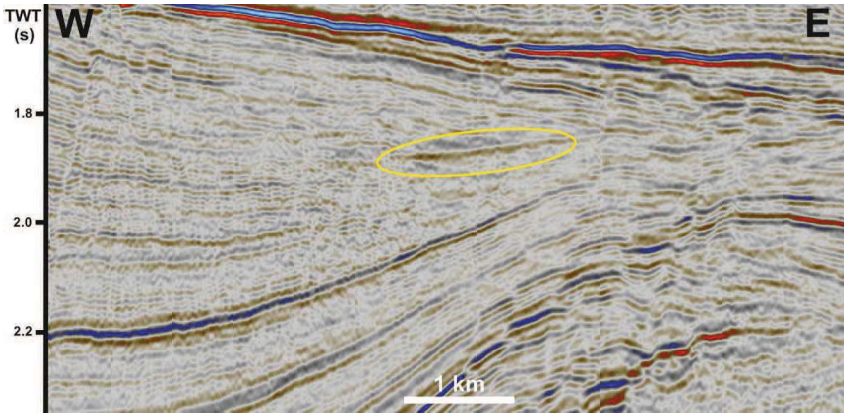

Figure 34. A, RMS amplitude map along intra Unit 9 reflector, displaying the map view signature of high amplitude feature within the discontinuous seismic reflectors. B, High amplitude, low frequency reflector surrounded by discontinuous seismic facies in Unit 9, Kimmeridge Clay Fm.

4. 3. Estimation of average sedimentation rates in the defined stratigraphic units

External and internal geometric characteristics of the defined units can provide insight into the spatial and temporal variations of differential subsidence. However, without any geologic time constraint the conclusions may include more than desirable uncertainties. Therefore, palynological data of the F03-03 well from the northern edge of the study area (Verreussel *et al.* 2015) was correlated with well F06-01 and was used to estimate the ages of the units' boundaries (which are based purely on seismic mapping) in the present project. Depth-to-time conversion was applied to well F06-01 in order to tie the well log information to the seismic cube available only in time domain. Since well data includes depth in meters, real thicknesses (along with TWT thicknesses) were estimated for the seismo-stratigraphic units at the location of the well. Absolute geologic age estimations of the units' boundaries, together with the thicknesses of the units, allowed to estimate average sedimentation rates for each tectonostratigraphic unit at the location of well F06-01. Since the well location is far from the margin, and targets the anticline of the F-03 Field, two other locations were chosen to represent the basin margin and basin axis areas which correspond to the locations used for the thinning rate calculations of chapter 4. 2. 3 (Figures 11-17.). In these two locations, the units' thicknesses in TWT were converted to depth in meters and so are calculated in meters/Myr. Time depth conversion factors are derived for each unit on the basis of TWT and depth thickness data of well F-06. These estimations include uncertainties from palynological analysis and the depth-time conversion but provide an insight into the order and amount of variation in sedimentation rates through time.

The estimated sedimentation rates at well F06-01, as well as in the basin axis and basin margin area, can be observed in Table 2. Figure 35 shows the temporal evolution of sedimentation rates at the three locations. It can be clearly seen that sedimentation rates significantly vary, even by an order of magnitude among the units, with an estimated minimum of 12 m/Myr for Unit 10 (Scruff Greensand Fm.) and 390 m/Myr during the deposition of the intra-Kimmeridge Unit 9 in the north-western edge of the study area.

Sedimentation during the Upper Jurassic in the study area can be divided into four phases (Figure 35). In the first phase, sedimentation began at a high rate during the deposition of the first two units (Unit 1, and 2), representing the Lower Graben Fm. In the second phase, sedimentation rate decreased and remained approximately the same pace during the deposition of the Middle- and Upper Graben Formations (Unit 3, 4 and 5) and the first part of the Kimmeridge Clay Fm (Unit 6). In the third phase, sediments of Unit 7 and 8 were deposited rapidly which make up the major part of the Kimmeridge Clay Fm. Decreased sedimentation rates of Unit 9 and 10 representing the latest Kimmeridge Clay Fm and the Scruff Greensand Fm define the fourth phase.

During the deposition of Unit 1 and 2, rapid sedimentation took place reaching an average of 333 m/Myr in the basin axis, and 111 m/Myr at the margin (Table 2 and Figure 35B). Unit 3 shows that sedimentation rate decreased almost to its fourth, to 86,7 and 40 m/Myr. Its 260 m thick basin axis package, representing the lower part of the Middle Graben Formation deposited during a period more than twice as long time (3 Ma) as the 400 m thick Lower Graben Formation (Unit 1-2) which deposited in only 1,2 million years.

Unit 4 represents the upper part of Middle Graben Formation and shows similar sedimentation rate as Unit 3. However, sedimentation rate increased slightly in the axis, but decreased slightly at the margin relative to Unit 3 (Figure 35).

Sedimentation rate during the deposition of Unit 5 increased, although not significantly. The increase was more pronounced in the basin margin (from 35,2 to 46,2 m/Myr) than in the basin axis where it increased from 92,4 to 112 m/Myr

Unit 6 shows a decrease in sedimentation rate at the axis and margin but the it remains still in the same range as the underlying units.

The biggest change in sedimentation rates between the margin and the basin axis can be observed from Unit 6 and 7 intra-Kimmeridge Clay Units. It rises by a factor of 5,4 in the axis and 6,7 at the margin. This order is maintained during the deposition of Unit 8. In contrast, Unit 9, being the uppermost Kimmeridge Clay Unit shows sudden drop from 438,8 to 55,7 m/Myr in the axis and 243,8 to 29,3 m/Myr at the margin.

Unit 10 indicates a slight decrease in sedimentation rate both at the margin and axis. At F06-01, sedimentation rate shows significant decrease from 25,4 in Unit 9 to 12,9 m/Myr observed in Unit 10.

Unit #	Top (m)	Base (m)	Top (ms)	Base (ms)	Thickness F06-01 (m)	Thickness F06-01 (ms)	Time to depth conversion factor	Age top (Ma)	Age Base (Ma)	Time period (myr)	**Sed. Rate F06-01(m/Myr)**	**Sed. Rate F06-01(ms/Myr)**	Thickness axis(m)	Thickness margin (m)	**Sed. Rate axis (m/Myr)**	**Sed. Rate margin (m/Myr)**
10	1686	1775	1603	1730	89	127	0,7	140	146,9	6,9	**12,9**	**18,4**	217,2	63,1	**31,5**	**9,1**
9	1775	1930	1730	1860	155	130	1,19	146,9	153	6,1	**25,4**	**21,3**	339,8	178,8	**55,7**	**29,3**
8	1930	2125	1860	2020	195	160	1,22	153	153,5	0,5	**390,0**	**320,0**	219,4	121,9	**438,8**	**243,8**
7	2125	2300	2020	2170	175	150	1,17	153,5	154	0,5	**350,0**	**300,0**	227,5	134,2	**455**	**268,3**
6	2300	2600	2170	2415	300	245	1,22	154	158	4	**75,0**	**61,3**	336,7	159,2	**84,2**	**39,8**
5	2600	2680	2415	2460	80	45	1,78	158	159	1	**80,0**	**45,0**	112	46,2	**112**	**46,2**
4	2680	2915	2460	2638	235	178	1,32	159	160,5	1,5	**156,7**	**118,7**	138,6	52,8	**92,4**	**35,2**
3	2915	3171	2638	2830	256	192	1,33	160,5	163,5	3	**85,3**	**64,0**	260	120	**86,7**	**40**
2+1	3171	*3631*	2830	3175	*460*	345	1,33	163,5	164,7	1,2	**383,3**	**287,5**	400	133,3	**33**	**11**

Table 2. Overview table depicting sedimentation rates at F06-01 well, in the basin axis and at the basin margin; along with variables needed for the estimations (e. g. thickness, age).

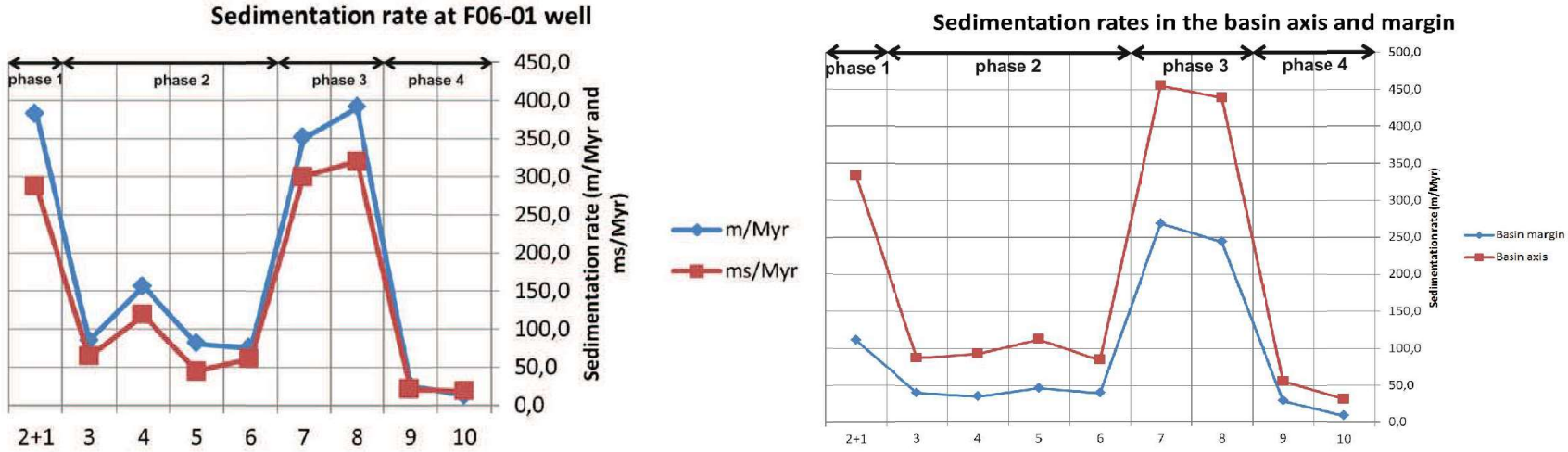

Figure 35. Estimated sedimentation rates (Y axis) of the defined tectonostratigraphic units (X axis) at F06-01 well (A) and two selected locations representing the basin axis and the basin margin (B), see Figure 11-17. for locations. Sedimentation rates are grouped into four phases and show peak values in unit 1-2, 7, and 8, while low values of the same range in units 3, 4, 5, 6, 9, and 10

4. 4. Overview of key results per tectono-stratigraphic unit

	Formation	Depositional environment *(Munsterman et al. 2012)*	Stratigraphic external forms	Stratal terminations	Amplitude features	Sedimentation rates (ms/Myr)		Thinning rate
						axis	margin	
Unit 10	***Scruff Greensand Fm***	Shallow marine, shoreface to offshore	Highly eroded apparent bowl (Fig. 17)	Onlap onto Kimmeridge Clay	-	44.9	13	3.4
Unit 9	***Kimmeridge Clay Fm***	Open marine, outer shelf	NNE-SSW trough in the N, radial thinning in the NW, depocenter in the SW (Fig. 16D)	-	Discontinuous seismic facies nex to S2 with high amplitude feature enclosed (Fig. 34)	46.7	24.6	1.9
Unit 8			NNE-SSW trough in the N, radial thinning in the NW, depocenter in the SW (Fig. 16B-C)		Discontinuous seismic facies nex to S2	360	20	1.8
Unit 7				-	-	390	230	1.7
Unit 6			NNE-SSW trough in the N, radial thinning in the NW, depocenter in the SW, Local bowl between salt wall and salt bodies (Fig. 16A)		SW-NE elongated high amplitude zone in the S (Fig. 28)	68.8	32.5	2.12
Unit 5	***Upper Graben Fm***	Marginal marine barrier-island system.	Heterogeneous thickness distribution with linear, circular and delta-like shapes, NNE-SSW trough in the northern edge Local bowl between salt wall and salt bodies (Fig. 15)	Small scale stratal terminations corresponding with amplitude patterns (Fig. 27)	Elongated, delta-like and circular features, corresponding with thickness distribution (Fig. 27)	63	26	2.42
Unit 4	***Middle Graben Fm***	Lacustrine; possible marine embayment	Roughly W-E thinning wedge (Fig. 14)	Onlaps, tips extend further basinward in the middle (Fig. 14)	Circular high amplitude patterns at the margin, at top and base of unit (Fig. 32&33)	70	26.7	2.63
Unit 3			W-E thinning wedge with depocenter in the S, Local bowl between salt wall and salt bodies (Fig. 13)	Prominent terminations along the margin (Fig. 19)	Linear feature with sinuous bend in the axis and abrupt bends at the margin (Fig. 23)	65	30	2.17
Unit 2	***Lower Graben Fm***	Fluvio-deltaic or coastal plain	W-E thinning wedge with curved strike of thinning. Increased thickness between the salt bodies (Fig. 12)	Prominent termination pattern following differences in thinning (Fig. 12)	Circular high amplitude feature west from salt bodies, linear feature in the north with side tracks (Fig. 21 & 31)	250	83.3	3.0
Unit 1			Confined bowl west from S2, otherwise w-E thinning wedge (Fig. 11)	Terminations bounding the bowl in the SW and (Fig. 18)	Discontinuous facies at the margin (Fig. 30)			

Table 3. Overview of the observations and findings of this study for each defined tectonostratigraphic unit (1-10) regarding external forms, prominent stratal terminations, amplitude features estimated sedimentation rates and thinning rates along with corresponding depositional environments from Munsterman *et al.* (2012

5. Discussion

5. 1. Tectono-stratigraphic implication of thickness distribution as an indicator of 3-D basin evolution

Prominent thickness changes, trending perpendicular to basin margins are widely considered to be controlled by syn-sedimentary structural elements, i.e. faulting, folding, or salt diapirism (Leeder Gawthorpe 1987; Giles and Rowan 2012). Normal fault bounded rift-basins are generally characterized by syn-rift sequences thickening towards the margins, which were deposited in the hanging walls of large normal rift faults. In contrast, in salt-bounded basins, syn-diapiric stratigraphic sequences characteristically thin towards the margin. In salt-bounded rift basins like the Dutch Central Graben, where salt diapirism occurs preferentially above pre-existing or active deep-skinned faults (ten Veen *et al.* 2012), both normal faulting and salt diapirism may play a role in determining the syn-deformational sedimentary architecture.

In the entire study area, stratigraphic units show thinning from the basin axis towards the basin margin, implying that their shapes in general were controlled preferentially by salt diapirism along the margin, rather than faulting. However, salt walls and diapirs represent rheologically weak sub-vertical heterogeneities and can facilitate normal faulting, which can result in local stratigraphic units thickening towards the salt. Another explanation of thickening towards salt structures is related to the evacuation salt. In this process, upward migration of the salt creates increased accommodation space next to the diapir or salt wall, resulting in thickening syn-diapiric wedges (e.g. Prather *et al.,* 1998, Weimer *et a.,* 1994, 1998), also referred as rim synclines.

In active rift basins, with or without salt diapirism involved, extension triggers basin subsidence. However, at the basin margins, uplift can occur, although only by an estimated 10% of the hanging wall subsidence values (Barr, 1987). Differential subsidence controls the amount and distribution of space available for sedimentation (also referred as accommodation). By definition, accommodation is created by vertical tectonic movements and absolute sea level changes (eustasy) (Catuneanu 2002). Since eustasy is a global controlling factor, differential subsidence and uplift create differential accommodation in a certain area.

In the tectonically active Dutch Central Graben during the Late Jurassic, eustasy, subsidence and differential subsidence can all be considered controlling mechanisms for accommodation creation, with the latter two being more dominant. Differential subsidence rate defines differential accommodation, while rate, style, and preferential direction of sedimentation govern where, and to what extent the accommodation space is filled (Banham & Mountney 2013).

It is assumed that depocenters defined by areas of increased thickness may correspond with areas of increased subsidence. However, it is important to add that sediment dispersal, lithofacies and sediment transport pathways are controlled by various processes beyond accommodation space, such as climate, and basin physiography. As a result of all the interplay between these processes, accommodation might not be fully filled up by sediments, so the sedimentary record may not necessarily represent the accommodation space created within a given geologic time range.

The thinning trends observed in isopach maps can be of different origin. True thinning occurs when no offlaps or truncations can be observed within the zone of thinning, therefore

likely representing the true stratigraphic thickness. These areas can serve as good indicators of the amount and spatial distribution of accommodation space. In contrast, where the zone of thinning is accompanied by erosional truncations, thinning represents, purely or partly, the effect of erosion, not the original stratigraphic thickness (see marginal areas beyond dashed lines in isopach maps (Figure 41). Local erosion may play a major role in the resulting thickness distribution in the basin margins, since footwall-uplift, or salt diapir-related uplift can expose the margin. Sediments deposited at the margin may be eroded and re-deposited in the basinal area or further downdip, as part of the subsequent stratigraphic unit. This type of erosion is observed only locally in the study area, at rather small scale, which indicates that most of the thinning observed in the produced maps in the present study reflects true thinning rather than erosional thinning. This means that the isopach maps produced can mainly be interpreted as structurally controlled stratigraphic thickness variation due to the evolution of the withdrawing and migration of salt that create rotation of the basin margins.

On the other hand, another type of erosion affects most of the units, the regional Cretaceous Unconformity. As a result of the Cretaceous inversion of the North Sea Basin, Upper Jurassic became widely exposed, especially the shallower marginal areas. The whole Kimmeridge Clay and the Scruff Greensand Formations are truncated at the margins (Figure 41.6-10), therefore locally do not record the original depositional thicknesses. In addition, Unit 2 is also widely affected by erosion, especially in the north and south of the area. Therefore, thinning towards the east from the marked erosion limits (Figure 41.2) show higher than original thinning rate.

Further limitations of using current thicknesses are the fact that thickness is only measured in two-way travel time in this study and that it does not account for the differential compaction of the sequences.. Amount of compaction is not only a function of the overlying load but the different lithological properties, e .g. porosity but such dynamic decompaction aspect was not included in this study.

When dealing with true preserved stratigraphic thicknesses, (i.e. not affected by regional erosion or differential compaction) it is assumed that the larger thicknesses correspond to larger accommodation space present during the deposition of the given unit. This also allows defining locations of maximum accommodation called depocenters within a tectono-stratigraphic unit.

According to the isopach maps, accommodation space and therefore likely the amount of subsidence, varied significantly in the study area during the Late Jurassic, as well as within each tectono-stratigraphic units. Thickness variation may not only allow to evaluate differential subsidence, but also to get insight into the rate of stratigraphic thinning at the margin i.e. higher thinning rates refer to higher rate of differential subsidence.

5. 2. Basin axis to basin margin transition

Thickness trends may provide good insight into changes in subsidence at the margin, but the transition from the basin to the margin is less revealed in terms of where the coastline is located and what kind of sediments were deposited. By incorporating results of attribute analysis together with seismic facies analysis, the sedimentary environments and their corresponding stratigraphic elements can be interpreted. For that purpose, well F06-01, located in the northwestern section of the study area (Figure 2) provides a valuable constraint on the potential depositional environments, even if the well data better represents the basin axis area due to the distance from the well to the basin margin.

Prominent amplitude differences along reflectors may refer to lithological changes, e.g. lateral distribution of sands. Deltas delineate the paleo-coastlines, and together with channels, reliably mark the dominant sediment transport direction. Onlaps may not always delineate precisely the coastlines but the most marginal points of sedimentation being of continental or marine origin. Therefore, onlaps provide information about the relative spatial shifts of the coastlines but not their exact locations. Distinct zones of discontinuous seismic facies (Figure 30) suggest the presence of mass flow deposits such as mass transport deposits (MTD, slumps and slides), debris flows or turbidite flows, which can reflect the changes of depositional slope, especially where small scale detachment faults are detected in the case of a slide.

5. 2. 1. Fluvio-deltaic and lacustrine depositional environments

The Lower Graben Formation is characterized by fluvio-deltaic sedimentation with tidal influence and the presence of lacustrine environment with no or minor marine incursions (Munsterman *et al.,* 2012). The stratigraphic succession is generally coarsening upwards, consisting of several smaller coarsening upwards cycles (Figure 2). Above the Lower Graben Formation., as the base of the Middle Graben Formation, a coal interval is present, which has a strikingly high, low frequency seismic signature in the form of one single reflector in most of the study area. Its marginal truncation can be seen in Figure 23 amplitude map and Figure 19 seismic section. The coarsening upward cycle within the fluvio-deltaic interval is capped by coal and indicates a decreasing accommodation/sedimentation ratio. Progradation of deltas filled the marginal areas of freshwater/brackish lakes. This is supported by a 100 – 1000 m wide delta shaped high amplitude features observed in amplitude maps (Figure 31) and are drawn in Unit 2 isopach map (Figure 41. 2). The delta shape, representing a one reflector thick interval corresponds to the middle area of Unit 2 with low thinning rate between the two salt bodies (Figure 41. 2.). This may suggest that the dispersal geometry was largely controlled by the location of the delta, rather than differences in subsidence. From another point of view, the delta may have evolved in that location due to higher differential subsidence in the middle part, which thus became less affected by subsequent erosion than the northern and southern areas (Figure 41. 2).

Tectonic control on Lower- and Middle Graben fluvial channels?

Based on stratigraphic and biostratigraphic studies (Munsterman *et al.* 2012) suggest that the Lower and Middle Graben Formations were deposited in fluvio-deltaic and lacustrine environments. The linear geobodies highlighted in the amplitude maps in these intervals are therefore interpreted as fluvial and distributary channels.

As an example, Channel system 2 in Lower Graben Formation (Figure 36, Figure 41. 2) roughly follows the SSE-NNW margin strike, suggesting that the basin margin orientation exerted a significant control on the channel orientation.

As it was described in the earlier sections, Channel 3 is located at the base of the Middle Graben Fm. and shows tight, 90 degrees bends in the marginal zone, which contrast with the large sinuous bend in the basin axis (Figure 37, Figure 41. 2). The straight pathway with sharp bends suggests tectonic control or confinement at the basin margin, while the sinuous bend refers to a lower energy environment lacking of significant tectonic forcing.

The seismic appearance of Channel 3 also shows different characteristics between the basin margin and axis. Although it is not challenging to recognize this channel in an attribute map, it is however challenging to see it in 2-D seismic cross sections, since amplitude anomalies or inclination of reflectors are minor and can barely be seen without the help of the map view

amplitude characteristics. In contrast, at the basin margin, Channel 3 is clearly observed in cross sections, as clear abruption of seismic reflectors and an anomalously high seismic amplitude pattern (Figure 37B). Unfortunately, channel 3 cannot be followed further to the east in this seismic dataset. Therefore, Channel 3 pathway can be interpreted in two ways.

1. Along a north-south section, immediately west from the salt body the channel shows a flat high amplitude seismic character (Figure 37B) and is bounded by elevated flanks on the sides. Highly speculative but corresponding with the flanks, opposite dipping faults can be interpreted, which may have controlled the channel pathway by creating a margin-parallel elongated depression. These normal faults may have originated from the collapse of the underlying salt body 1. In this case the channel pathway would continue above the salt body. Therefore, the channel in this marginal area (Figure 37A) can be considered an incised valley due to salt diaper collapse.
2. Another possible interpretation is that the channel continues right next to salt body 1. In this scenario, the evacuation of salt could have created a rim syncline locally, which could have triggered the channel to flow in a confined local depression in the proximity of the salt at the margin area. The presence of the channel-bounding faults and the fact that the stratigraphic level – although affected by it– lies well above the salt body, i.e. they are not in direct contact, favour the first interpretation.

The interpretation of the updip part of Channel 3 as an incised valley is based on its external geometry (map and cross section views) and not on its internal structures, that are likely below seismic resolution.

The widespread coal layer at the top indicates that sedimentation eventually outpaced the accommodation creation, which may refer to the decreasing rate of subsidence.

The coal layer(s) at Base Unit 3 (Middle Graben Formation) suggest the presence of swamps, mires surrounding the river preserved as Channel 3. Although sinuous, the channel does not show any sign of avulsion but its path is rather confined in an approximately 600 m wide zone. This type of channel track can be triggered by raised swamps at the sides, which keep overbanks from flooding and avulsion (Reading 1996). The raised swamps are indicative of abundant vegetation.

Another striking characteristics of the channel is its abrupt termination, and the lack of any sign for a delta. Since the overlying fined-grained early Middle Graben sediments represent marine conditions, a possible explanation is marine erosion (ravinement) during the subsequent transgression, which eliminated the more basinal section of the channel.

Extensive fluvio-deltaic system in the Upper Graben Formation

Well log data indicates that the Upper Graben Formation (Unit 5) is mainly comprised of sandstone with siltstone and coal stringers at the top of the unit. Amplitude mapping revealed a well-developed channel-delta system (Figure 38 and 41. 5). Purely based on the channel and fan shapes observed in the amplitude maps, this interval could be interpreted as of deep-water origin. However, the presence of coal stringers strongly supports the fluvial origin of the channels and deltas. These observations suggest that the Upper Graben Formation represents another period of low subsidence rate, and filling up of the basin.

The most prominent channel (Channel 5.1, Figures 38 and 41.5) is oriented SE-NW and ends up in a 4 km wide delta in the basin axis. The other main trend represented by Channel 5. 2 deflects from the SE-NW one to the SW and terminates in a circular shaped distinct zone, which can be interpreted as a delta or a crevasse splay (Figure 38 and 41. 5). In this interval the coastline is well delineated by the basinward edges of the deltas.

In addition, dense stratal slicing of Upper Graben Formation revealed the migration of individual channel elements (Figure 27B), and an overall shift in channel pathway. Channels right below Upper Graben fluvio-deltaic system show northeastward migration.

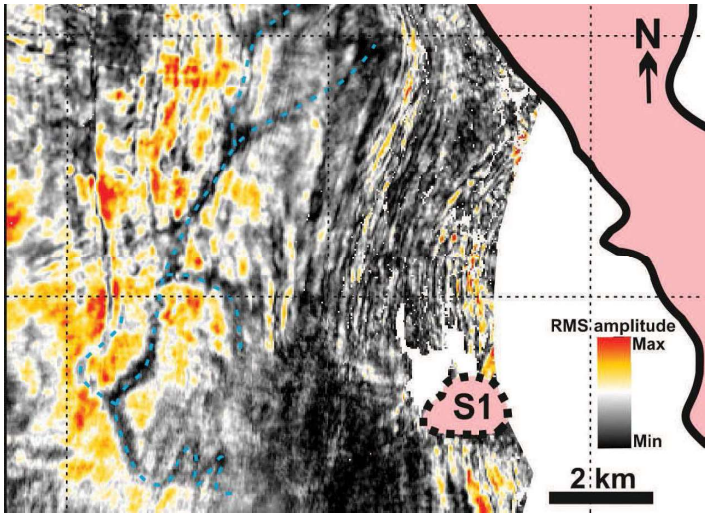

Figure 36. RMS amplitude map from Unit 2, Lower Graben Fm, depicting linear low amplitude features interpreted as fluvial *channel system 2* in the northern part of the study area.

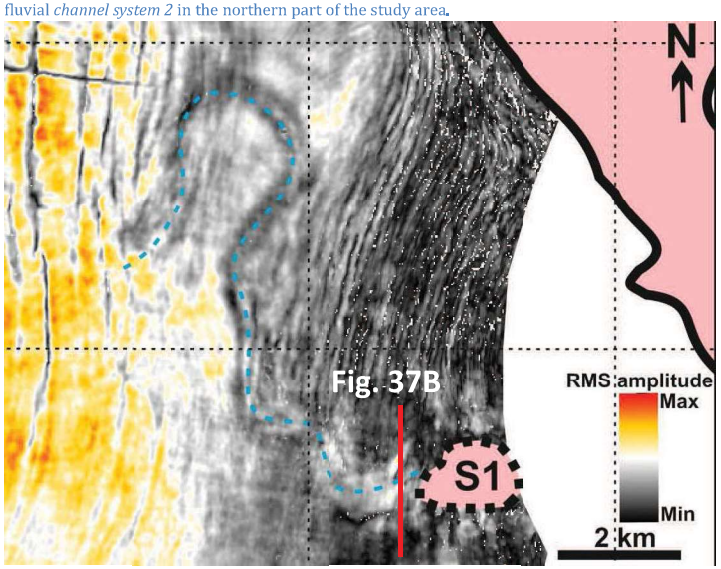

Figure 37A. RMS amplitude map from the base of Unit 3, Middle Graben Fm, showing fluvial *Channel 3* pathway.

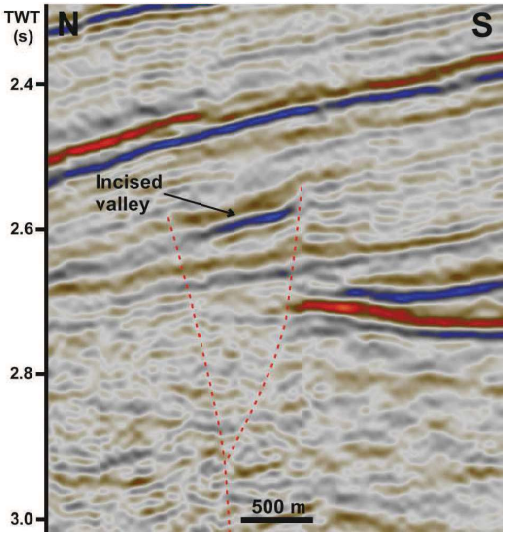

Figure 37B. N-S seismic cross section highlighting the 2-D character of the fluvial *channel 3* revealed in amplitude maps, adjacent to salt body 1 (see map view in Figure 37A).

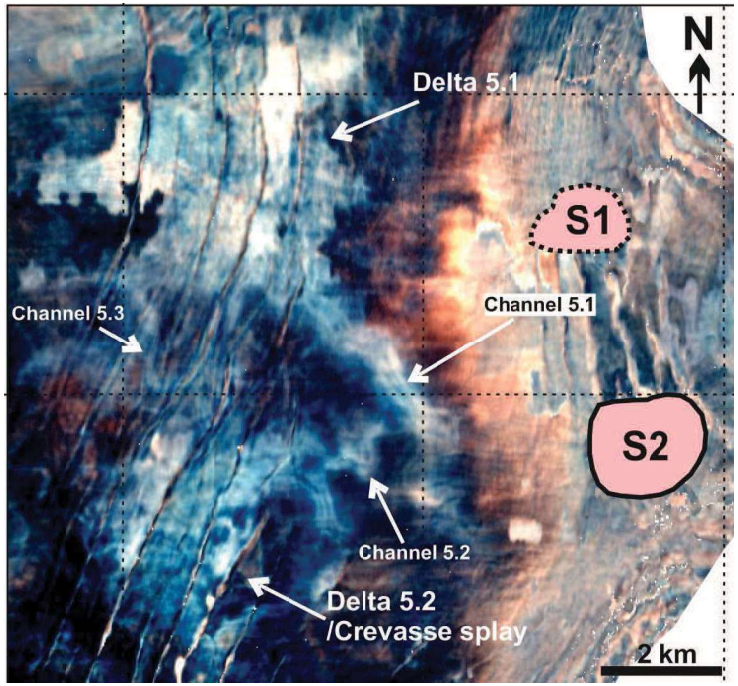

Figure 38. Color-blended spectral decomposition map from the upper part of Upper Graben Formation (Unit 5), highlighting linear elements terminating in well-defined delta-like or circular zones.

Varying fluvial sediment transport directions

Channel orientations suggest varying directions of sediment transport from the basin margin towards its axis in the three identified fluvial and fluvio-deltaic systems described above.

Channel system 2 in the Lower Graben Formation suggests dominantly north-south axial flow in the basin axis, with tributaries flowing perpendicular into the main channel (Figure 36 and 41. 2). Channels were not observed and/or are not preserved along the margin itself which does not allow robust interpretation on flow direction at the margin. However, the presence of a delta (Delta 2.1) indicate that marginal sediment pathway were active and that lateral sediment sources were already active during this period.

In contrast, Channel 3 originates clearly from the eastern basin margin, although seismic resolution is not sufficient to fully capture its pathway toward the east up onto the Schill Grund High. The confined channel pathway suggests that preferential sediment transport direction was east to west at the margin at the time of deposition of the youngest Middle Graben sediments, with the main source area in the east (Figure 41.3). In contrast, the younger fluvio-deltaic system observed in the Upper Graben Formation suggests a third dominant sediment transport direction, oriented SE-NW, with the source area located to the south-east (Figure 41. 5.).

Amplitude mapping provided the clearest channel patterns along levels that are located at boundaries of sharply different seismic facies. According to lithostratigraphic data, these levels also correspond to sharp lithologic boundaries at the tops of coarsening upward trends. Channel 3 is overlain by the fine-grained claystones of Middle Graben Formation. Upper Graben fluvial channel system is preserved right at the boundary with the deeper marine Kimmeridge Clay. The boundary can be interpreted as a transgressive surface. These might suggest that the channels, deltas, or other depositional elements preserved preferentially at levels where depositional environment rapidly changed, i.e. widespread flooding deposited finer grained sediments on top of relatively coarser grained clastics of continental-fluvial origin.

5. 2. 2. Open marine depositional environments

Large number of studies focus on the evolution of deepwater environments with special attention to submarine channel evolution in tectonically active basins (e.g. Posamentier, 2003, Beaubouef and Rossen 1999). Size, stacking pattern, and sinuosity of channels together with deepwater fans can provide good insight into the tectonic evolution of basin margins (Posamentier and Kolla 2003). In addition, deepwater gravity flow deposits such as turbidites, debrites and MTDs can also serve as good indicators of tectonic activity. In this study, purely based on seismic character, turbidites, slumps and a deepwater channel belt are interpreted in the open marine Kimmeridge Clay Formation.

Base Kimmeridge Clay Formation (Base Unit 6) represents a sharp change in grain size, lithology, and depositional environment. The formation is dominated by clays with thin, dolomitic interbeds. Grain size trend can be observed only in the upper section of the formation, slightly coarsening upwards, below the transition with the overlying Scruff Greensand Formation. This may imply rapid relative sea level rise at the boundary of Upper Graben Fm. and Kimmeridge Clay, which refers to increased rate of subsidence as well as, likely, an absolute sea level rise. Otherwise, the Kimmeridge Clay Fm. reflectors show few terminations, and characteristically drape the underlying sediments in the marginal area as well. Marginal boundary of the Kimmeridge Clay units is either eroded during the Cretaceous inversion or terminates against the salt wall.

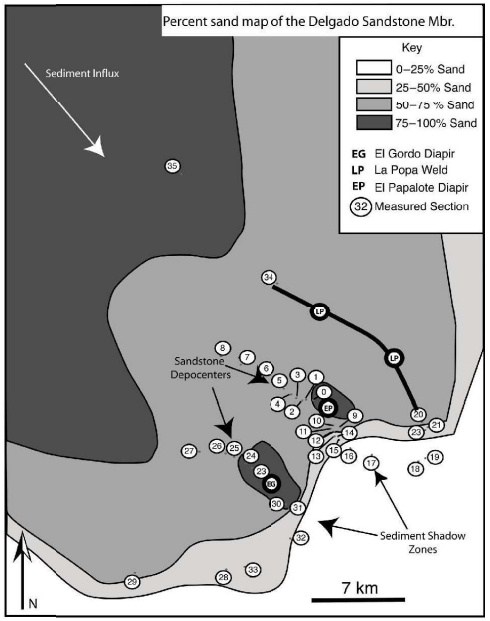

Figure 39. Sand distribution in the vicinity of salt diapirs, from Aschoff &Giles (2005). Higher sand content is found adjacent to salt diapirs regardless of the regional sediment dispersal pattern and transport direction

Salt diapirism-triggered deepwater slumps?

At the basin margin, zones of discontinuous facies have been detected in Unit 8-9 , with a preferred orientation NW-SE (Figures 34 and 41.8-9). These can be interpreted as debris flows, slumps or turbidites.

In Unit 9, within the discontinuous zone, a high amplitude feature can be traced in a fan-like shape (Figure 22 and 25. 9). High seismic amplitude can refer to sandier strata or contrasting fluid content within the coarser sediments enclosed in the overall clayey interval. Therefore, we interpret this feature as turbidite deposits. It is striking that the potential slumps and turbidites are located adjacent to salt body 2. These deposits can be induced by instability and/or tilting of depositional slope. In this case, the emergence of salt body 2 may have created the increase in slope gradient, which destabilized the unconfined sediments, and redeposited them at deeper areas. The turbidites or slumps are characterized by higher sand content than the surrounding sediments. The sediment dispersal observed adjacent to a single salt diapir in Unit 9 (Figure 41.8-9) is somewhat comparable with results of Aschoff and Giles (2005) (Figure 39). In their model, the general depositional trend and sand content distribution is disturbed due to individual salt diapirs. The diapirs elevate the topography, and while exposing the overlying sediments, locally provide source area for redeposited sediments. The eroded clastics originating from above the diapirs are redeposited adjacent to the diapirs. Since the regional sediment source is located far from the diapirs, the coarser sediments from older stratigraphic units were uplifted, eroded and ended up being redeposited in the Kimmeridge Clay Fm., and therefore, surrounded by finer grained clastics (Figure 34).

A submarine channel complex

In the lower part of Kimmeridge Clay (Unit 6), WSW-ENE oriented, elongated high amplitude zone is interpreted as a submarine channel complex (Figure 28 and 40), trending perpendicular to the basin margin from the position of salt body S2. The interpretation of this feature as a deep-water channel or channel complex is supported by the fact that the channel path is oriented roughly perpendicular to isopach lines, i.e. runs towards the depocenter of the unit wide (Figure 41.6). The high amplitude zone have a very large aspect ratio, being only one reflector thick, 10 km long and 1 km wide. In addition, no actual channel forms can be observed internally within this feature, and so it is interpreted as a channel complex (similar to features described in Weimer & Slatt, 2004 and Bouroullec & Pyles, 2010). The individual channels may be laterally stacked, giving the channel complex a low aspect ratio.

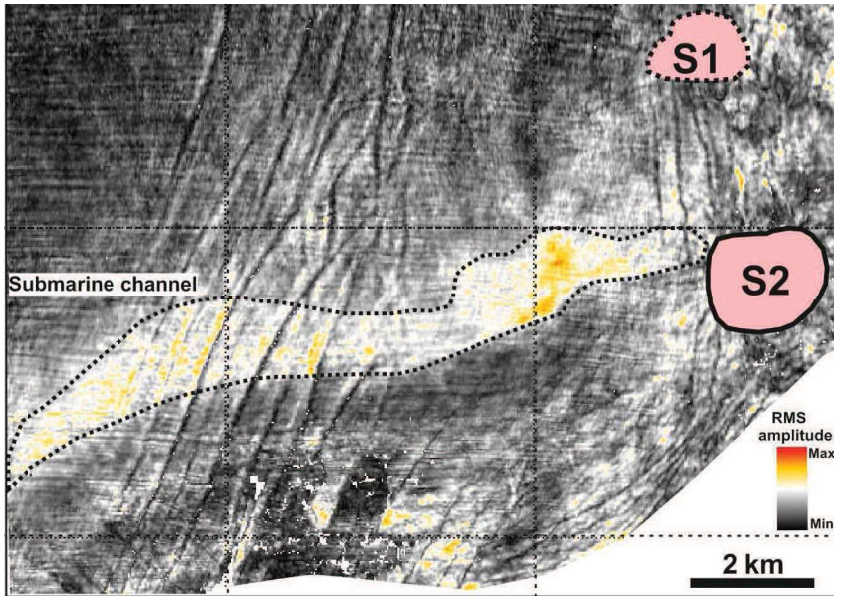

Figure 40. RMS amplitude map from the middle of Unit 6, Kimmeridge Clay Fm, depicting NW-SE oriented elongated high amplitude zone, interpreted as a submarine channel complex.

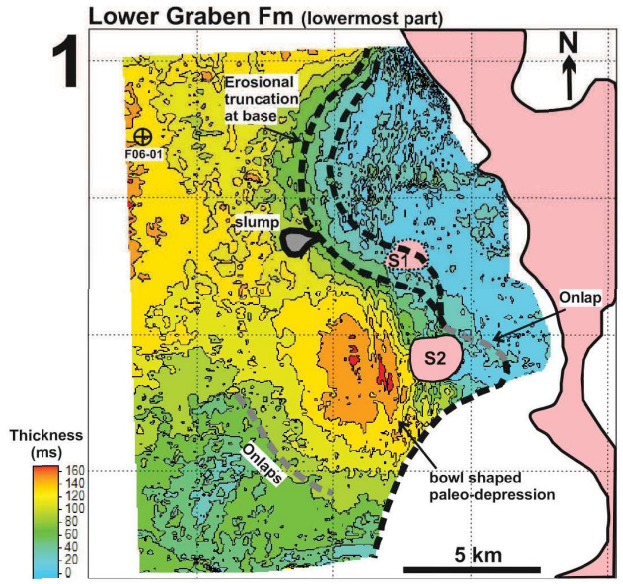
1
Lower Graben Fm (lowermost part)
N
Erosional truncation at base
F06-01
slump
S1
Onlap
S2
Onlaps
bowl shaped paleo-depression
5 km
Thickness (ms)
160
140
120
100
80
60
40
20
0

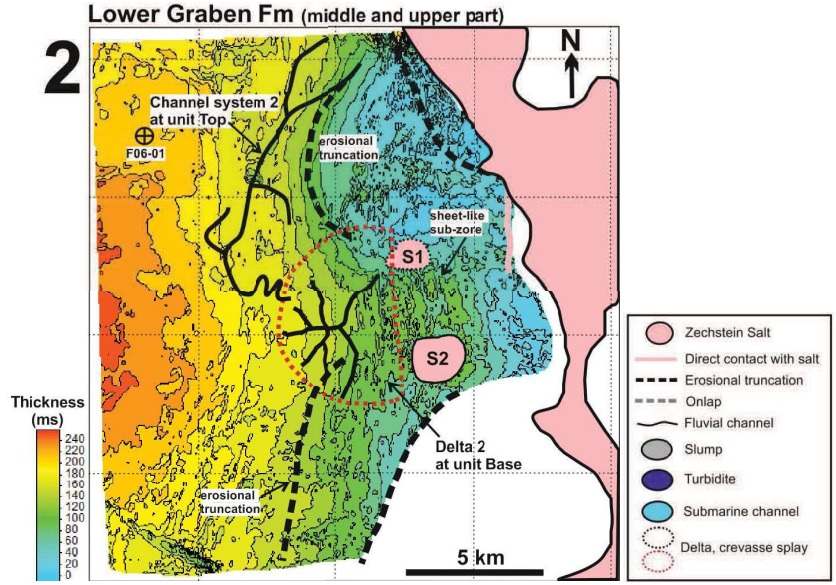
2
Lower Graben Fm (middle and upper part)
N
Channel system 2 at unit Top
F06-01
erosional truncation
sheet-like sub-zone
S1
S2
Delta 2 at unit Base
erosional truncation
5 km
Thickness (ms)
240
220
200
180
160
140
120
100
80
60
40
20
0
Zechstein Salt
Direct contact with salt
Erosional truncation
Onlap
Fluvial channel
Slump
Turbidite
Submarine channel
Delta, crevasse splay

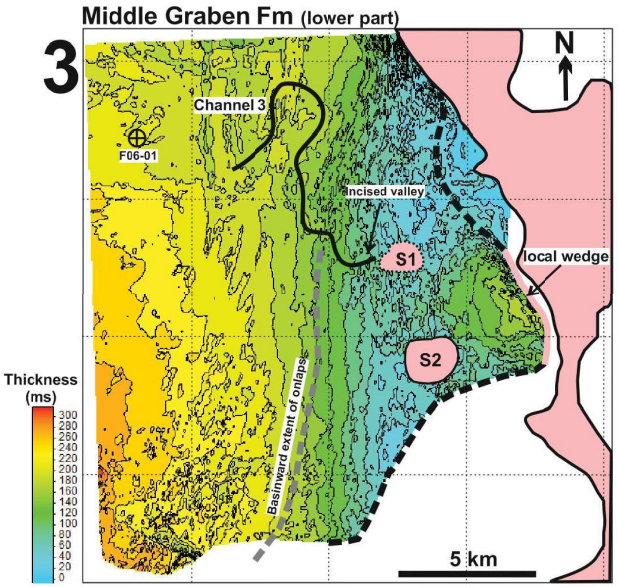
3
Middle Graben Fm (lower part)
N
Channel 3
F06-01
incised valley
S1
local wedge
S2
Basinward extent of onlaps
5 km
Thickness (ms)
300
280
260
240
220
200
180
160
140
120
100
80
60
40
20
0

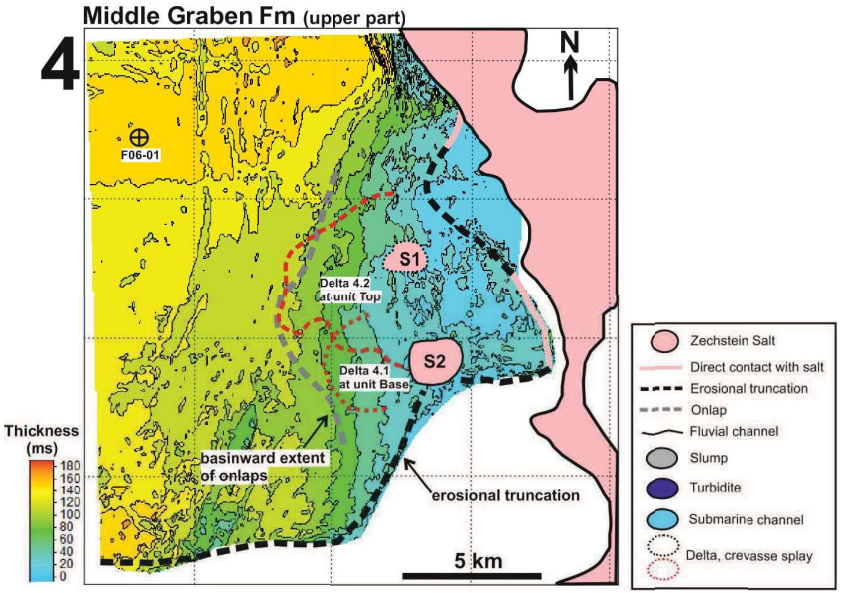
4
Middle Graben Fm (upper part)
N
F06-01
S1
Delta 4.2 at unit Top
S2
Delta 4.1 at unit Base
basinward extent of onlaps
erosional truncation
5 km
Thickness (ms)
180
160
140
120
100
80
60
40
20
0
Zechstein Salt
Direct contact with salt
Erosional truncation
Onlap
Fluvial channel
Slump
Turbidite
Submarine channel
Delta, crevasse splay

Upper Graben Fm

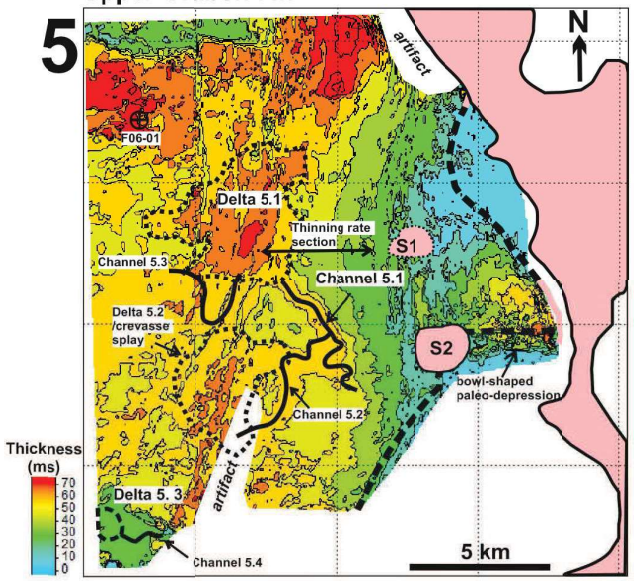

Kimmeridge Clay Fm (lowermost part)

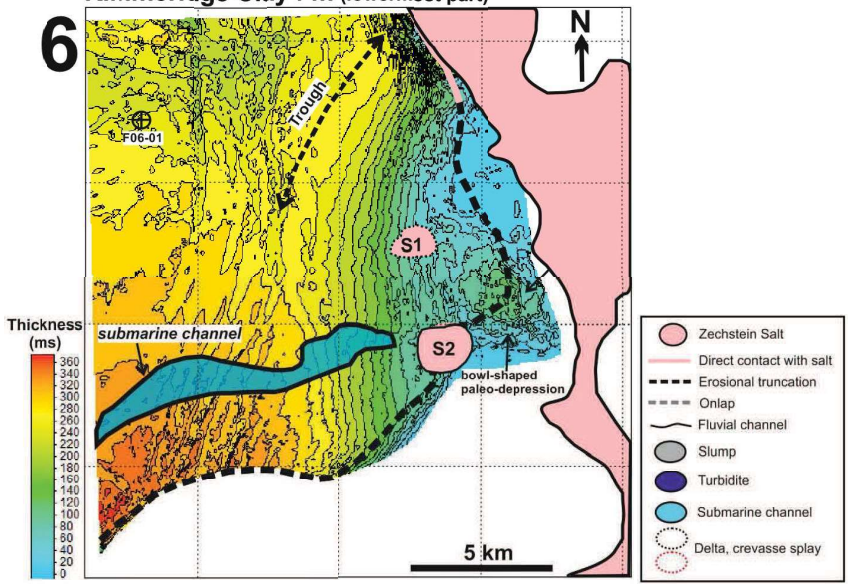

Kimmeridge Clay Fm (lower middle part)

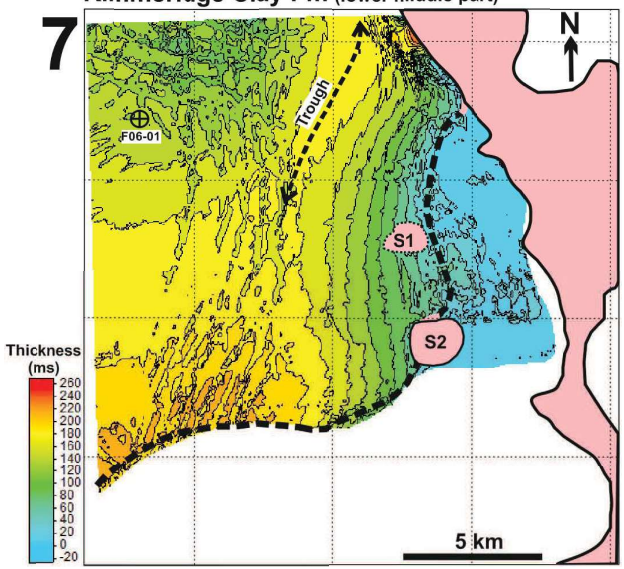

Kimmeridge Clay Fm (upper middle part)

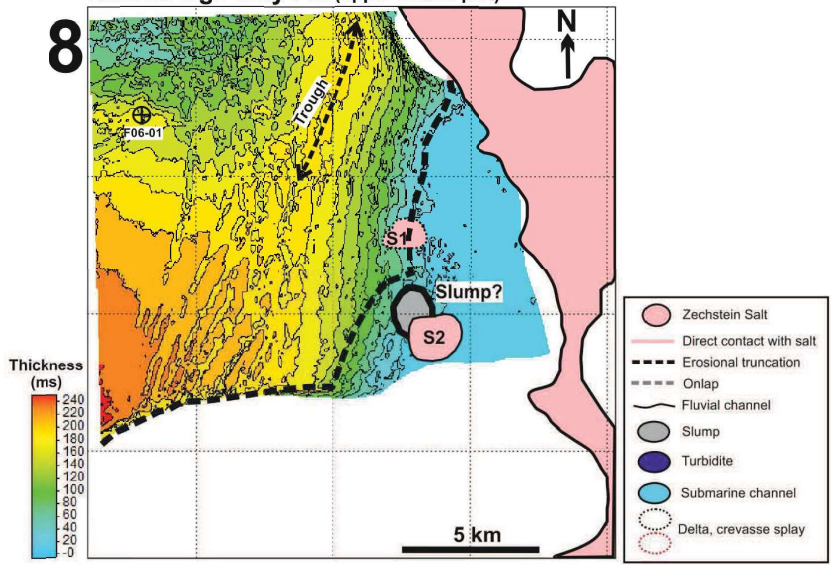

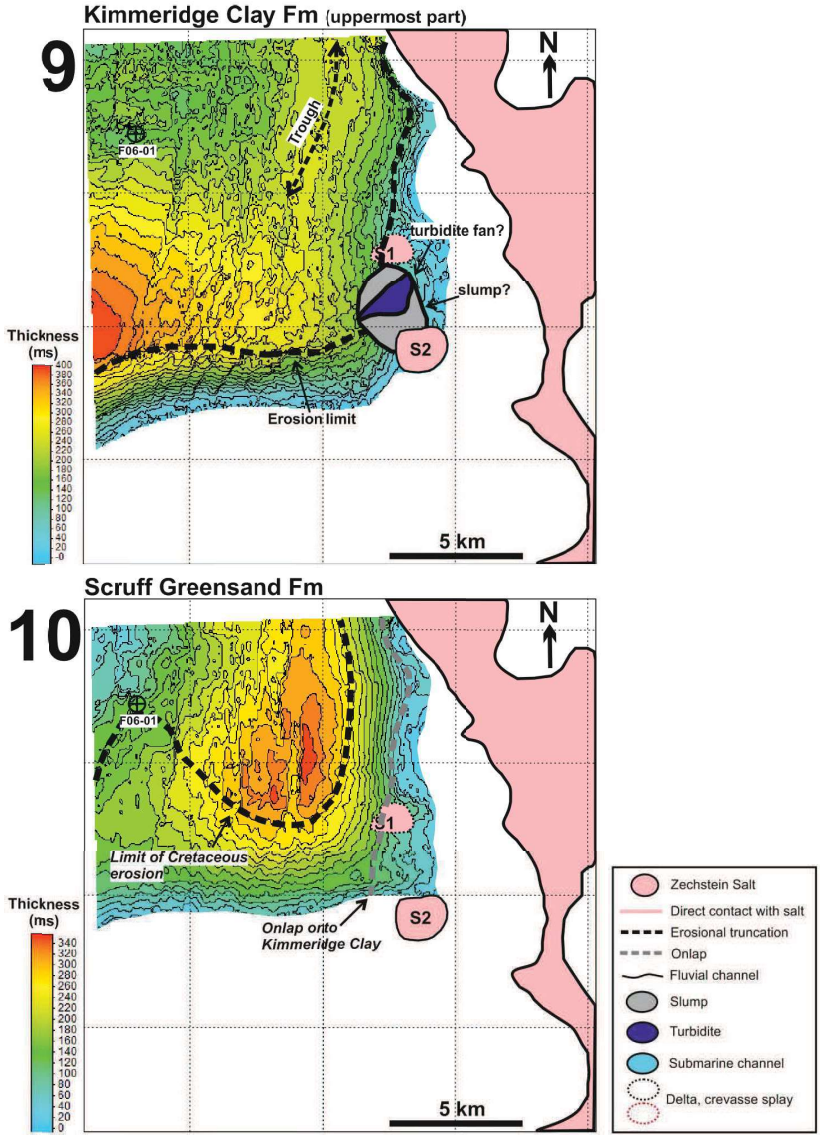

Figure 41.1 -10. Isopach maps of tectonostratigraphic units defined in this study with interpretations from amplitude mapping and seismic facies analysis

5. 3. Paleo-topographic evolution of an active salt basin

Basin margin to basin axis transition varies between rift basins involving or lacking salt, especially in terms of paleo-topography and the resulting sediment dispersal pattern. In fault bounded rift basins, footwall uplift plays a major role by providing abundant source for transverse canyons and fans. In contrast, in salt bounded basins, salt with sufficient thickness (see ten Veen *et al.* 2012 for quantitative estimation) does not allow faults to penetrate through the suprasalt succession. Salt diapirism generates a relatively smooth depositional profile and promotes axial or transverse development of deltaic-shallow marine sequences (Alves, 2003).

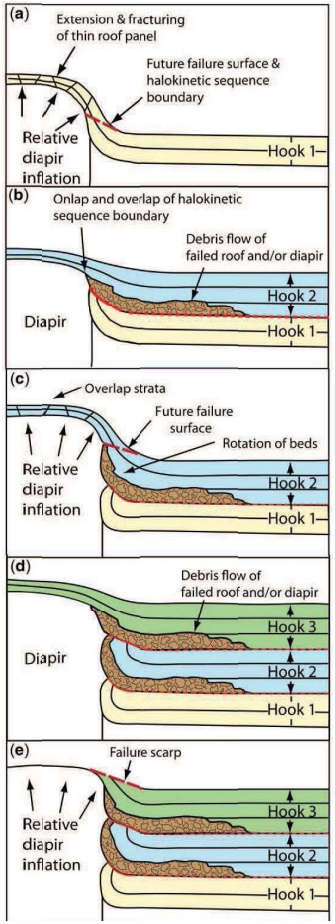

Figure 42. Genetic model for syn-diapiric sequences in case of high salt rise/sediment accumulation ratio. Emergence of salt triggers debris flow. From Giles and Lawton (2012)

Salt diapirism controls sedimentation by modifying contemporaneous topography, being the free surface at the basin axis or margins. Rise of salt bodies along the margins can increase slope gradient increase erosion and/or confinement of sediments. At its apex, diapirism can trigger the exposure of basin margins, which can become subject to erosion and act as an additional local sediment source (Rowan & Weimer 1998). In intra-slope salt-minibasins, such as in the Gulf of Mexico, salt withdrawal from below the mini-basins can create new accommodation space for turbidites to accumulate along the mini-basin axis and margins (Prather *et al.* 1998). Pathways of turbidity currents can be deflected or constrained by topography exerted by salt diapirism (e. g. Kane *et al.* 2012) and have a complex dispersal pattern related to local paleo-topography.

In order to discuss the timing, rate and spatial distribution of salt bodies' rise and overall basin margin evolution, a few assumptions need to be made. The ratio of the rate of salt wall rise and sediment accumulation controls the resulting external shapes as well as internal layer terminations of growth units in terms of how abruptly the thinning occurs in the vicinity of diapirs (Giles and Lawton 2002, Hearon et al. 2014).

Draping reflectors are related to little or no differential subsidence between the basin margin and the basin axis, i.e. tectonic quiescence. In contrast, onlaps may refer to significant differential subsidence.

More abrupt thinning trends between the axis and the margin (e.g. Unit 4, Figure 41. 4 and Table 1) are considered to relate to higher differential subsidence (higher subsidence at the basin axis or higher marginal uplift due to salt body rise). Onlaps can be considered to roughly delineate paleo coastlines and/or the actual location of the basin margin and are regarded as good indicators for high values of accommodation.

In a salt-bounded basin, paleo-topography is highly influenced by salt movements, which exerts a big

impact on the evolving sedimentary pattern. Salt body rise elevates the topography at the margin, which creates accommodation space in the basin. Heterogeneities in the geometry and rate of salt body rise, as well as salt evacuation can define local paleo-topographic lows and highs at the margins and within the basin, which may control the sediment pathways. Local depression in the salt wall can allow rivers to cross the margin perpendicularly, which is likely the case with channel 3 at the base of Middle Graben Formation (Figure 41.3 and 37). This is very different in the case of a fault bounded rift basin where the marginal sediment inputs are controlled by fault ramps and their evolution (e.g. Gawthorpe & Leeder, 1999). However, it is important to note that sedimentation pattern is not only a consequence of paleo-topography but also influences it. As one 0of the main triggering mechanism of salt diapirism is the sediment load itself (Hudec and Jackson, 2007), the evolving sedimentary pattern also influences the 3-D evolution of salt walls, i.e. thicker sediment load may induce higher salt rise, resulting in different rates of salt rise along the basin margin strike.

It is worth noticing that debris flows and/or slides can be also seen in non-deep-water setting in the study area. They refer to occasional, local failure of the margin as it can be observed at the boundary of unit 1 and 2 in the Lower Graben Fm (Figure 30 and 41.1) and potentially in the Kimmeridge Clay Fm in Unit 8 and 9 (Figure 34 and 41. 9). In a salt-bounded basin, failure of the margin can be caused by increased local salt body rise, which locally increases the topographic relief and triggers MTDs. These MTDs may be erosional, as it can be observed in Figure 30. This process is predicted in previous studies in salt-bounded basins and suggested to be mark of increased rate of salt rise (Figure 42) (Giles and Lawton 2012).

The channel trajectory can also be affected by paleo-topography. The geometry of Channel 2 in the Lower Graben Formation (Figures 36 and 41.2) is interpreted as being controlled by local topography control on its river pathway. This may be a result of increased rate of salt body rise, which elevates the marginal area. In turn, areas adjacent to the margin subside and triggers channels to modify their trajectory and flow parallel to the margin when it reached the channel axis.

Channel 3 pathway (Figure 37 and 41. 3) suggests that significant paleo-topographic relief was exerted at the time of its deposition which forced the river to flow in restricted valley with sharp bends at the margin. However, in the basin, tectonic control was negligible based on the large sinuous bend of Channel 3 (Figure 37A).
The transverse entering point of Channel 3 is possibly related to local topographic lows perpendicular to the margin. These depressions can be caused by heterogeneous salt wall height in salt bounded basins, which is a result of differential salt wall rise or salt evacuation. The basin margin representation of these channels are often incised valleys as it is interpreted in case of channel 3 (Figure 37B).

The fluvial system of Upper Graben Fm. (channels 5.1-5.4 in Figure 38 and41.5) evolved in a period with low topographic relief exerted by the basin bounding salt bodies. Characteristic indications for the unrestricted flow are the extensive deltas (Deltas 5. 1 and 5.3 in Figures 38 and 41.5) that are laterally and possibly compensionally stacked in different location and at different orientations.

According to field-work based models such as of Andrie et al. 2012 (Figure 43), channels are situated closer to salt diapirs when rate of salt rise and differential subsidence increases. In the Upper Graben Fm., however, the migration of the channels (Figure 27B) are more likely of depositional origin. After the filling up the accommodation in one area, the channel was forced to flow along another pathway, where sufficient accommodation was s still present.

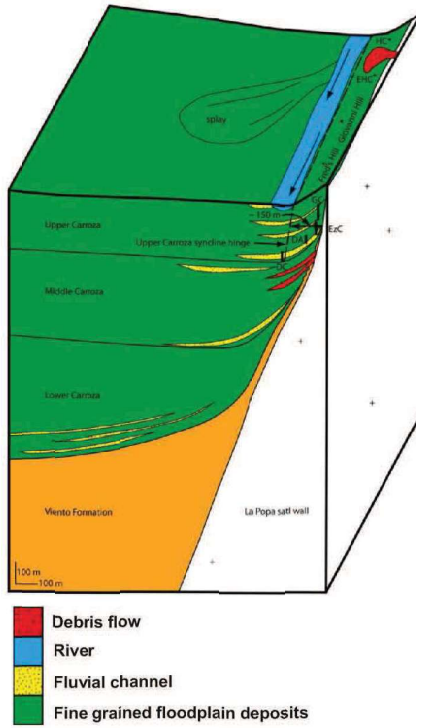

Figure 43. Depositional model of Andrie et al. (2005) for the fluvial succession of the Eocene Carroza Formation in the La Popa salt withdrawal minibasin. Accelerating salt rise resulted in significant changes in fluvial channel morphology and stacking pattern, as well as the external shapes of subsequent syndiapiric stratigraphic unit (Lower- to Upper Carroza).

The faulted margin area (Figures 7-8) reveals the significant effect of changes in paleo-topography on the preserved sedimentary pattern. Faults at the margin area can be observed in almost all units (Unit 1-9), though they are rarely continuous vertically, but steps can be observed along fault planes at certain levels (Figure 7-8). Especially in the lower units (Unit 1, 2, 3), but also at the lower part of Kimmeridge Clay Fm (in Unit 6), small, one-two reflector scale small detachment faults can be detected. These may have formed related to salt wall rise, which triggered increase in topography and slope dip. During syn-depositional diapirism, unconsolidated sediments are especially prone to destabilization. If the rate of salt wall rise is sufficiently high, these sediments tend to move downdip on the slope, which is accommodated by small scale normal faults. The detachment level of the faults likely corresponds with clayey beds which act as rheologically weak zones, being ideal to accommodate fault slip. Interbedded clayey layers are characteristic in fluvio-deltaic successions such as the Lower and Middle Graben Formations, corresponding to high gamma ray well log response (Figure 2). According to the north-south oriented fault pattern, the direction of these mass movements was east to west at the margin. Based on the vertical extent of the faults, faulting moved towards the east with younging (Figure 7). This suggests that the basin margin migrated generally towards the east during the Upper Jurassic. It is in agreement with the overall fining upward, transgressive trend of the basin fill.

5. 4. Tectono-stratigraphic evolution

Based on the derived external forms, thinning rates, sedimentation rates and interpreted tectonically influenced geobodies, the tectonostratigraphic evolution of the Upper Jurassic sequence is described below to further constrain qualitatively the differential subsidence (i.e. that of the basin margin and the basin axis), overall subsidence and relative base level changes (Table 4) occurring during the Upper Jurassic in the study area. It was generally assumed that high sedimentation rates may refer to high subsidence rate, while high thinning rates may refer to high differential subsidence. Estimation of relative base level changes were derived with the aid of previously published depositional environment interpretations, along with subsidence rates and geobodies defined in this study and summarised in Table 4.

5. 4. 1. Lower Graben Formation

The lowermost Upper Jurassic is characterized by a local depression (Unit 1), referred as a bowl external shape. The base of the unit is erosive most of the study area and is related to the thermal doming-related exposure during the Middle Jurassic.

It is known that after the collapse of the thermal dome, rifting started again along pre-existing fault pattern, resulting in the syn-tectonic Upper-Jurassic sequences (De Jager 2007, Munsterman 2012). However, based on the thickness distribution of Unit 1 (Figure 41. 1.), it is possible that accommodation during this initial stage of the Upper Jurassic was not created by extensive rifting-related fast subsidence yet. Instead, local accommodation space was created by the thermal relaxation and sinking of the mantle dome involving no or little rifting and so local depressions filled up on top of the previously erosive top of the Lower Jurassic Altena Group.

The main depocenter within the bowl is located close to salt body 2. In the basin axis, thickness increases from 40 milliseconds to 120 milliseconds, suggesting higher rate of subsidence in the north.

During the deposition of the rest of the Lower Graben Formation (Unit 2) subsidence occurred more homogenously in the study area as well as at a higher rate (Table 4), resulting in wedge forms thinning towards the eastern margin in the entire study area. However, a thicker package can be observed locally between the two salt bodies. Without looking at the internal reflector truncations this area would suggest higher differential subsidence in the middle of the area resulting in a local depocenter. However, the basinward extent of truncating reflectors identified (Figure 41.2) suggests that the northern and southern part of the unit was significantly eroded. Therefore, the higher thickness in the middle is a result of differential preservation in Unit 2, which suggests that the northern and southern areas became exposed at the end of the deposition of Lower Graben Formation. The exposure in this period corresponds with the continental sediment record (coal, fluvial Channel 3) at the boundary of Lower and Middle Graben Formation.

In the middle of the study area, thinning rate of early Unit 2 sequence is low, i.e. reflectors are draping the basin margin (Figure 19, Table 4), which refers to widespread flooding of the whole basin and low differential subsidence between the margin and the axis. The basin preferentially filled up by the westward progradation of few km-scale deltas, among which one is revealed in amplitude maps (Figure 31), and resulted in regression of the lake.

Sedimentation occurred at a high pace during the deposition of the Lower Graben Formation, which suggests that sedimentation could keep up with significant accommodation space related to the start of rifting and related salt diapirism.

Based on its thickness trend, Unit 2 marks the actual start of rifting and accordingly increased salt diapirism in the study area. This interpretation may be supported by the debris flow interpreted at the boundary of Unit 1 and 2 (Figure 30 and 41.1), although the feature bears only local extent. High sedimentation rate suggests that overall subsidence during the deposition of Unit 2 occurred at high pace while differential subsidence of the margin and the basin axis was high in the northern part of the study area but remained low in the south (Table 4).

5. 4. 2. Middle Graben Formation

After the relative uplift and exposure of the northern and southern areas, subsidence renewed shortly after the deposition of the Lower Graben Formation. Rapid change in sedimentation style is marked by fine-grained claystone on top of base Middle Graben coal. Unit 3 strata onlap onto Unit 2 Lower Graben units (Figure 19 and 41. 3) and overlie the prominent, truncated coal layer at the base. This suggests that early Middle Graben deposits postdating the basal coal layer are partly originate from the erosion and redeposition of marginal Lower Graben (Unit 2) sediments. Since onlapping strata of Unit 3 extend further to the margin with younging, and are composed of claystone, it can be concluded that the first half of Middle Graben deposition marks overall transgression. This interpretation may be supported by the drop in sedimentation rate at the transition from Lower Graben to Middle Graben Formation (Table 4). During this transgression, relative base level rise resulted in the eastward migration of the paleo-coastline, roughly marked by the onlaps (Figure 19) and triggered the deposition of fine grained sediments. Munsterman et al. (2012) suggests minor marine influence during the deposition of Middle Graben, therefore this transgression may have occurred in an eustarine environment.

During the deposition of the Middle Graben Formation (Unit 3-4), the basin axis depocenter moved southward in the study area compared with the Lower Graben Fm. At the eastern margin, a local depression developed between the salt wall and the two salt bodies (S1 and S2). This wedge-shaped stratigraphic package thickens to the NE towards the salt wall (Figure 20 and 41.3), which can be a result of either faulting along the western side of the salt wall during this period, or local salt evacuation from the salt wall, which results in a rim syncline. Thinning rate of Unit 3 suggests lower rate of differential subsidence than for Unit 2.

The upper part of Middle Graben Formation (Unit 4) shows high thinning rate referring to high differential subsidence but low sedimentation rates suggests low overall subsidence rate (Table 4), similar to that of Unit 3.

At the start of deposition of Unit 4, sedimentation shifted westward, marked by the onlap configurations (Figure 41.4) that suggests an outward curved coastline, located closer to the basin axis in the middle of the study area. This coastline trajectory is also reflected in the deltaic amplitude pattern show in Figure 32 and 33 and drawn in Figure 41.4 ispopach map outlines the margin-ward limit of sedimentation and potentially the coastline locally at the start, and at the end of Unit 4 deposition.

5. 4. 3. Upper Graben Formation

Since Unit 5 is a very thin unit of up to 100 meters, its irregular thickness distribution is controlled largely by sedimentation pattern, i.e. the distribution of fluvial channels and deltas (Figure 41. 5). Sedimentation continued at nearly the same pace as during the deposition of the Middle Graben Fm. Based on the extensive fluvial channel-delta system highlighted, with fluvial channels, distributary channels and possible associated crevasse splays (Figure 38 and 41.5),

subsidence is minor and differential subsidence remained unclear during this period. Although thinning clearly occurs in the unit, apparent high rate of thinning is not considered a reliable value due to the small thickness differences within this thin unit which does not allow very precise thickness estimations and especially time-depth conversion.

Low accommodation/sedimentation ratio resulted in the deltaic systems filling up of the basin axis and the W-NW progradation of the coastline.

The stratigraphic wedge observed in Unit 3 reappears in Unit 5 but has slightly shifted toward the SE and seems to have a V-shape that could be related to a point-source sediment input to the SE that can be considered a transition toward a fan-shaped paleothick toward the NW between salt bodies S1 and S2) (Figure 41. 5.).

5. 4. 4. Kimmeridge Clay Formation

The Kimmeridge Clay Formation marks the most pronounced change in the distribution of accommodation in the study area during the Upper Jurassic. The main thickness trends are similar in the entire formation (Units 6-9, Figures 41.6-9). The main depocenter is oriented NNE-SSW, with the maximum thickness located in the southwest. During the deposition of the Kimmeridge Clay Fm., the northwestern area may have subsided with a lower rate than its surroundings, which resulted in a NNE-SSW oriented trough (Figure 41.6-9).

Within the Kimmeridge Clay Formation, the boundary of Unit 7 and 8 represents the boundary of tectonic sequence 1 and 2 (Abbink *et al.* 2006). Based on thickness trends, no major change can be observed, since depocenters are located at the same places. However, the rate of thinning is much higher in Unit 6, referring the higher rate of differential subsidence during the deposition of the Kimmeridge Clay Fm (Table 4).

A small turbidite fan and a slump (Figure 34 and 41. 9) are interpreted adjacent to salt body 2 in Unit 9, which may refer to the direct relationship between salt piercement and slope instability. Emerging salt locally may have elevated the topography and slope gradient which triggered mass flows on the shelf.

Sedimentation rate rose enormously within the Kimmeridge Clay Formation (Table 2 and 4, Figure 35). Unit 6 shows similar rates as the underlying units but Unit 7 marks a major increase. This can be a result of rapid subsidence creating large accommodation within a short time interval which accompanied by sufficient sediment input to fill the available space. Age estimation within the Kimmeridge Clay bears relatively high uncertainty due to the limited amount of palynological constraints, meaning that the estimated sedimentation rates can be even higher within the Kimmeridge Clay. The exact value of sedimentation rate increase is also uncertain, but the notion of low sedimentation rate during the early Kimmeridge Clay Fm. followed by a rapid increase can be considered a reasonable estimation. The uppermost part of Kimmeridge Clay, however, deposited at a much lower rate, comparable to the earliest part of the formation in Unit 6 (Table 2 and 4, Figure 35), which implies that that subsidence slowed down during the deposition of Unit 9.

Paleo-depocenters are located at roughly the same place all through the depositional time of the Kimmeridge Clay Fm, referring to no significant spatial variation of differential subsidence within the study area during the deposition of the formation. This evokes the idea that potentially local (5-10 km scale) salt withdrawal during the Lower-, Middle- and Upper Graben Formations changed to a more basin wide (25-30 km-scale) salt withdrawal during the deposition of the Kimmeridge Clay Fm. However, thinning rates suggest a difference of subsidence in the basin axis and basin margin between Unit 6 and Units 7-9, being higher during the deposition of Unit 6 than the rest of the Kimmeridge Clay (Table 2 and 4). This can also be seen in the stratigraphic record, with thinning locally accompanied by onlaps in Unit 6, while Unit 7-9 show no onlaps. Higher rate of differential subsidence during the deposition of Unit 6 may have been caused by salt diapirism-inducing relative uplift at the margin with coeval subsidence in the basin axis, while the draping reflectors of Unit 7 and 8 correspond to very high sedimentation rates and overall subsidence in the whole basin (Table 4).

5. 4. 5. Scruff Greensand Formation

The Scruff Greensand Formation (Unit 10) is only preserved in the northwestern part of the study area. This smaller preserved part of Unit 10 is related to post-depositional erosion, thus its true thickness trends can be examined only in the half of the unit. Its depocenter is located in the north, representing a bowl. It is the only representation of sequence 3 (Abbink *et al.* 2006) in the study area, but based on its thickness, no major change can be detected compared to sequence 2 units (Figure 25. 10). Unit 10 onlaps onto Unit 9 and Scruff Greensand reflectors dip at a shallower angle than the underlying Kimmeridge Clay reflectors.

Sedimentation rate is approximately the same as in the latest Kimmeridge Clay Formation. Apparent high thinning rate is a result of erosion affecting preferentially the basin margin zone.

	Formation	Depositional environment	Tectonically influenced geobodies	Relative base level	Sedimentation rate		Thinning rate	Differential subsidence	Subsidence rate
					Basin axis	Basin margin			
Unit 10	Scruff Greensand Fm	Shallow marine, shoreface to offshore	-	Regression	44,9	13	3,44	-	Low
Unit 9	Kimmeridge Clay Fm	Open marine, outer shelf	Deepwater slump, turbidite (Figure 34)	Transgression	46,7	24,6	1,9	Low	Low
Unit 8			Deepwater slumps (Figure 34)		360,0	20	1,8	low	Very high
Unit 7			-		390,0	230	1,7	Low	Very high
Unit 6			Submarine channel NE-SW (Figure 28)		68,8	32,5	2,12	Medium	Low
Unit 5	Upper Graben Fm	*Fluvio-deltaic*	Channels 5.1 -5. 4, fluvio-deltaic system (Figure 27)	Regression	63,0	26	2,42	High	Low
Unit 4	Middle graben Fm	Eustarine - lacustrine	Deltas (Figure 32 & 33)	Regression	70,0	26,7	2,63	High	Low
Unit 3			Fluvial channel 3 (Figure 37)	Transgression	65,0	30	2,17	At start: exposure of the margin in the north and south; otherwise low	Low
Unit 2	Lower Graben Fm	Fluvio-deltaic or coastal plain	Fluvial channel 2system (Figure 36)	Regression	250,0	83,3	3,0	North and South: High Middle Low	High
Unit 1			Shallow water MTD (Figure 30)	Transgression				Medium	Low

Table 4. Overview table of interpretations in this study, including tectonically controlled geobodies, relative base level changes, thinning rates, differential subsidence, and subsidence rates. Note fluvio-deltaic depositional environment proposed in the Upper Graben Formation, which differs from marginal marine barrier-island system after Munsterman *et al.* (2012)

6. Applications for hydrocarbon prospectivity

The Upper Jurassic interval has been subject of oil and gas exploration for more than forty years in the Dutch Offshore and altogether seventeen fields has been developed (see Table 5 for overview). Abbink *et al.* (2006) identified two main play types in the Dutch Central Graben and the neighbouring Terschelling Basin, the two preferential area where Upper Jurassic is preserved. The paralic – fluvial stratigraphic/structural play is located in sequence 1, while the shallow marine Scruff Spiculite play is part of Sequence 3. One of the proven, and producing fields is the F03-FB, which is partly located in the northwestern corner of the study area.

In the following sections, the potential elements of a hydrocarbon system in the study area are described, including reservoirs, source, seals and trapping mechanisms.

6. 1. Reservoirs:

Well log data suggests the abundance of interbedded sandstone and claystones in Sequence 1, preferentially in the Lower, Middle, and Upper Graben formations. Discontinuous seismic facies may represent distinct sand bodies, fluvial or tidal channel sandstone, surrounded by clayey floodplain or lagoonal deposits (Abbink *et al.* 2006).

In agreement with the literature, distinct fluvial channel zones were identified in the Lower, Middle and Upper Graben Formations which can have good reservoir potential. The most extensive channel system was found in the Upper Graben Formation, where channel or stacked channel width can reach 600 metres (Figure 27 and 41.5). In the Middle Graben Formation, Channel 3 shows width of 600-700 metres (Figure 23 and 41.3). Apart from channels, the prominent high amplitude zone at Base Lower Graben Formation (Figure 29) suggests a possible distribution pattern of sands. In the north, high amplitudes correspond with the truncation of a single reflector, and can represent a combined structural-stratigraphic trap.

Base Lower Graben Formation high amplitude zones can refer to sand distributions at the onset of renewed sedimentation. In the east, these potentially sand zones are truncated along the margin. This stratigraphic truncation along with the dipping nature of the stratigraphy may provide good trapping potential.

Additionally, Sequence 2 may also provide potential reservoir zones. The strikingly high amplitude feature in the lower part of Kimmeridge Clay (Unit 6) is interpreted as a submarine channel complex,which represents a sandier zone enclosed within the fine-grained Kimmeridge Clay (Figure 28).

Shallower in the Kimmeridge Clay, a distinct high amplitude feature has been mapped and interpreted as turbidite in Unit 9. Its anomalously high amplitude can be a result of fluid content.

Since hydrocarbon content significantly decreases average density, oil or gas bearing rocks can create higher impedance contrast with respect to the surrounding, water bearing sediments. Therefore, the observed local amplitude anomalies within the Kimmeridge Clay can be created or enhanced by the presence of hydrocarbons.

6. 2. Source and charge:

The Lower Jurassic Posidonia shale acts as a source rock for all Late Jurassic oil plays, while the Carboniferous for gas plays (Abbink *et al.* 2006).

6. 3. Seal and trapping mechanism:

In general, sealing capacity within the Lower-, Middle and Upper Graben Formations might not be excellent, since interbedded claystones have relatively low continuity and thickness. Therefore hydrocarbons might not characteristically be trapped in most of the underlying discontinuous, paralic/fluvial sand beds. Abbink *et al.* (2006) suggests that intra-formational seals may be sufficient for trapping oil but not gas.

However, the identified channels, especially channel 3 (Figure 23 and 41.3) and channels 5.1 5. (Figure 27 and 41.5), are located at levels that are overlain by extensive clayey interval. Channel 3 can be found at the boundary of rapid lithological change from coal to Middle Graben claystone, which can potentially serve as a good seal. Upper Graben sandstones of channel 3 are capped by the Kimmeridge Clay which provides excellent sealing capacity with its high thickness and continuity.

Kimmeridge Clay may serve as a good seal for Unit 6 submarine channel sandstone, as well as for Unit 9 turbidite within the formation. The proposed fluvial or submarine channel and turbidite reservoirs are sealed in a purely stratigraphic manner. In contrast, elongated high amplitude zone in the north at Base Lower Graben Formation may represent a combined structural/stratigraphic trap.

F-03 field, partly within the study area bears oil and gas in the Lower-, Middle and Upper Graben paralic – fluviodeltaic formations, which correspond to the proposed levels in this study. Therefore, it can be concluded with relatively good certainty, that mature source rock an sealing rocks are present and the proposed channels can be of good reservoir quality. However, the F-03-FB field is located right above a salt pillow, or turtleback structure in the basin axis, which created a round shaped anticline in the overlying. This anticline provides an ideal structure for fluid accumulation. Such an efficient or even comparable structuration cannot be observed elsewhere in the study area, which decreases the potential for trapping in case of the proposed reservoirs.

Field	Discovery well	Discovery date	Stratigraphy	Sequence	Fluid	Remark
B18-FA	B18-03	1982	Lower Graben Fm.	Seq. 1	Oil	stranded
F03-FA	F03-01 (type well) (F03-08)	1971 (1982)	Lower Graben Fm. &. Scruff Greensand	Seq. 1&3	Gas	stranded
F03-FB	F03-03 (F3-FB-101) (type well)	1974 (1992)	Lower, Middle and Upper Graben Fm.	Seq. 1	Oil & gas	producing
F03-FC	F03-07	1981	Scruff Greensand	Seq. 1	Oil	stranded
F14-A	F14-05	1986	Lower Graben Fm.	Seq. 1	Oil	stranded
F17-FA	F17-03	1982	Schieland Group	Seq. 1	Oil & gas	stranded
F17-FB	F17-04 (type well)	1982	Schieland Group	Seq. 1	Oil	stranded
F18-FA	F18-01 (type well)	1970	Schieland Group	Seq. 2	Oil	stranded
G16-FA	G16-01	1985	Scruff/Zechstein	Seq. 3&1	Gas	Production planned
L01-FB	L01-03	1985	Schieland Group	Seq. 1	Oil	stranded
L05-FA	L05-05	1988	Terschelling Sandstone Mb.	Seq. 1	Oil	stranded
L06-FA	L06-02	1990	Terschelling Sandstone Mb.	Seq. 2	Gas	Production planned

Table 5. Overview of discovered oil and gas fields in the northern and middle Central Graben from Abbink *et al.* (2006). F03-FB field is located partly in the northwestern edge of the study area.

Conclusion

Tectono-stratigraphic analysis of the Upper-Jurassic – Lower Cretaceous interval based on three-dimensional seismic data in the NE margin of the Dutch central Graben provided the following results in terms of the evolution of paleo-topography, subsidence and the resulting sedimentary development.

- Thickness distributions show relatively high variability of differential subsidence during the deposition of the Lower-, Middle, and Upper Graben Formations. In contrast, internal units of the Kimmeridge Clay Formation show little spatial changes in subsidence, since paleo-deeps and highs are located approximately at the same locations in the basin axis and the basin margin, as well Smaller scale salt withdrawal during the deposition of the Lower-, Middle and Upper Graben Formations changed to a more basin wide salt withdrawal during the deposition of the Kimmeridge Clay Formation.

- Sedimentation rate estimations were used to constrain qualitatively the temporal changes in basin subsidence and suggests four main phases during the Late Jurassic – Early Cretaceous. High subsidence rate during the deposition of the Lower Graben Fm. was followed by a calmer period during the deposition of the Middle- and Upper Graben Fm, as well as the lowest Kimmeridge Clay Fm, when subsidence rate remained low. Thick package of the middle Kimmeridge Clay represents a period of rapid subsidence, which decreased later during the deposition of the uppermost Kimmeridge Clay Fm. and the Scruff Greensand Fm.

- Differential subsidence between the margin and the basin axis areas are described by the rate of thinning within the syn-diapiric sequences. High thinning rates in the Middle and Upper Graben Formation, and locally the Lower graben Formation suggests high differential subsidence, while low thinning rate values in the Kimmeridge Clay Formation refer to less pronounced differential subsidence. These refer to higher ratio of salt wall rise vs. sedimentation rate during the deposition of the Lower- and Middle graben Formations, and lower salt wall rise – sedimentation rate ratio in case of the Kimmeridge Clay Formation, which correspond to peak subsidence rate values during the deposition of the main part of the Kimmeridge Clay Formation.

- Attribute analysis of several key horizons revealed tectonically influenced geobodies such as fluvial and submarine channels, delta systems and mass transport deposits. Fluvial channels are present in Callovian Lower Graben Formation and at the base of Middle Graben Formation which show that source area was located to the east of the study area. Fluvio-deltaic system detected in the Upper Graben Formation suggest SE-NW sediment transport direction and extensive deltaic sedimentary development. A submarine channel in the lower part of Kimmeridge Clay Formation. Slumps and a potential turbidite fan are detected in the upper part of the Kimmeridge Clay Formation that were triggered by allochthonous salt diapirism.

- Small-scale detachment faults at the basin margin refer to repeated periods of depositional slope failure which moved unconsolidated sediments downdip. Increase in topography and depositional slope dip was likely triggered by periods of increased salt diparism.

- Some of the detected geobodies of this study such as deltas and fluvial channels in the Lower-, Middle and Upper Graben Formation or submarine channels and turbidites in the Kimmeridge Clay Formation may suggest the presence of hydrocarbon reservoirs and can encourage future hydrocarbon-related investigation in the these stratigraphic intervals in the Dutch Central Graben and its surroundings.

Acknowledgements

I would like to thank everyone for their support who was involved to any extent in my half-year long master's research internship at TNO (Netherlands Institute of Applied Research) in the Petroleum Geosciences Group.

First of all, I am grateful to Renaud Bouroullec for his systematic and critical supervision, always thought-provoking remarks and the high level of involvement in the Petroleum Geosciences Group. I would like to thank Geert de Bruin for his support and special technical advice, as well as Roel Verreussel, Kees Geel and Mart Zijp for sharing their opinion and expertise on particular subjects. I am thankful to Jeroen Smit and Dimitrios Sokoutis from Utrecht University for their help and valuable remarks during the project.

I would also like to thank Eliis for providing an extended license of PaleoScan, which software played an essential role in producing valuable results in this project and I am thankful to Johan ten Veen for proposing the possibility of using this software.

References

Abbink, O.A., Mijnlieff, H.F., Munsterman, D.K. & Verreussel, R.C.M.H., (2006) New stratigraphic insights in the 'Late Jurassic' of the Southern Central North Sea Graben and Terschelling Basin (Dutch Offshore) and related exploration potential. Netherlands Journal of Geosciences 85: 221-238.

Alves, T. M., Manupella, G., Gawthorpe, R. L., Hunt, D. W., Monteiro, J. H. (2003) The depositional evolution of diapir- and fault-bounded rift basins: examples from the Lusitanian Basin of West Iberia

Andrie, J. R.,. Giles, K. A., Lawton, T. F., Rowan, M. G. (2012) Halokinetic-sequence stratigraphy, fluvial sedimentology and structural geometry of the Eocene Carroza Formation along La Popa salt weld, La Popa Basin, Mexico

Aschoff, J. L., Giles, K. (2005) Salt diapir-influenced, shallow-marine sediment dispersal patterns: Insights from outcrop analogs

Barr, D. (1987) Structural/stratigraphic models for extensional basins of half-graben type

Beaubouef, R. T., Rossen, C., Zelt, F. B., Sullivan, M. D., Mohrig, D.C.,. Jennette, G. D.C. (1999) Course Notes 40: Deep-Water Sandstones, Brushy Canyon Formation, West Texas

Bouroullec, R., Pyles, D. R. (2010) Sandstone Extrusions and Slope Channel Architecture and Evolution: Mio-Pliocene Monterey and Capistrano Formations, Dana Point Harbor, Orange County, California, U.S.A.

Bouroullec, R., Weimer, P., Serrano, O. (in press) Petroleum Geology of the Mississippi Canyon, Atwater Valley, Western Desoto Canyon, and Western Lloyd areas, Northern Deep-Water Gulf of Mexico: Part 1, Traps, Reservoirs, and Tectono-Stratigraphic Evolution: AAPG Bulletin.

Brun, J.-P., Fort, X., (2011) Salt tectonics at passive margins: geology versus models. Marine and Petroleum Geology 28

Catuneanu , O. (2002) Sequence stratigraphy of clastic systems: concepts, merits, and pitfalls

Dawers, N.H., Underhill, J.R. (2000) The role of fault interaction and linkage in controlling synrift stratigraphic sequences: Late Jurassic, Statfjord East area, northern North Sea

Doornenbal, H., Stevenson, A. (ed.) (2010) Petroleum geological atlas of the Southern Permian Basin Area

De Jager, J. (2007) Geological development, in Geology of the Netherlands

Gawthorpe, R.L., Leeder, M.L. (1999) Tectono-sedimentary evolution of active extensional basins

Hearon, T. E., Rowan, M. G., Giles, K. A., H. Hart, W. H. (2014) Halokinetic deformation adjacent to the deepwater Auger diapir, Garden Banks 470, northern Gulf of Mexico: Testing the applicability of an outcrop-based model using subsurface data

Hudec, M. R. , Jackson, M. P. A. (2007) Terra infirma: Understanding salt tectonics

Jackson, M.P.A. & Vendeville, B.C., (1994) Regional extension as a geological trigger for diapirism. Geological Society of America Bulletin 106: 57-73.

Kane, I. A., McGee, D. T. and Jobe, Z. R. (2010) Halokinetic effects on submarine channel equilibrium profiles and implications for facies architecture: conceptual model illustrated with a case study from Magnolia Field, Gulf of Mexico

Kolla, V., Posamentier, H.W., Wood, L. J. (2007) Deep-water and fluvial sinuous channels—Characteristics, similarities and dissimilarities, and modes of formation

Mannie, A. S. Jackson C. A. - L. and Hampson G. J. (2014) Structural controls on the stratigraphic architecture of net-transgressive shallow-marine strata in a salt-influenced rift basin: Middle-to-Upper Jurassic Egersund Basin, Norwegian North Sea

Munsterman, D. K., Verreussel, R.M.C.H., Mijnlieff, H. F. Witmans, N. Kerstholt-Boegehold. S. & Abbink, O.A. (2012) Revision and update of the Callovian-Ryazanian Stratigraphic Nomenclature in the northern Dutch offshore, i.e. Central Graben Subgroup and Scruff Group

Poliakov, A.N.B. van Balm, R., Podladchikov, Yu. Daudre, B., Cloetingh, S., and Talbot, C. (1993) Numerical analysis of how sedimentation and redistribution of surficial sediments affects salt diapirism

Posamentier, H. W. (2003) Depositional elements associated with a basin floor channel-levee system: case study from the Gulf of Mexico

Posamentier, H.W., Kolla, Y. (2003) Seismic geomorphology and stratigraphy of depositional elements in deep-water settings

Reijenstein, H. M., Posamentier, H. W., Bhattacharya, J. P. (2011) Seismic geomorphology and high-resolution seismic stratigraphy of inner-shelf fluvial, estuarine, deltaic, and marine sequences, Gulf of Thailand

Remmelts, G. (1996) Salt tectonics in the southern North Sea, the Netherlands, *in* Geology of Gas and Oil under the Netherlands

Rowan, M. G. & Weimer, P. (1998) Salt-Sediment Interaction, Northern Green Canyon and Ewing Bank (Offshore Louisiana), Northern Gulf of Mexico

Rowan, M. G., Frank J. Peel, F. J. Bruno C. Vendeville, B. C., Gaullier, V. (2012) Salt tectonics at passive margins: Geology versus models e Discussion

Van Wijhe, D.H. (1987) Structural evolution of inverted basins in the Dutch offshore. Tectonophysics 137: 171–219.

Vendeville, B.C. & Jackson, M.P.A., (1992) The rise of diapirs during thin skinned extension. Marine and Petroleum Geology 9: 331-353.

Verreussel, R., Houben, S., Munsterman, D., Janssen, N., Kerstholt-Boegehold, S. (2015) The Justrat Project: New Stratographic framework for the Upper-Jurassic Lower Cretaceous in the southern North Sea using integrated novel techniques, TNO report.

Weijermars, R., Jackson, M.P.A. & Vendeville, B. (1993) Rheological and tectonic modeling of salt provinces

For more information and questions, please contact:

Friso Veenstra
✉ friso.veenstra@tno.nl
✆ +31 (0) 88 866 53 55

TNO innovation for life

TNO Applied Geosciences | PRINCETONLAAN 6 | POSTBUS 80015 | 3508 TA UTRECHT | +31 88 866 42 56 | wegwijzer@tno.nl